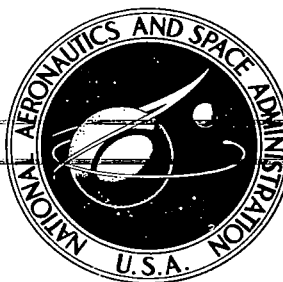


**NASA CONTRACTOR
REPORT**

NASA CR-2804



NASA CR-2804

C.1

0061389



TECH LIBRARY KAFB, NM

LOAN COPY: RETURN TO
AFWL TECHNICAL LIBRARY
KIRTLAND AFB, N. M.

A FIELD STUDY OF WIND OVER A SIMULATED BLOCK BUILDING

Walter Frost and Alireza M. Shahabi

Prepared by

THE UNIVERSITY OF TENNESSEE SPACE INSTITUTE

Tullahoma, Tenn. 37388

for George C. Marshall Space Flight Center

NATIONAL AERONAUTICS AND SPACE ADMINISTRATION • WASHINGTON, D. C. • MARCH 1977



0061389

1. REPORT NO. NASA CR-2804		2. GOVERNMENT ACCESSION NO.		3. RECIPIENT'S CATALOG NO.	
4. TITLE AND SUBTITLE A Field Study of Wind Over a Simulated Block Building				5. REPORT DATE March 1977	
				6. PERFORMING ORGANIZATION CODE	
7. AUTHOR(S) Walter Frost and Alireza M. Shahabi				8. PERFORMING ORGANIZATION REPORT # M-201	
9. PERFORMING ORGANIZATION NAME AND ADDRESS The University of Tennessee Space Institute Tullahoma, Tennessee 37388				10. WORK UNIT NO.	
				11. CONTRACT OR GRANT NO. NAS8-29584	
12. SPONSORING AGENCY NAME AND ADDRESS National Aeronautics and Space Administration Washington, D. C. 20546				13. TYPE OF REPORT & PERIOD COVERED Contractor	
				14. SPONSORING AGENCY CODE	
15. SUPPLEMENTARY NOTES					
16. ABSTRACT A full-scale field study of the wind over a simulated two-dimensional building is reported. The study develops an experiment to investigate the structure and magnitude of the wind fields. A description of the experimental arrangement, the type and expected accuracy of the data, and the range of the data are given. The data are expected to provide a fundamental understanding of mean wind and turbulence structure of the wind field around the bluff body. Preliminary analysis of the data demonstrates the reliability and completeness of the data in this regard.					
17. KEY WORDS Wind Shear Wake Turbulence Wind Profile				18. DISTRIBUTION STATEMENT Category: 47	
19. SECURITY CLASSIF. (of this report) Unclassified		20. SECURITY CLASSIF. (of this page) Unclassified		21. NO. OF PAGES 131	
				22. PRICE \$6.00	

AUTHORS' ACKNOWLEDGMENTS

The research reported herein was supported by the National Science Foundation (NSF), Contract GK-42942, and by the National Aeronautics and Space Administration, Contract NAS8-29584, supported by Mr. John Enders of the Aviation Safety Technology Branch, Office of Advanced Research and Technology, NASA Headquarters.

The authors wish to express their appreciation to Dr. George K. Lea for his assistance and guidance during the course of this investigation. The authors are also especially indebted for the assistance of Dr. George H. Fichtl of the NASA/Marshall Space Flight Center.

TABLE OF CONTENTS

CHAPTER	PAGE
I. INTRODUCTION	1
Background	1
II. EXPERIMENTAL DESCRIPTIONS	15
Introduction	15
Description of Available Data	15
Channel Arrangement	18
Contour of Field Site	19
III. INSTRUMENTATION	22
Horizontal Wind Speed Sensor	22
Wind Direction Transmitter	25
Vertical Wind Speed Transmitter	27
IV. DATA REDUCTION PROCEDURE	34
Introduction	34
Reduction of Digitized Data	34
Fluctuating Velocity Components	38
Computation of Statistics	41
V. RUNS DOCUMENTATION	53
VI. SMOKE STUDY	67
VII. INTERPRETATION OF DATA	79
Description	79
Raw Velocity Data	79
Turbulence Characteristics of the Flow	88

CHAPTER	PAGE
VIII. CONCLUSIONS	103
BIBLIOGRAPHY	105
APPENDIX	108
VITA	120

LIST OF TABLES

TABLE	PAGE
I. Tower Location and Elevation	21
II. Specifications of Climet 011-1 Wind Speed	
Transmitter	23
III. Manufacturer's Calibration of Climet Wind	
Speed Transmitter	24
IV. Specifications of Climet 021-1 Wind Speed	
Transmitter	26
V. Run Number Versus Mean Wind Angle	54
VI. Run Numbers for Which Data Is Available	55
VII. Computer Printout of Horizontal, Direction and	
Vertical Mean Speeds	56
VIII. Computer Printout of Root Mean Square of u' , v'	
and w'	62
IX. Smoke Pattern Measurement of the Wake Extent . .	75
X. Measurement of Wind Speed at Different Heights .	77
A-I. Tower and Levels Associated with the Given	
Channel Number	115

LIST OF FIGURES

FIGURE		PAGE
1.	Flow Around a Cross-Section of a Rectangular Building in a Steady, Uniform Flow	2
2.	The Effects of Shear in the Incident Wind on the Flow Around a Building	4
3.	Flow Around a Rectangular Building in a Turbulent Wind [2]	5
4.	Definition of Flow Zones Near a Sharp-Edged Building [5]	7
5.	Vertical Profile of Longitudinal Mean Velocity Behind the Building Model [6]	10
6.	Vertical Profile of Longitudinal Turbulence Intensity Behind the Building Model [6]	11
7.	The Variation of Mean Wind Speed with Height [7]	13
8.	Eight Tower Facility Site	16
9.	Cross-Section of Eight Tower Array	20
10.	Propeller Calibration (Wind Speed Versus Propeller rpm	29
11.	Response of Four Blade Propeller to Wind Speeds from Threshold to 5 Ft/Sec	30
12.	Propeller Response Versus Wind Angle (Four Blade Polystyrene Propeller)	31
13.	Propeller Response Versus Wind Angle Between 60 and 120 Degrees (Four Blade Polystyrene Propeller)	32

14.	Digitization of Data for Simple Continuous	
	Random Record $V(t)$	35
15.	Average Wind Speed and Wind Direction	37
16.	Definition of Wind Fluctuations u' and v'	39
17.	Trend Removal	39
18.	Typical Plot of u''' with Time (Not Complete	
	Record Length)	42
19.	Statistics of u'''	43
20.	Kurtosis Variation with Respect to Normal Curve . .	46
21.	Typical Plot of Accumulative Probability	
	Distribution	47
22.	Typical Autocorrelation $B(\tau)$	50
23.	Typical Power Spectral Density	52
24.	Top View of the Eight Tower Facility Site (All	
	Dimensions in Meters)	68
25.	Upstream Flow Separation	69
26.	Wake Formation	70
27.	Recirculation and Reattachment Flow	71
28.	Vortex Shedding	72
29.	Basic Data for Test Number 8540-42	81
30.	Correlation of Reference Velocity, Tower	
	Number 6	83
31.	Wind Speed Nondimensionalized with Reference	
	Wind Speed	84
32.	Decay of Velocity Deficit Along Center Line of	
	Wake	87

FIGURE	PAGE
33. Plan View of Tower Array	89
34. Variations of Longitudinal Velocity Fluctuation σ_u (No Building Case)	90
35. Variations of Longitudinal Velocity Fluctuation σ_u (Building Case)	91
36. Variations of the Lateral σ_v and Vertical σ_w Velocity Fluctuations	94
37. Turbulent Regions in Shear Layer	95
38. Turbulence Intensity (No Building Case)	97
39. Test 8044, Tower Number 3, Nondimensionalized Spectral Density (No Building)	98
40. Test 8044, Tower Number 6, Nondimensionalized Power Spectral Density (No Building)	99
41. Test 8504, Tower Number 3, Nondimensionalized Spectral Density (Building Case)	101
42. Test 8504, Tower Number 6, Nondimensionalized Spectral Density (Building Case)	102
A-1. Tower Arrangements; Runs 8001 Through 8057, Recorded Between December 30, 1971 and May 22, 1972	110
A-2. Tower Arrangements; Runs 8058 Through 8062, Recorded Between January 3, 1973 and January 22, 1973	111
A-3. Tower Arrangements; Runs 8063 Through 8079, Recorded Between March 1, 1973 and April 27, 1973	112

FIGURE

PAGE

A-4.	Tower Arrangements; Runs 8401 Through 8409, Recorded Between March 19, 1974 and May, 1974	113
A-5.	Tower Arrangements; Runs 8501 to Present, Recorded Between November, 1974 to Present	114

NOMENCLATURE

A	Constant coefficient
B	Constant coefficient
$B_u(t)$	Autocorrelation
C	Constant coefficient
$f_1(\omega)$	Power spectral density
h	Height of building
IRIG "B"	Intro range instrumentation group coded "B"
K	von Karman constant
L	Distance of traverse
m	Constant, $\tau/\Delta t$
N	Total number of data samples
$S(\eta)$	Power spectral density
T	Time constant
T	Tower
t	Time interval
t_o	Initial time
T_p	Total time period of the data recorded
u_i	Indicated speed
u'	Tunnel equilibrium speed
U	Stream velocity
\bar{u}	Mean meridional velocity
\tilde{u}	Horizontal mean speed
u_*	Friction velocity
V_H	Horizontal wind speed

\bar{v}	Mean zonal velocity
\bar{v}	Vertical mean speed
w	Vertical wind speed
x	Longitudinal distance
z_o	Surface roughness
z	Elevation
α	Angle of wind attack
θ	Direction of the wind
δ	Height of ground relative to zero at base of tower number 3
η	Frequency
σ	Standard deviation
τ	Lag time

Subscripts

\mathcal{C}	Center line
P	Polynomial
k	Number of increment
i	Tower number
j	Level of instrument
b	Begin
e	End
∞	Free stream

CHAPTER I

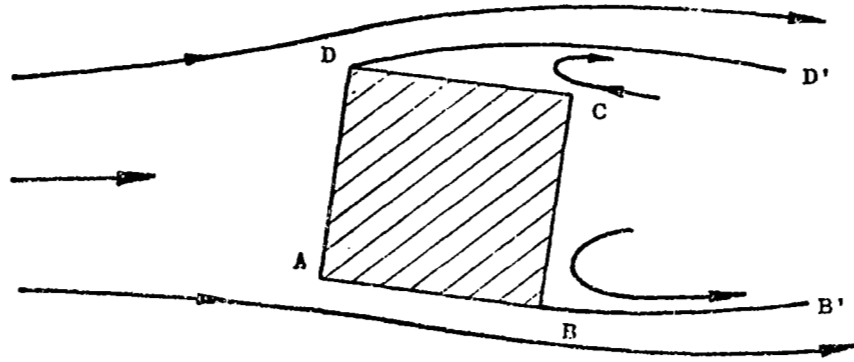
INTRODUCTION

I. BACKGROUND

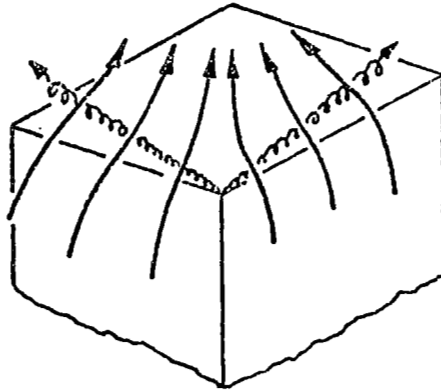
Measurements of turbulence in the atmospheric boundary layer have been made for many years. Little study has been devoted, however, to the way in which obstacles on the ground, such as buildings or woods affect the structure of the turbulent atmospheric flow which is of considerable importance when considering the takeoff and landing of conventional and V/STOL aircraft on runways or landing pads close to such obstacles. The flow around buildings induced by natural winds is also of increasing importance to architects and design engineers since these winds create significant loading of high-rise buildings, influence and affect the comfort of shoppers in the surrounding malls and direct the dispersion of pollutants.

Figure 1 shows typical streamlines for flow around a tall building in a uniform and steady incident flow with low turbulence intensity [1].¹ The region B B' C D D' is said to be separated and to form a wake, Figure 1a. Inside the wake and for a certain distance on either side of the building, the wind is very turbulent having, as well as a steady

¹Numbers in brackets refer to similarly numbered references in the Bibliography.



(a) Typical stream line for flow around a tall building



(b) Vortices on the roof of a rectangular building [2]

Figure 1. Flow around a cross-section of a rectangular building in a steady, uniform flow.

velocity component, a fluctuating velocity component which can be as high as 40 percent of the steady component. The fluctuating component is greatest on the boundaries of the wake BB' and DD' which are referred to as the shear layers. Over the roof, the flow also separates and two strong vortices are created as illustrated in Figure 1b.

The effect of shear in the approaching flow which was not considered in the previous discussion generates a vortex near the ground upstream of the building causing a down-wash on the front face of the building, Figure 2. This can be explained as the piling up of vortex lines swept in by the incident flow (Figure 2b), which also explains the swirling flow found downwind on either side of the building.

The addition of higher turbulence levels to the incident flow effects both the steady and the fluctuating velocity near the building. The two basic effects of the turbulence are to force the wake to start nearer the rear of the building, and to thicken the shear layers which bound the wake region. Figure 3 illustrates the former effect where the turbulence in the incident wind forces the stream separating along D to reattach at D' and to separate again at C; this is in contrast to the flow shown in Figure 1 for low turbulence level. Since the natural wind is always turbulent it is probably true that flow around surface obstacles experience both of the aforementioned effects.

Further description of the distorted flow region around building can be made by dividing the flow region

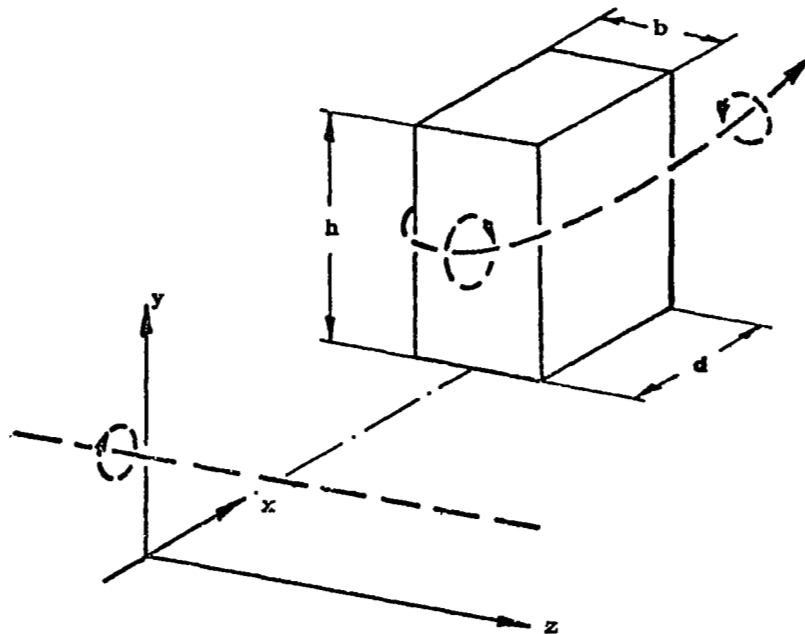
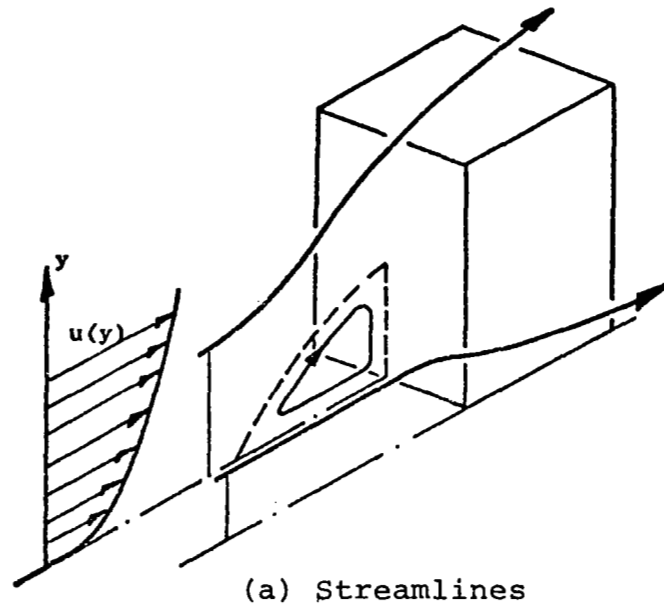


Figure 2. The effects of shear in the incident wind on the flow around a building.

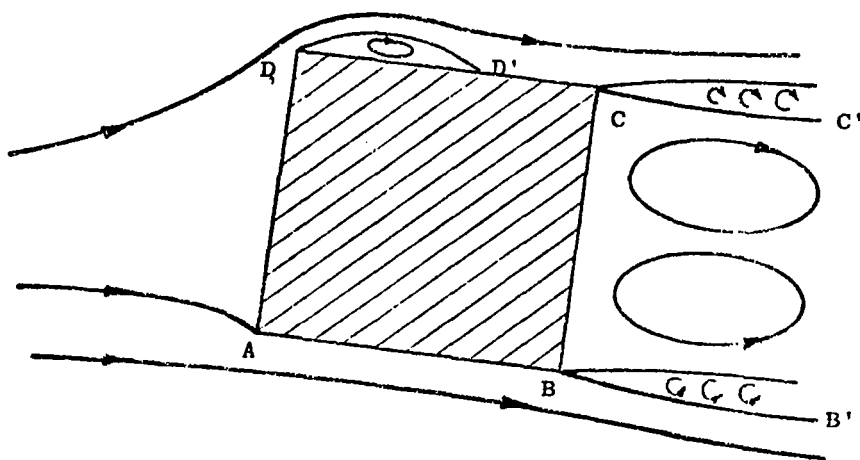


Figure 3. Flow around a rectangular building in a turbulent wind [2].

into three zones, Figure 4: (1) the displacement zone, (2) the wake zone which includes the rear separation bubble, called at times the cavity zone, and (3) the upstream separation bubble or downwash zone.

Chang [3] has compiled an extensive survey of the flow separation literature. Two necessary conditions for flow separation to occur in the downwash zone are an adverse pressure gradient, and viscosity. Retardation of the fluid particles due to viscosity close to the body surface leads to a rapid thickening of the boundary layer and eventually to the onset of reversed flow. The longitudinal position on the surface where reversed flow occurs is identified as the separation point. At this point the velocity gradient at the surface in the direction normal to the wall, passes through zero as does also the wall shear stress. The weakness of this definition is that steady, two-dimensional, incompressible, laminar flow, is the only case where the onset of separation of the boundary layer is unambiguously correlated with the occurrence of zero wall shear stress and flow reversal at the wall.

Nash [4] points out that these convenient surface flow diagnostics are frequently not as well defined when applied to complex flows typical of the turbulent and three-dimensional flows about buildings. In interpreting the literature and the results of experiments and, in particular, extrapolating two-dimensional studies to field situations,

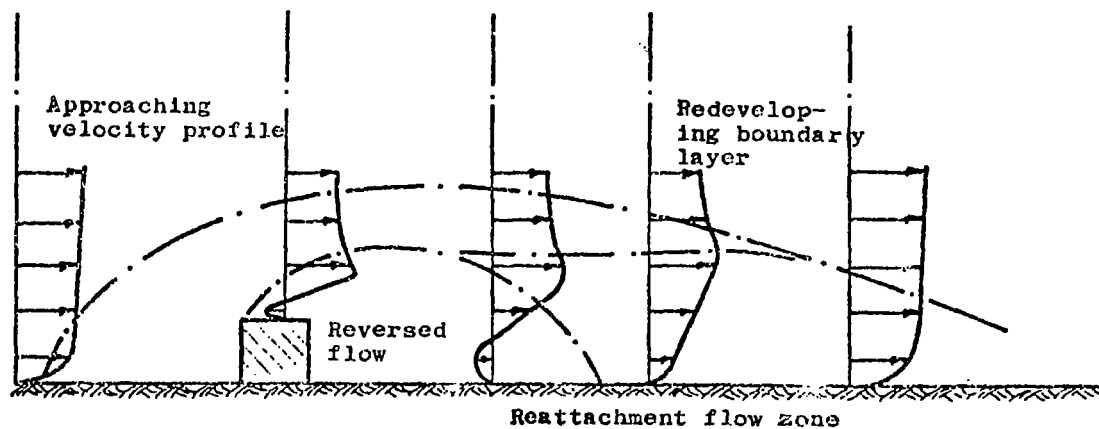
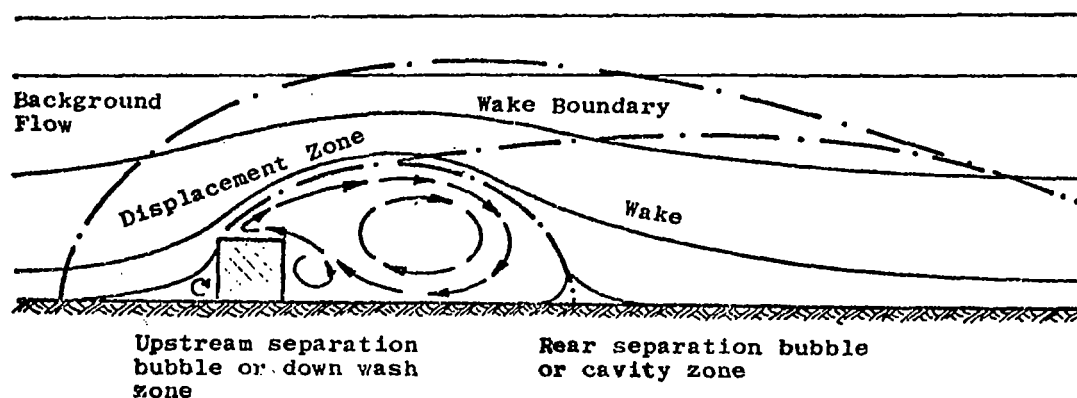


Figure 4. Definition of flow zones near a sharp-edged building [5].

cognizance must be taken of the ambiguities surrounding turbulent and three-dimensional flow separation.

The above described flow phenomena has been qualitatively determined mainly from wind tunnel studies. A summary of related flow phenomena is given in Reference [1]. In order to establish a comparison with the natural atmospheric flow, a study of wind about a simulated block building in an open field has been conducted and is reported in this investigation. Simultaneously, a wind tunnel study sponsored by NASA (National Aeronautics and Space Administration) modeling the NASA field arrangement used in this study is being carried out in the CSU (Colorado State University) wind tunnel. This study is concentrated on measuring mean velocities, longitudinal turbulence intensities, and wake geometries measured at the same appropriately scaled locations to coincide with the locations of the wind tower instrumentation, at the field site. For a selected set of test conditions, the data for the preliminary report of CSU [6] is directly comparable to the results of this study as will be discussed subsequently. The CSU study is continuing with measurement of two-point correlations, longitudinal spectra, and auto-correlations in the wake.

Wakes generated by buildings or other obstacles are characterized by increased turbulence, a mean velocity defect, and in certain situations by organized, discrete standing vortices. Two points are noted from the wind tunnel study; first, the three-dimensional wake narrows in

the horizontal plane at greater heights above the ground. Second, though the wake is strongest near the edges of the wake at low heights, the intermediate heights show the strongest wake near the wake centerline. As it is noted, these differences are quite small [6].

Another related observation from the CSU wind tunnel study is related to the influence of a line of trees upstream of the building at the field site. Figures 5 and 6 show vertical profiles from Reference [6] of turbulence intensity and mean velocity taken with and without the tree line in the tunnel but with all other conditions the same. It can be seen that the trees cause a definite but small change in the wake strength. The effect of the tree line is to give the flow approaching the building a higher turbulence level and a higher exponent in the power-law velocity profile (from 0.25 without the trees to 0.35 with trees).

Also of interest is that the wind tunnel study shows the wake to have a completely different nature when the wind approaches the building at an angle of 47 degrees. It appears that the vortices shed from the corners of the building extend into the far wake of the building, suggesting that the vortex is an extremely stable flow pattern. The only mechanism available to dissipate the angular momentum of a vortex is viscous or turbulent stress acting to produce a moment about the vortex axis [6].

Reference [1] also discusses field studies related to flow about buildings. Literature on this subject is

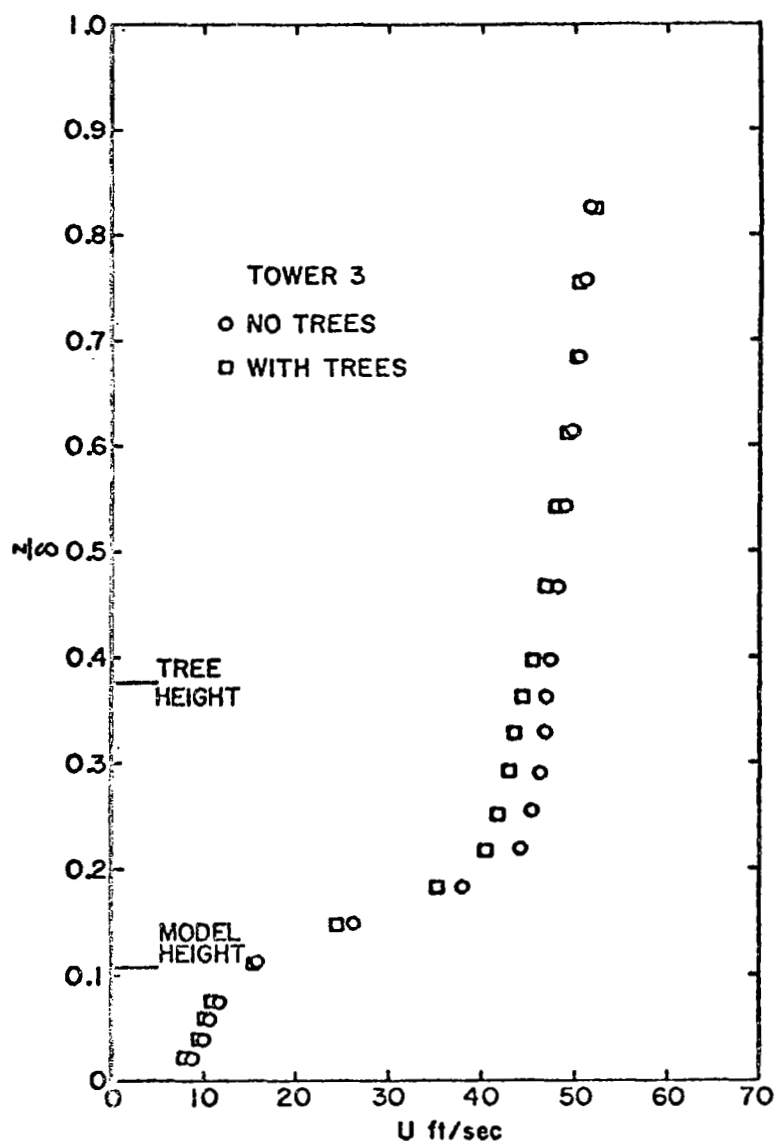


Figure 5. Vertical profile of longitudinal mean velocity behind the building model [6].

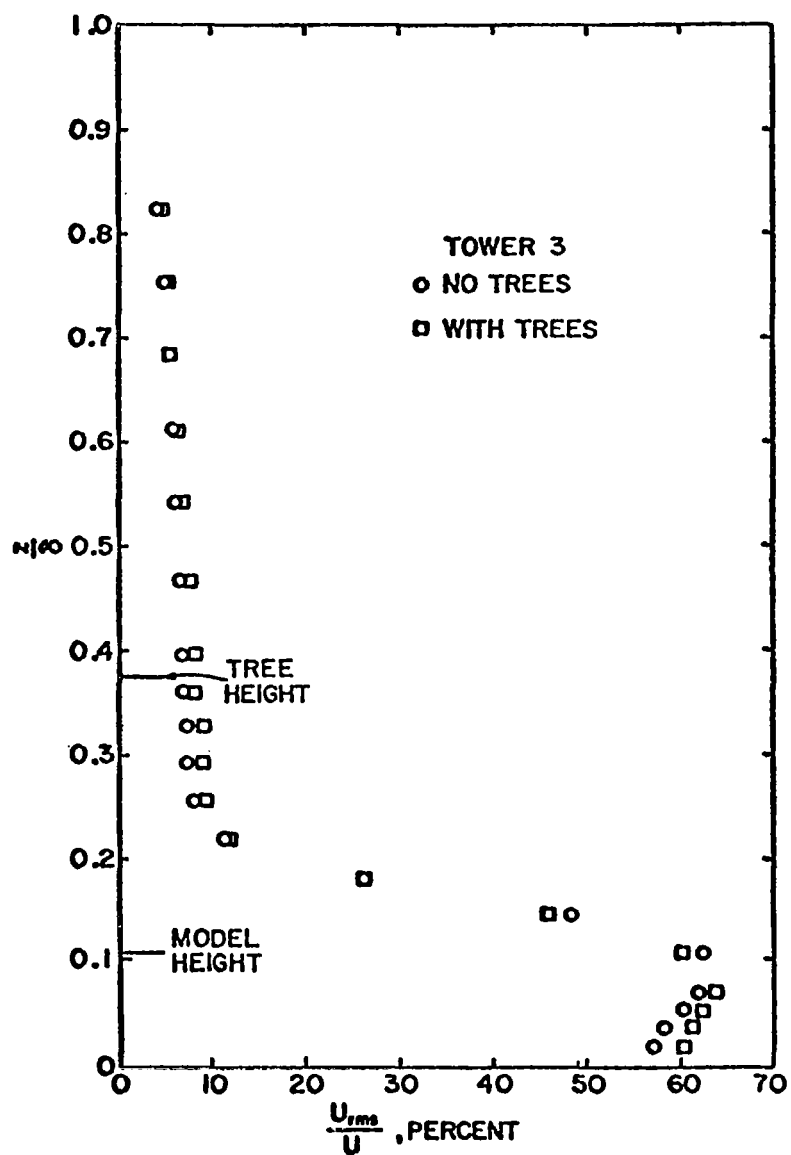


Figure 6. Vertical profile of longitudinal turbulence intensity behind the building model [6].

scarce but one report of limited results pertaining in particular to this work is given by Colmer [7].

The experiment performed by Colmer [7] at RAE (Royal Aircraft Establishment), Bedford, England was designed to investigate in full scale, the wake of an isolated hangar. Evaluation of the turbulence structure and the magnitude of the wind effect is reported. This study reports that at five building heights downstream of the hangar, the mean wind is reduced from the upstream value at all levels below the building height due to the sheltering effect of the hangar, Figure 7. Just above the height of the building there is a slight increase in mean wind speed as a result of the flow accelerating over the top of the hangar. This mean wind profile is very similar to those [7] measured profiles behind obstacles of a similar shape. Also, the data shows that at 14 building heights downstream the velocity deficit is nearly zero at one building height above the ground, which suggests that the effect of the hangar on the mean velocity near the ground soon decays.

Since many questions regarding atmospheric flows about buildings remain unanswered, this study describes an experiment designed to investigate the structure and magnitude of the wind fields about a simulated building. A fundamental understanding of the mean wind and turbulence structure about a bluff obstacle is the expected outgrowth of the experiment.

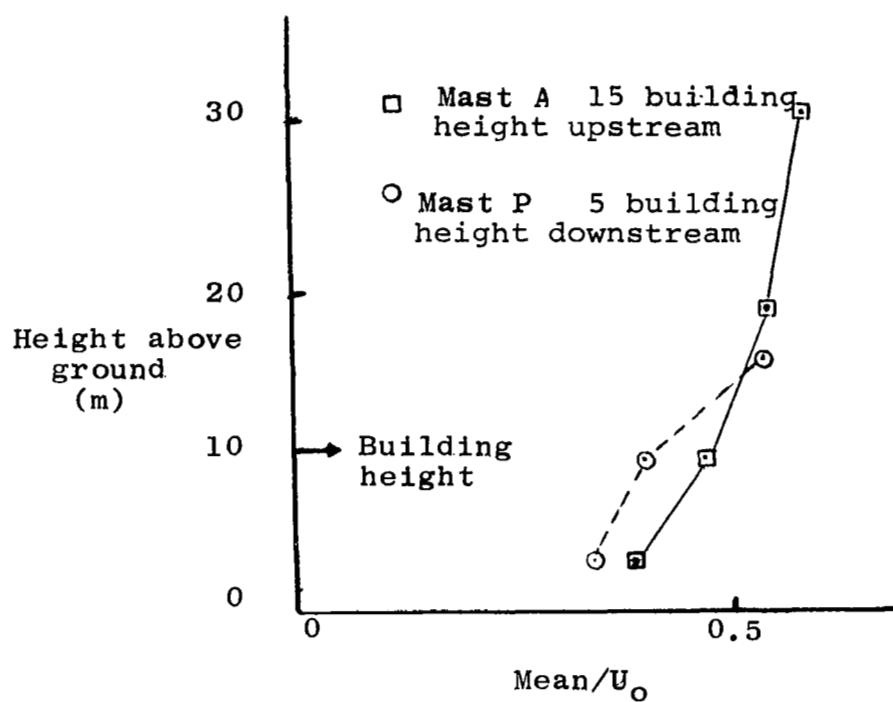


Figure 7. The variation of mean wind speed with height [7].

The present study describes the experimental arrangement, the type and expected accuracy of the data, the extent to which data has been collected at the time of this writing and the data reduction procedure. The currently available data is classified and catalogued and an initial analysis of selected data is given.

CHAPTER II

EXPERIMENTAL DESCRIPTIONS

I. INTRODUCTION

The experiments were conducted in the NASA Marshall Space Flight Center, Aerospace Environment Division Atmospheric Boundary Layer Facility (ABLF), located in Huntsville, Alabama. This facility is essentially an eight wind tower array located in a large open field, Figure 8. All towers are instrumented at approximately the 3, 6, 12 and 20 meter levels, with a three cup anemometer, Climet model 011-1 (horizontal wind speed sensor), a Climet model 012-1 vane (horizontal wind direction sensor) and a Gill model 27100 propeller anemometer (vertical wind speed sensor). The data acquisition and handling system is composed of seven 14 channel model CP100 Ampex magnetic tape recorders.

Approximately 100 experimental runs have been conducted to date for various wind conditions and various geometrical arrangements of the eight towers. The Appendix illustrates these tower arrangements, and the type and the location of the data acquired.

II. DESCRIPTION OF AVAILABLE DATA

Sixty-two experimental runs have been carried out with the facility for the case where no building is present

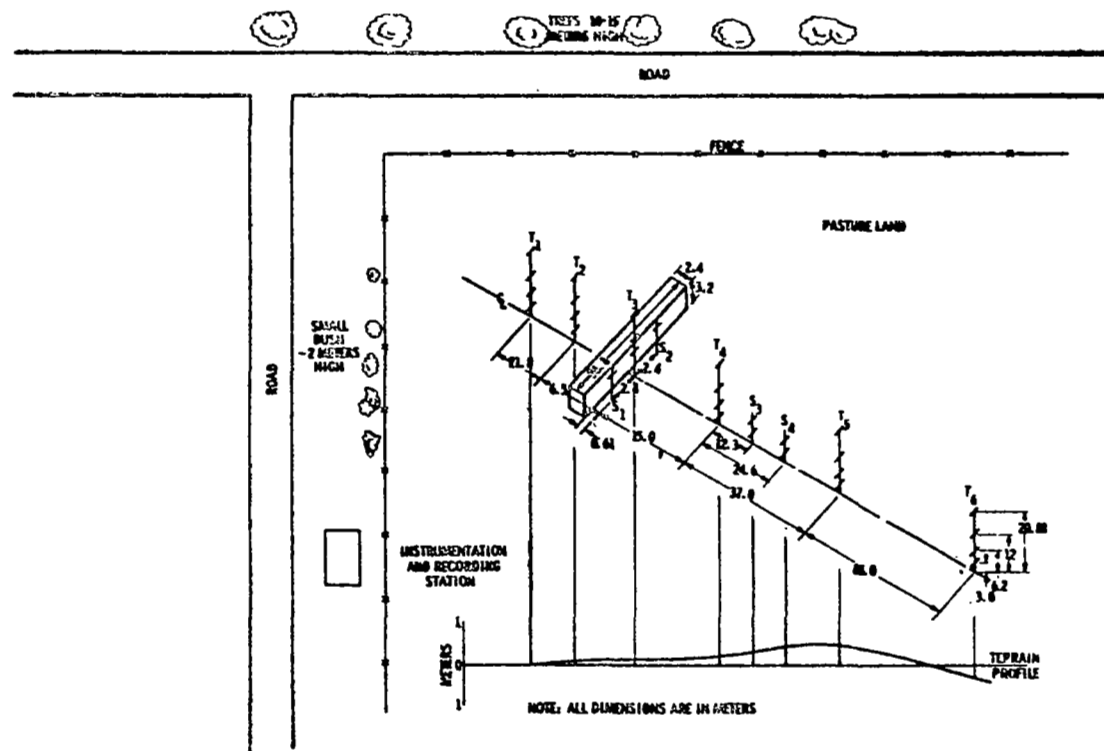


Figure 8. Eight tower facility site.

(no building case). These runs were in two parts; the first runs were made during the period of December 30, 1971 to May 22, 1972, and are numbered 8001 through 8057. The second runs were made during the period of January 3, 1973 to January 22, 1973, and are numbered 8058 through 8062. These runs provide data which serves as a no building reference cases and Figures A-1 and A-2 of the Appendix show the field site and tower arrangement for them. The difference between runs 8001-8057 and runs 8058-8062 is that tower number 1 has been moved 21.8 meters forward from tower number 2 for the latter runs.

Sixteen runs have been carried out with a simulated building (2.4 m deep, 3.2 m high and 7.95 m long) located 2.1 meters forward from tower number 2; this setup is referred to herein as the small building case. Four short towers were mounted laterally on either side of tower number 2 and number 3 during these runs (see illustration in the Appendix, Figure A-3) which are numbered 8063-8079 and were recorded between March 1, 1973 to April 27, 1973.

Following this series of runs, a longer building (2.4 m deep, 3.2 m high and 26.8 m long) was positioned in the array to better simulate a two-dimensional building--the large building case. Data for a two-dimensional building can more directly be compared with wind tunnel and theoretical results which are in greater abundance for two-dimensional geometries.

Nine runs were carried out with this building which was located between tower number 2 and tower number 3 (see illustrations in Appendix, Figure A-4), 0.61 m from tower number 3. Also the two short towers S3 and S4 were moved 12.3 m and 24.6 m respectively up the array from tower number 4. These series of runs are numbered 8401-8409 and were recorded between March 19, 1974 through May, 1974.

The latest series of runs numbered 8501 through 8524 were recorded starting in November, 1974. Also three special runs, numbers 8540, 8541 and 8542, were carried out during the writing of this study and are reported subsequently. Additional data is still being taken and will be reported in future reports. The field site and tower arrangement for the 8500 series are exactly as described for the previous case with the exception that the instrumentation on tower number 3 at level four (21.0 m) was moved to the 9 meter level to give better detail of the building influence (see Appendix, Figure A-5).

III. CHANNEL ARRANGEMENT

The reported data for the various instrumentation locations are listed according to channel numbers. There are 96 channels. The arrangements are as follows: Channels 1-32 record horizontal wind speed, channels 33-64 record wind direction, and channels 65-96 record vertical wind speed.

Figures A-1 through A-5 and Table A-I in the Appendix indicate the corresponding field site positions, tower and levels, associated with the given channel numbers. The nomenclature T_iL_j in the Appendix denotes tower i at level j . Note that T_3L_4 for runs 8501-8524 now corresponds to the 9 meter level. Also short towers S_3 , S_2 correspond to T_7L_1 , T_7L_2 and T_8L_1 , T_8L_2 , respectively, but the short towers S_1 and S_4 correspond to T_7L_3 , T_7L_4 and T_8L_3 , T_8L_4 , respectively. Note that all short towers S_1 , S_2 , S_3 and S_4 are instrumented on 3 meter and 6 meter levels only.

IV. CONTOUR OF FIELD SITE

The field site is not exactly level, having slight undulations along the line of towers. The elevation of the ground with respect to the profile of the towers array is shown in Figure 9. The measurement of elevation with tower number 3 as the zero elevation datum plane are given in Table I. These data indicate the instrumentation levels relative to the building site. One observes that the building is located on an approximately 6.3:1 upgrade.

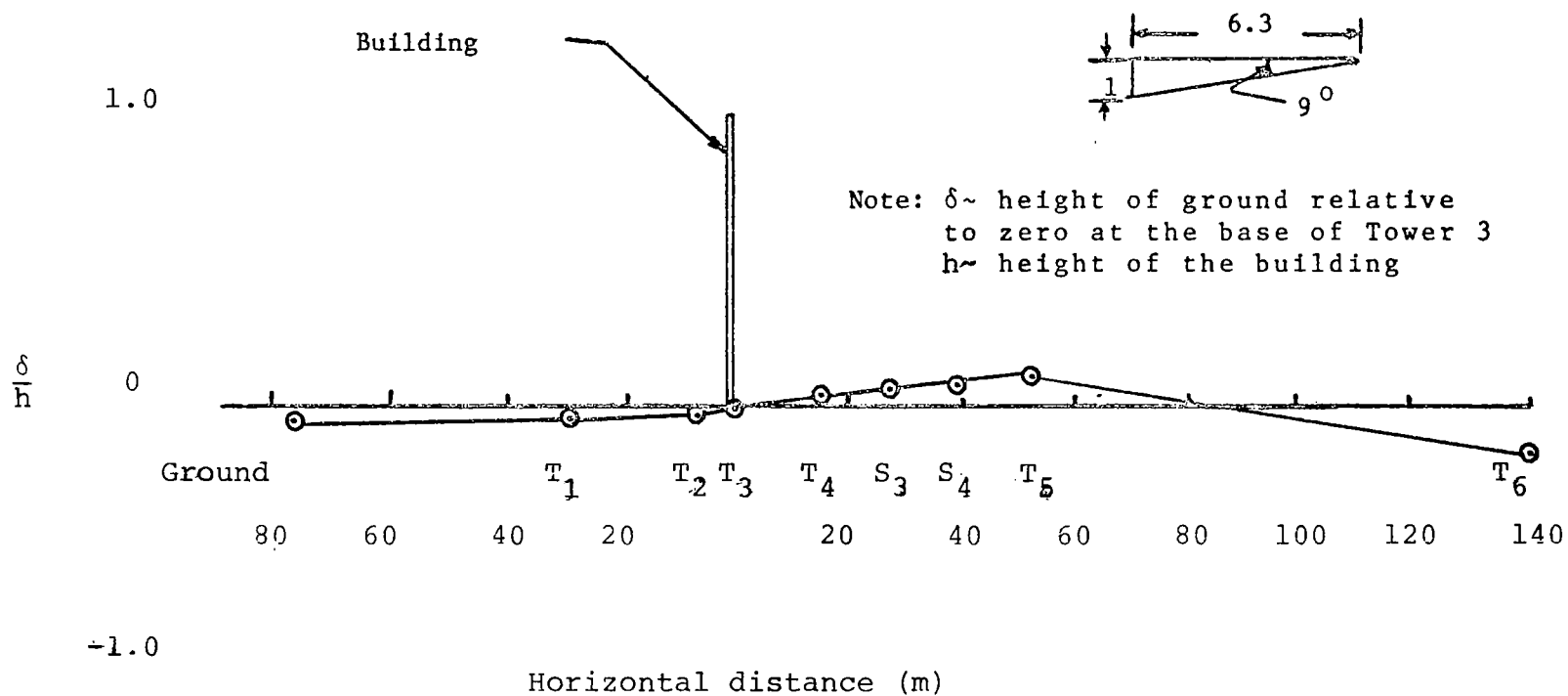


Figure 9. Cross-section of eight tower array.

TABLE I
TOWER LOCATION AND ELEVATION

	Horizontal		Elevation	
	Building Heights	Meters	Building Heights	Meters
Ground	-24.125	-77.20	-0.045	-0.146
Tower #1	-9.040	-28.91	-0.039	-0.128
Tower #2	-2.220	-7.11	-0.008	-0.027
Building*	-0.190	0.61	-0.002	-0.005
Tower #3 ⁺	--	--	--	--
Tower #4	4.687	15.00	0.043	0.140
Tower #S3	8.530	27.30	0.076	0.247
Tower #S4	12.375	39.60	0.087	0.283
Tower #5	16.250	52.00	0.103	0.335
Tower #6	43.750	140.00	-0.156	-0.506

*Building dimensions:
 Height = 3.25 m
 Width = 2.44 m
 Length = 26.72 m

⁺Tower #3 instrument levels:
 Level 1 = 3.17 m
 Level 2 = 6.37 m
 Level 3 = 12.18 m
 Level 4 = 21.01 m

CHAPTER III

INSTRUMENTATION

I. HORIZONTAL WIND SPEED SENSOR

The Climet 011-1 wind speed transmitter is a research sensor designed for measurement of horizontal wind velocity. The model 011-1 uses a three cup anemometer assembly and precision light beam chopper to produce an amplified pulsed electrical output whose frequency is proportional to wind speed (Table II).

Table III gives the calibration of the Climet wind speed transmitter. A 12 volt supply to the anemometer results in a 0-12 volt square wave being proportioned to the frequency of rotation. The sensor output can be filtered through a translator and recorded as a 0-1 volt continuous output or processed through a capacitor and recorded as a spike without regard for the amplitude of the signal.

In the present study, the manufacturer's calibration is accepted and only the tape recorder is calibrated before each run. The procedure consists of first shorting out the oscillator plug to give zero voltage and secondly employing a Hewlett Packard oscillator to give a 1409 cps record on each channel. From Table III, this corresponds to 44.74 mph (20 m/sec) which is taken as full scale in the data reduction. Each calibration is run one minute and a microphone is

TABLE II
SPECIFICATIONS OF CLIMET 011-1 WIND SPEED TRANSMITTER

Model 4 Description	Climet Model 011-1
Power requirements	10.6 to 12.6 V at 15 ma
Operating range	0 to 110 mph
Calibrated range	0.6 to 90 mph
Signal output	Approximately 10 V P-P* square wave
Output	Less than 50 Ω
Accuracy	$\pm 1\%$ or 0.15 mph, whichever is greater
Threshold	0.6 mph
Distance constant ⁺	<5 ft
Operating temperature	-50 °F to 155 °F
Weight	14 oz
Height	18.5 in
Housing dimension	3.5 in h x 2.25 in w
Connector	Climet 49-2004

*P-P is peak-to-peak.

⁺The distance constant is the length of a column of air which passes an anemometer after it has been distributed by a sharp gust until it reaches 63 percent ($1-1/e$) of the new equilibrium value.

TABLE III

MANUFACTURER'S CALIBRATION OF CLIMET WIND SPEED TRANSMITTER

Meters/Second ^a		Miles/Hour ^b		Knots ^c	
v	f	v	f	v	f
0	-16.57	0	-16.57	0	-16.57
0.232	0	0.519	0	0.561	0
0.250	1.25	5.000	142.80	5.000	166.90
1.000	54.73	10.000	302.10	10.000	350.40
2.000	126.00	15.000	461.50	15.000	533.90
3.000	197.30	20.000	620.80	20.000	717.40
4.000	268.60	22.500	700.50	25.000	900.90
5.000	339.90	25.000	780.20	30.000	1084.40
7.000	482.50	30.000	939.50	35.000	1267.90
10.000	696.40	35.000	1098.90	40.000	1451.40
15.000	1052.90	40.000	1258.20	45.000	1634.90
20.000	1409.40	45.000	1417.60	50.000	1818.40
25.000	1765.90	50.000	1576.90	60.000	2185.40
30.000	2122.40	60.000	1895.60	70.000	2552.40
35.000	2478.90	70.000	2214.30	80.000	2919.40
40.000	2835.40	80.000	2533.00	90.000	3286.40
60.000	4261.40	90.000	2851.70	100.000	3653.40
		100.000	3170.40		

^a $f = 71.30 v - 16.57$, $f = \text{Hz}$, $v = \text{meters/second}$

^b $f = 31.87 v - 16.57$, $f = \text{Hz}$, $v = \text{miles/hour}$

^c $f = 36.70 v - 16.57$, $f = \text{Hz}$, $v = \text{knots}$

Best fit using $y = ax + b$, least mean squares approximation. Data from NBS #6.13/172567, August 10, 1962.

employed to inform the computer laboratory of the beginning of each calibration input. This microphone is also used to communicate with the computer laboratory as to the point on each tape where simultaneous reduction of test data is to begin. There is additionally an IRIG "B" timing unit for synchronizing events occurring on different tapes.

II. WIND DIRECTION TRANSMITTER

A Climet model 021-1 wind direction transmitter delivering a 0-4.8 volt DC signal proportional to horizontal wind direction is employed to measure wind direction. The sensing potentiometer which proportions the voltage signal is contained within the housing of the transmitter, thereby being provided maximum protection from contamination by means of a teflon sealed bearing "o" ring seal. Table IV shows the characteristic of the sensor.

The voltage amplitude output of the direction transmitter is proportioned to the wind direction. The Climet wind direction sensor is a 10 K Ω continuous turn potentiometer. A 4 volt input is proportioned according to wind vane position. The instrument is calibrated:

- 1 volt--90 degrees
- 2 volt--180 degrees
- 3 volt--270 degrees
- 4 volt--360 degrees

The 180 degree position has been aligned straight down the tower array in the present installations. A rifle scope is

TABLE IV

SPECIFICATIONS OF CLIMET 021-1 WIND DIRECTION TRANSMITTER

Model 4 Description	Climet Model 012-1
Power requirements	4.8 volts DC
Mechanical range	0 to 360° continuous
Electrical range	354° ± 2°
Signal output	0 to 4.8 v corresponding to 0-360°
Output impedance	Potentiometric output, impedance varies from approximately zero to maximum of 10 KΩ
Linearity	±1/2%
Threshold	0.75 mph
Damping ratio	0.4 with Climet 014-6 vane
Distant constant	Less than 3.3 ft
Operating temperature	-50° to +155 °F
Weight	14 oz
Height	18.5 in
Housing dimension	3.5 in h x 2.25 in w
Connector	Climet 49-2001

used to align the alignment collar on each tower. The towers were initially aligned with a surveyor's transit. The alignment procedure is generally conducted prior to each major measurement program. Calibrations of the recording tapes are performed with a precision power supply.

III. VERTICAL WIND SPEED TRANSMITTER

The Gill propeller anemometer model 27100 is a sensitive precision air speed measuring instrument employing a foamed polystyrene propeller molded in the form of a true generated helicoid. The horizontally positioned propeller is designed to provide one revolution for each foot of vertically passing air. Extensive wind tunnel tests have shown that the propeller actually rotates 0.96 revolutions per foot of air for all wind speed above 2.7 mph (4 ft/sec). Increasing slippage occurs down to the threshold speed of 0.5 mph (0.8 ft/sec). In the standard instrument the propeller drives a miniature DC tachometer generator providing an analog voltage output which is directly proportional to wind speed.

The propeller anemometer will measure both forward and reverse air flow. When the propeller rotation reverses the generator signal polarity reverses. Thus the meter or recorder can be calibrated to read both plus and minus from the central zero position.

Calibration of the instrument is as follows: The positive or negative DC voltage amplitude is directly

proportional to the vertical velocity. At 1800 rpm (0.96 actual propeller revolutions per foot of air) equals 69.9 mph (31.25 ft/sec). Figures 10 and 11 are used to find the vertical velocity, $w(t)$, when the revolutions per minute are known. The output voltage signal for an updraft is recorded as a positive voltage and for a downdraft as a negative voltage. Also the output signal is calibrated to 26.6 mph, at an 1800 rpm. Propeller response follows the cosine law within ± 3 percent in the range of 60 to 120 degrees (± 60 degrees each side of stall). The propeller responds when the component of the wind is parallel with its axis of rotation. Four blade polystyrene propellers provide slightly better symmetry of response to various wind angles especially near the stall region. Figures 12 and 13 show the variation of wind angle with propeller and percentage of response. The model 27100 was designed for optimum dynamic response in wind ranging from threshold to 50 mph.

As angle of attack approaches 90 degrees, the distance constant L equals $T u'$ where T is the time constant and u' the tunnel equilibrium speed. The percentage of response is given by u_i/u' where u_i is the indicated speed. Also the ratio is the cosine of the angle of attack

$$\cos \alpha = u_i/u'.$$

The tape recorders are calibrated prior to each run by recording on each tape -0.2 volts for one minute and +0.2 volts for one minute supplied by a precision power

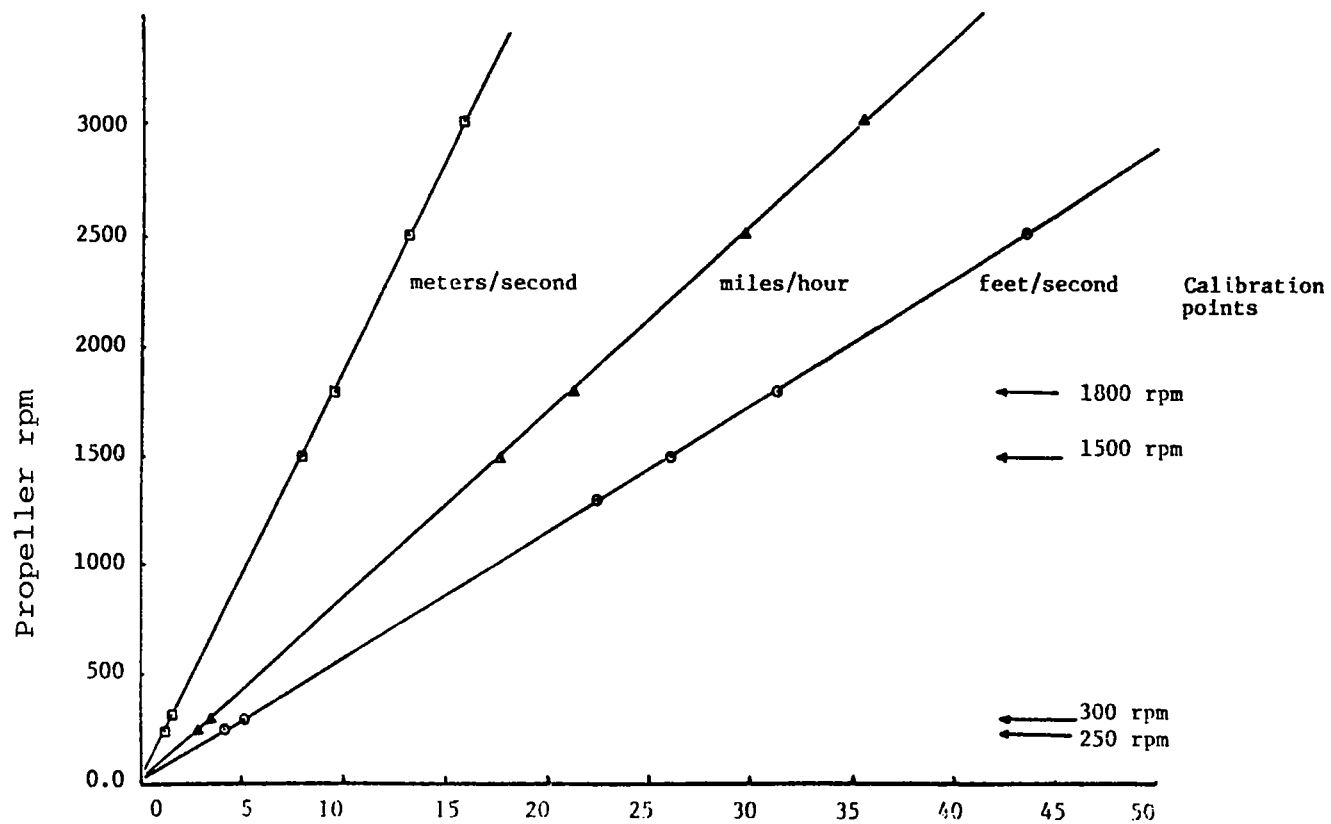


Figure 10. Propeller calibration (wind speed versus propeller rpm).

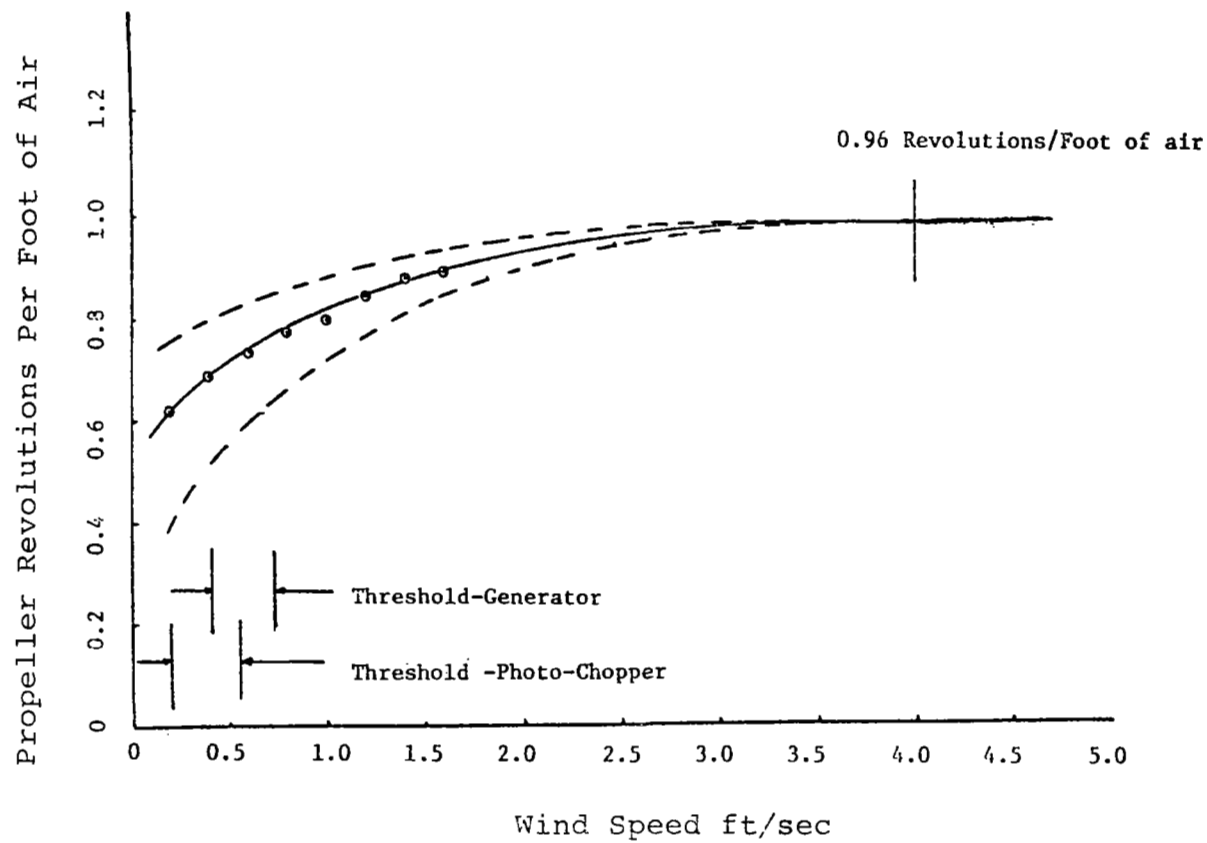


Figure 11. Response of four blade propeller to wind speeds from threshold to 5 ft/sec.

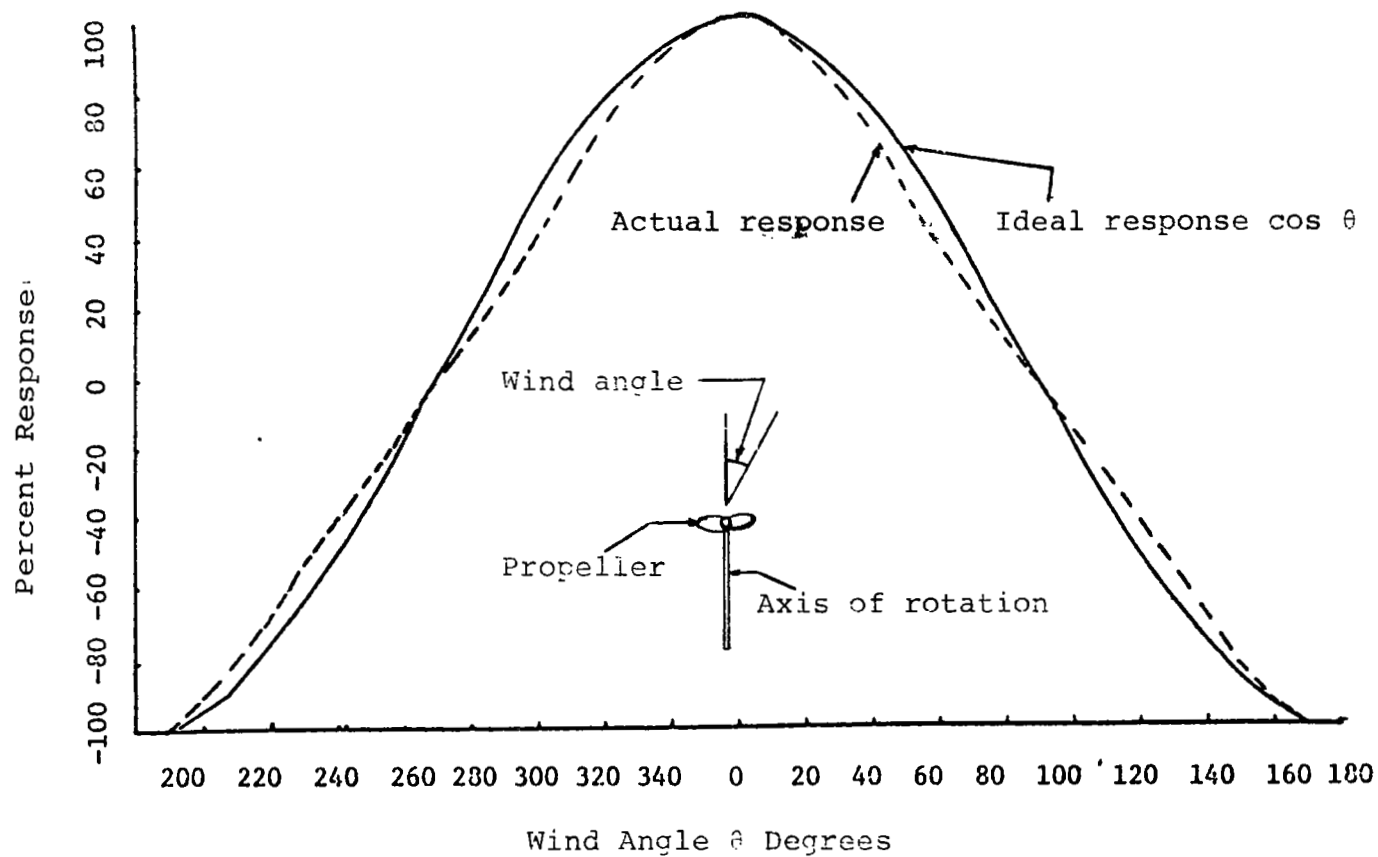


Figure 12. Propeller response versus wind angle (four blade polystyrene propeller).

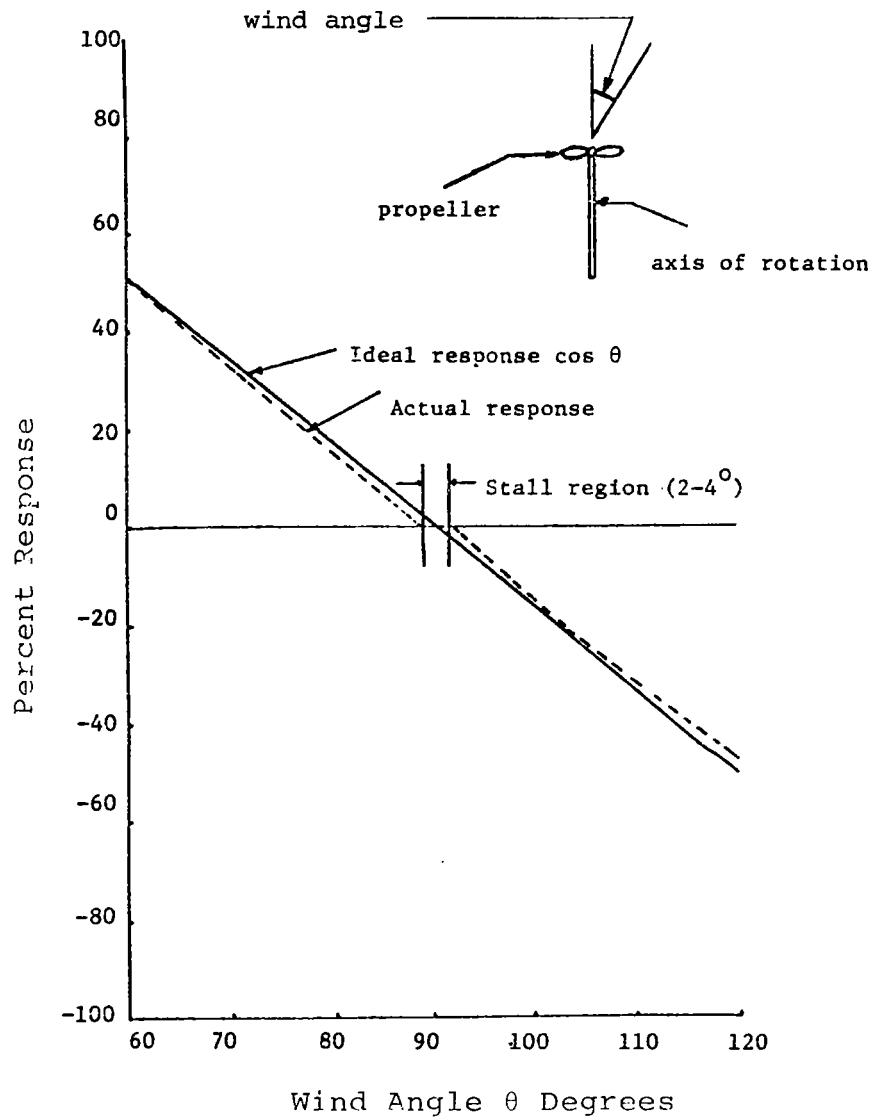


Figure 13. Propeller response versus wind angle between 60 and 120 degrees (four blade polystyrene propeller).

source. The computer laboratory in reducing the data then assigns 0 to the -0.2 volt reading and 1000 to the +0.2 volt reading, thus dividing a range of -10.64 to 10.64 mph into 1/1000 increments.

CHAPTER IV

DATA REDUCTION PROCEDURE

I. INTRODUCTION

The data are digitized with an analog to digital convertor in the NASA Marshall Space Flight Center computer laboratory. The converted data consists of 1/10 sec. averages of horizontal wind speeds, V , horizontal wind directions, θ , and vertical wind speeds, w . As an example of the digitization procedure, consider Figure 14 to represent a continuous analog record of the horizontal wind speed $V(t)$. Let V_n be the average value of $V(t)$ over the time increment Δt between t_n and t_{n-1} . The frequency of sampling, n , is given by $n = 1/\Delta t$. The mean velocity is then given by $\bar{V} = \frac{1}{N} \sum_{n=1}^N V_n$ where N is the total number of time increments $(t_N - t_0)/\Delta t$. The time $t_p = (t_N - t_0)$ is the total time period of the data record.

II. REDUCTION OF DIGITIZED DATA

The digitized data are first bulk averaged with the relationships

$$\bar{u} = \frac{1}{N} \sum_{n=1}^N V_n \cos \theta_n$$

$$\bar{v} = \frac{1}{N} \sum_{n=1}^N V_n \sin \theta_n$$

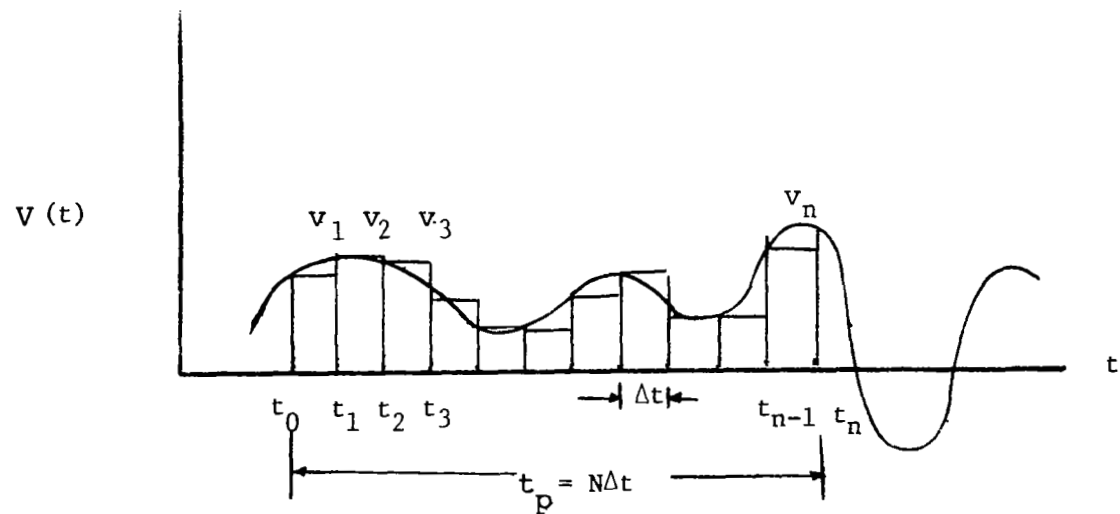


Figure 14. Digitization of data for simple continuous random record $V(t)$.

$$\bar{w} = \frac{1}{N} \sum_{n=1}^N w_n$$

The average horizontal wind speed and wind directions are then given by

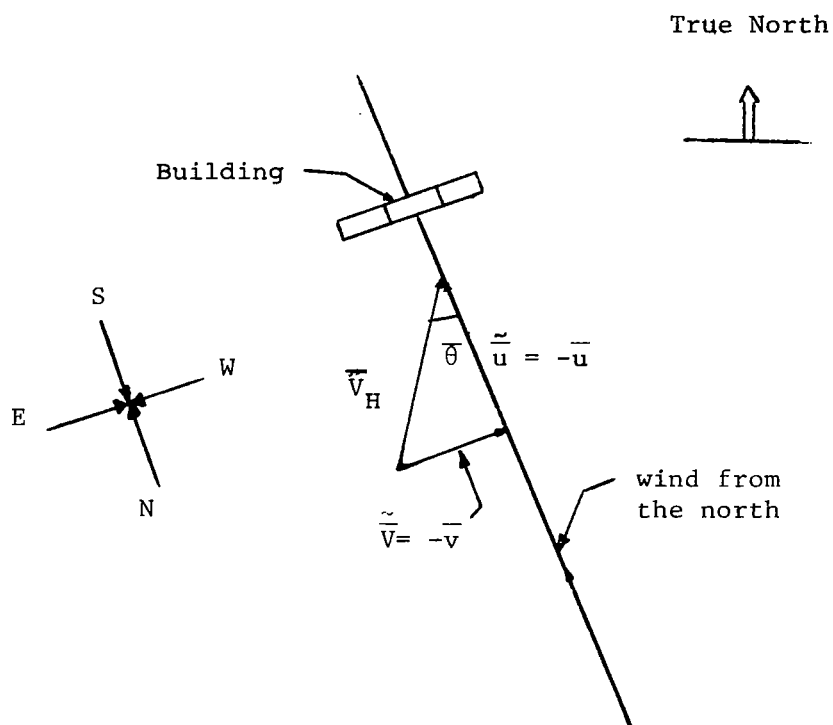
$$\bar{V}_H = (\bar{u}^2 + \bar{v}^2)^{1/2}$$

and

$$\bar{\theta} = \tan^{-1}(\bar{v}/\bar{u})$$

respectively. Figure 15 illustrates the direction of the velocity components \bar{u} and \bar{v} relative to the tower array. Recall that $\theta = 180^\circ$ is defined as the direction a wind would blow if air flow is along the tower array from tower #1 to tower #6. For convenience, north relative to the array is defined to have the direction as shown in Figure 15, and hence, a wind from the north, $\theta = 0$, blows in the direction from tower #6 to tower #1. True north, however, is 52 degrees measured clockwise from the defined north.

According to the above definitions, \bar{u} becomes the component of wind from the north and \bar{v} the component of wind from the east. The wind components are then redefined as a mean zonal wind component \bar{v} perpendicular to the array and a mean meridional wind component \bar{u} down the array (from T_1 to T_8) as shown in Figure 15. \bar{v} is then a positive wind component from the west or a positive wind component toward the



Note: Wind from 0 degree is from the north, and wind from 180 degrees is from the south.

Figure 15. Average wind speed and wind direction.

east. Similarly, \bar{u} is a positive wind component toward the north or a positive wind component from the south.

III. FLUCTUATING VELOCITY COMPONENTS

The mean horizontal wind velocity, \bar{V}_H , defines a new coordinate system from which the fluctuations are measured. Figure 16 defines lateral and longitudinal fluctuations relative to the horizontal mean velocity. The fluctuating components of the wind in the vertical direction, v' , and in the horizontal direction u' reported herein are therefore perpendicular and parallel to the mean wind direction, respectively. The following relationships may be employed to compute v'_k and u'_k for the k th time increment $t_k = t_0 + (2k - 1)\Delta t/2$

$$v'_k = V_k(t) \sin(\theta'_k - \bar{\theta})$$

$$u'_k = V_k(t) \cos(\theta'_k - \bar{\theta}) - \bar{V}_H$$

These new fluctuations are computed in the present study on the basis of 1/2 sec. averages.

The resulting fluctuating components will appear as shown in Figure 17 having in many cases a trend with time. The trend is removed by taking a least squares fit of a polynomial throughout the data, i.e., $V_p = C + Bt + At^2$. The values of A , B , and C are obtained by solving the system of equations:

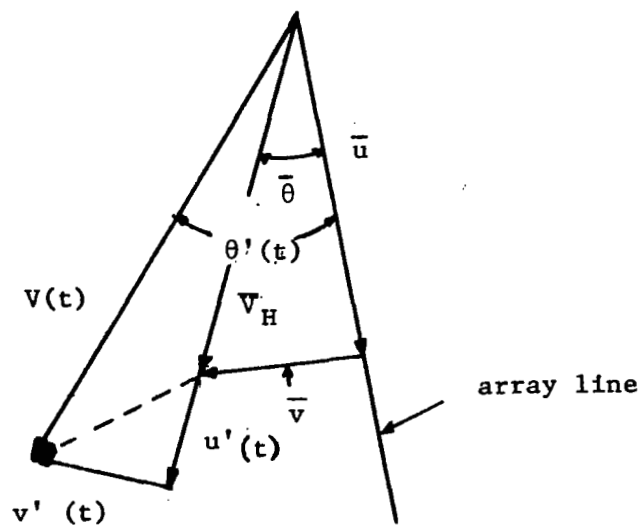


Figure 16. Definition of wind fluctuations u' and v' .

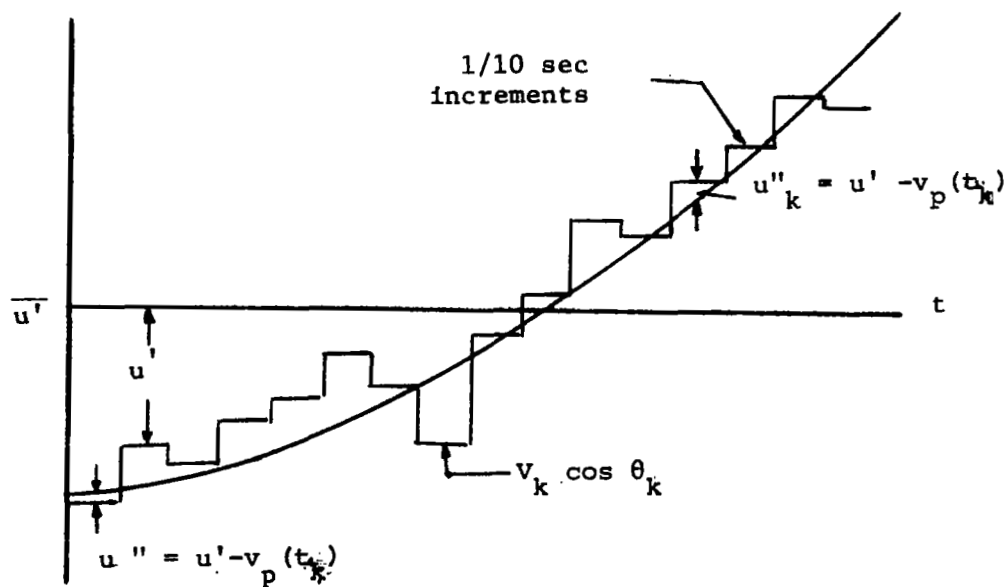


Figure 17. Trend removal.

$$NC + B\sum t_k + A\sum t_k^2 = \sum u'_k$$

$$C\sum t_k + B\sum t_k^2 + A\sum t_k^3 = \sum t_k u'_k(t)$$

$$C\sum t_k^2 + B\sum t_k^3 + A\sum t_k^4 = \sum t_k^2 u'_k(t)$$

where A, B, and C are unknown constant coefficients, $t_k = t_0 + (2k - 1)\Delta t/2$ and u'_k is the kth value of u' . The mean of the fluctuating velocity u' is then calculated from

$$\bar{u}' = \frac{1}{N} \sum_{k=1}^N u'_k$$

where N is the total number of data samples. The computed parabolic curve fit gives the parabolic variations of the 1/2 sec. averaged data with time. With the curve fit a new random variable is defined as:

$$u''_k = u'_k - (C + Bt_k + At_k^2)$$

$$v''_k = v'_k - (C_1 + B_1 t_k + A_1 t_k^2)$$

$$w''_k = w'_k - (C_2 + B_2 t_k + A_2 t_k^2)$$

Averaging the three components u'' , v'' , and w'' we get

$$\bar{u}'' = \frac{1}{N} \sum_{k=1}^N u''_k$$

$$\bar{v}'' = \frac{1}{N} \sum_{k=1}^N v''_k$$

$$\bar{w}'' = \frac{1}{N} \sum_{k=1}^N w_k''$$

The mean of the double primed quantities will not in general be zero, hence a final set of conditioned fluctuating velocities u''' , v''' and w''' are defined so as to have zero mean, i.e.,

$$u''' = u'' - \bar{u}''$$

$$v''' = v'' - \bar{v}''$$

$$w''' = w'' - \bar{w}''$$

IV. COMPUTATION OF STATISTICS

The statistics of the triple prime random variable are computed and plotted by the NASA Computer Laboratory. A packet of reduced data for each channel is provided per run. A sample set of the provided data for one channel is presented and described in the following. Such data is available for all channels for almost all runs.

Figure 18 is a typical plot of u''' versus time. The significant information tabulated above the figure is the test number, 8515, the channel number, 1, the sample rate, 2/sec, and the variance 1.168 m/s which is erroneously labeled in the tables as standard deviation or rms value.

Figure 19 shows the probability density distribution functions compared with a Gaussian distribution. The probability density distribution is computed by dividing the

DATE 03/03/75		SEG NO = 1030		1
TEST	8515	CAL. RANGE	0.000 TO 0.000	
LINK/CHAN	POWER=1	SAMPLE RATE	2.000 /SEC.	
SLICE TIME	4.071E+04 TO 5.107E+04	SE-COMP-RAP	453-2733	
PEAS. NO.	CHAN 1	COMP. RMS	1.168	

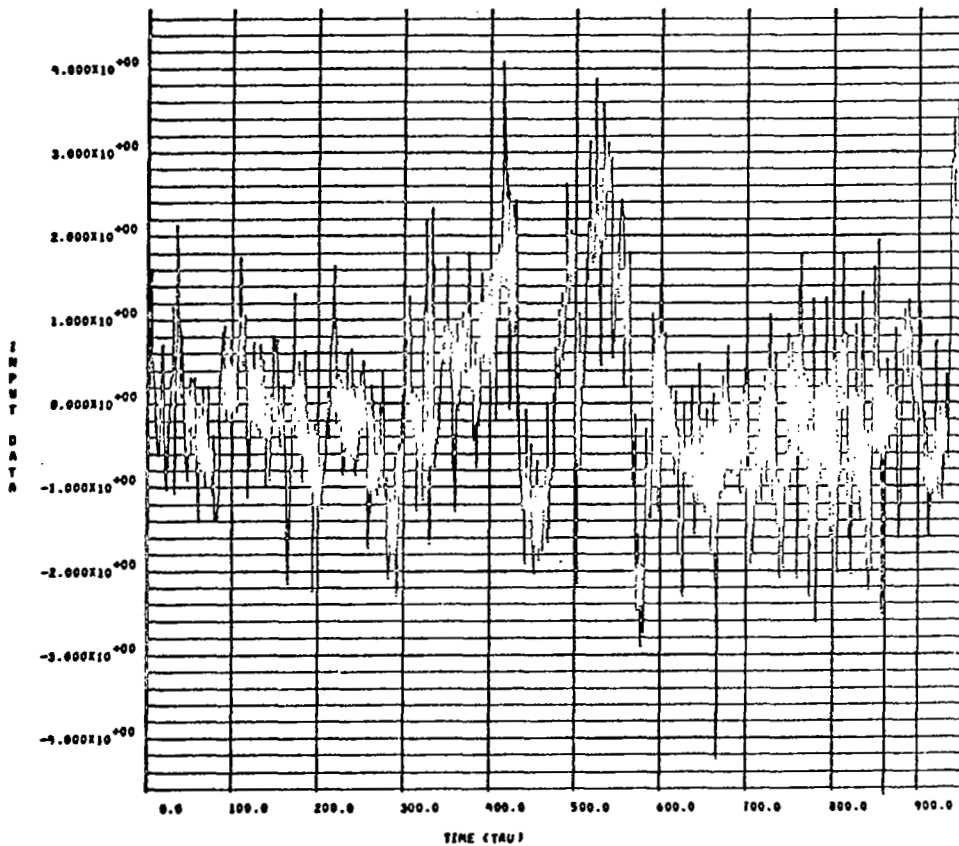


Figure 18. Typical plot of u''' with time (not complete record length).

range of u''' into increments $\Delta u'''$. The number of data points which lie in each $\Delta u'''$ increment are then summed and divided by the total number of data points. This gives the density of points in the increments $\Delta u'''$. The density is then plotted versus \tilde{u}'''/σ as shown in Figure 19. \tilde{u}''' is the mid-point value of $\Delta u'''$. As an example, consider a point at $\tilde{u}'''/\sigma = -1.4$ in Figure 19. The interval surrounding this point is approximately -0.9 to -1.9 and the value of the ordinate is 16 percent. Thus 16 percent of the data points lie between $-0.9 < \tilde{u}'''/\sigma < -1.9$ or $-0.97 \text{ m/s} < u''' < -2.05 \text{ m/s}$. In addition to the standard information listed on all the computer plots, the mean, standard deviation, skewness and kurtosis along with other statistics are tabulated above Figure 19.

A brief description of these statistics is defined as follows:

1. Mean. $\bar{u}''' = \frac{1}{N} \sum_{k=1}^N u'''_k$

\bar{u}''' should be very close to zero. From Figure 19
 $u''' = 1.175 \times 10^{-5} \text{ m/sec}$.

2. Standard deviations. The standard deviation is the root mean square value of u'''^2 , i.e.,

$$\sigma = \left[\frac{1}{N} \sum_{k=1}^N (u'''_k)^2 \right]^{1/2}$$

Note, $\sigma^2 = 1.168 \text{ m/s}$ is tabulated in Figure 19.

3. Skewness. Skewness is the tendency of a distribution to depart from a symmetrical form.

Interest in this parameter lies in its measure of the amount of departure or skewness from a symmetrical frequency distribution

$$\text{Skewness} = \frac{1}{N} \sum_{k=1}^N (u'''_k)^3 / \sigma^3$$

From Figure 19, page 43, the calculated skewness is 0.482.

4. Kurtosis. A curve of a probability density distribution may conceivably be perfectly symmetrical yet differ from a normal curve as shown in Figure 20. In case 1 the curve is higher and narrower than the normal distribution curve. This is called leptokurtic. In case 2 the curve is lower and wider than a normal distribution curve and is called platykurtic.

$$\text{Kurtosis} = \frac{1}{N} \sum_{k=1}^N (u'''_k)^4 / \sigma^4$$

From Figure 19 the calculated kurtosis is 4.038 and since it is higher than the value of three for the Gaussian curve, this particular data is leptokurtic.

The range of the u''' data is also listed in Figure 19. The maximum (4.702 m/sec) and the minimum (-4.638 m/sec) are the range of values of u''' recorded for that channel during the given run. Figure 21 is a plot of the accumulative probability distribution.

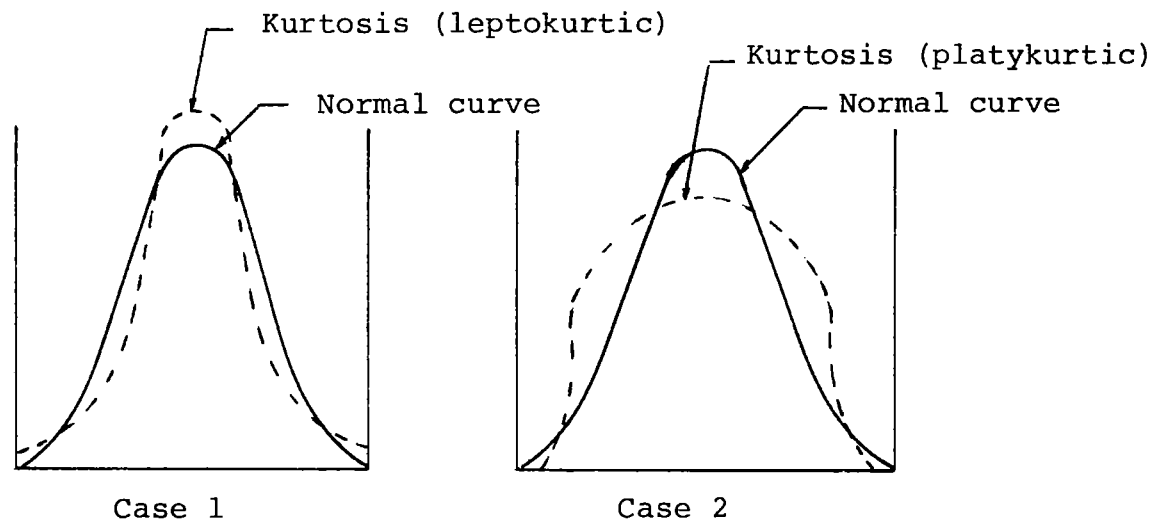


Figure 20. Kurtosis variation with respect to normal curve.

DATE 03/03/75		SEQ NO = 1030		6	
TEST	0515	POWER=1		FILTER B.W.	6.666E-03 HZ
LINE/CHAN	9.871E+04	TO	5.107E+04	SAMPLE RATE	2.000 /SEC.
SLICE TIME	CHAN 1			SE-COMP-RAP	453-2733
MEAS. NO.				COMP. NYS	1.168

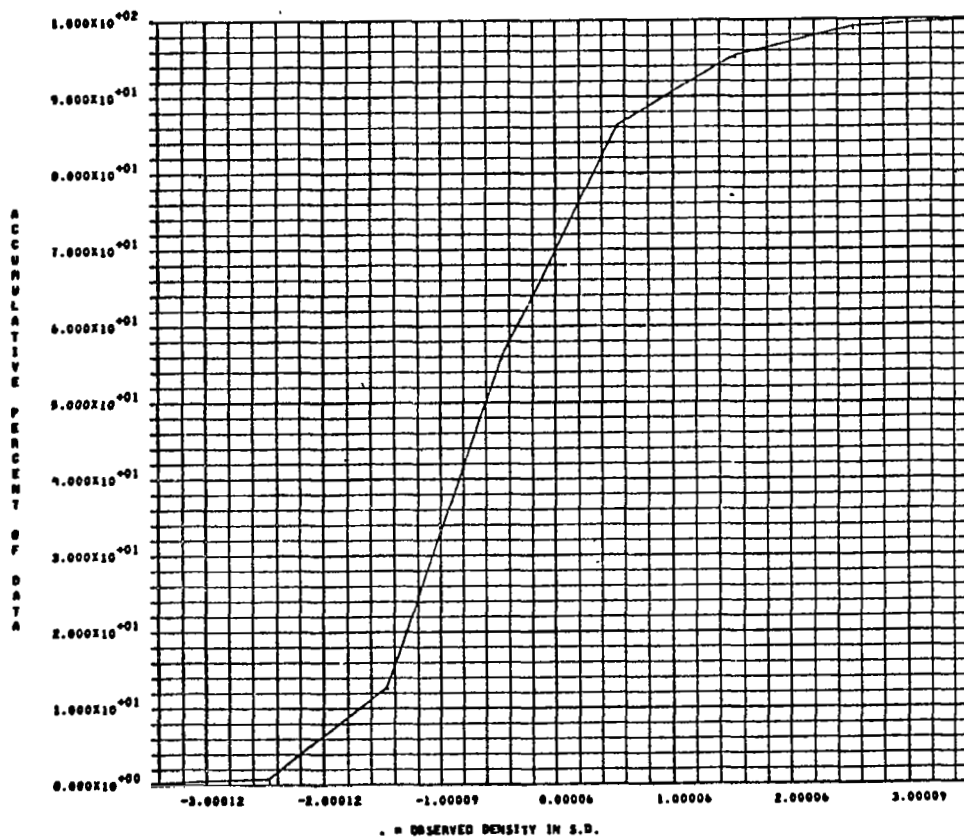


Figure 21. Typical plot of accumulative probability distribution.

The autocorrelation and power spectral density are also part of the computer laboratory output. A description of these parameters is as follows:

Autocorrelation

Given a sample voltage time history record $u(t)$ from a stationary random signal, the autocorrelation function $B(\tau)$ of the signal is defined as

$$B(\tau) = \frac{1}{T} \int_0^T u(t) u(t + \tau) dt$$

With digitized data rather than a continuous record $B(\tau)$ is approximated with

$$\begin{aligned} B(\tau) &= \frac{1}{N} \sum_{k=1}^N u'''(k\Delta t) u'''(k\Delta t - \tau) \\ &= \frac{1}{N} \sum_{k=1}^N u'''_k u'''_{k-m} \end{aligned}$$

where

$$m = \frac{\tau}{\Delta t}$$

$\Delta t \sim$ is the digitized interval (1/2 sec in this case).

In words, the autocorrelation function is estimated by the following operations:

1. The signal is delayed by a time displacement equal to τ seconds called the lag time.

2. The signal value at any instant is multiplied by the value that had occurred τ seconds before.
3. The instantaneous product values are averaged over the sampling time.

In the sample experimental data shown here the maximum overlap is 10 percent. For 6000 data points the run time is 3000 sec and the maximum delaying of the signal is therefore $\tau_{\max} = 300$ sec. The lag time τ is taken in 1 sec increments, hence the calculations proceed as indicated below and give 300 values of $B(\tau)$ for the corresponding 300 values of τ .

$$B(0) = \frac{1}{N} \sum_{k=1}^N u_k^2 \quad \text{at } \tau = 0$$

$N_{\max} = 6000$ points

$$B(1) = \frac{1}{N} \sum_{k=1}^N u_k u_{k-2}$$

at $\tau = 1$ sec
 $m = \frac{1}{1/2} = 2$
 $N = 5998$ points

$$B(300) = \frac{1}{N} \sum_{k=1}^N u_k u_{k-600}$$

at $\tau_{\max} = 300$ sec
 $N = 5400$ points

A plot of $B(\tau)$ versus τ which is a typical autocorrelation of the data taken in this investigation is shown in Figure 22.

Power Spectral Density Function

For stationary random data, spectral density function can be calculated as follows:

DATE 03/03/75		SEQ NO = 1030		2	
TEST	0515	POWER=1		FILTER B.W.	6.66E-03 HZ
LINK/CHAN	9.071E+04	TO 5.107E+04		SAMPLE RATE	2.000 /SEC.
SLICE TIME	CHAN 1			SE-COMP-RAP	453-2733
MEAS. NO.				COMP. RMS	1.168

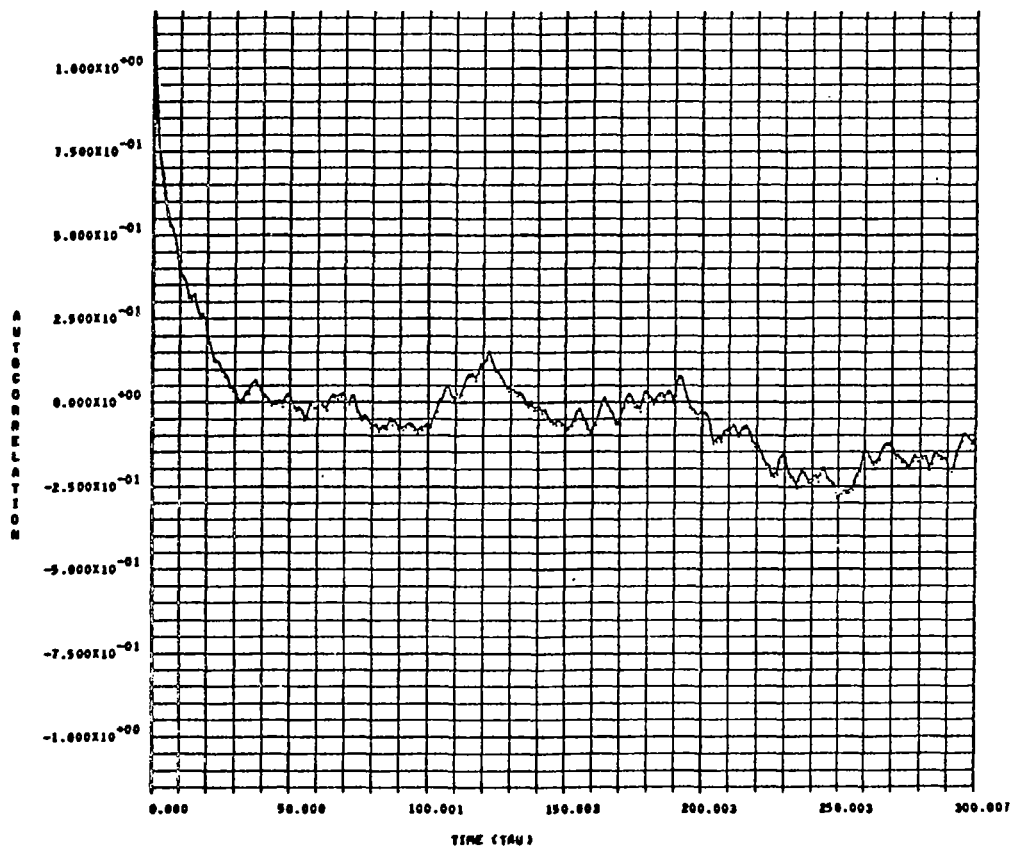


Figure 22. Typical autocorrelation $B(\tau)$.

By definition

$$B(\tau) = \int_0^{\infty} f_1(\omega) \cos \omega \tau d\omega$$

$$f_1(\omega) = \frac{2}{\pi} \int_0^{\infty} B(\tau) \cos \omega \tau d\tau \quad (1)$$

where $f_1(\omega)$ is the power spectral density function. The power spectral density function uses the 300 values of $B(\tau)$ and numerically integrates Equation 1. Selecting a frequency as often as you pick a lag time, the power spectral density $f_1(\omega)$ is numerically approximated by

$$f_1(\omega) = \frac{2}{\pi} \sum_{n=1}^{n=(300-1)} B[(n-1)\Delta\tau] \cos \omega[(n-1)\Delta\tau] \Delta\tau$$

The values of $f_1(\omega)$ for given frequencies then become

$$f_1(0 \text{ rad/sec}) = \frac{2}{\pi} \sum_{n=1}^{300-1} B[(n-1)\Delta\tau] \Delta\tau$$

$$f_1\left(\frac{1}{k} \text{ rad/sec}\right) = \frac{2}{\pi} \sum_{n=1}^{300-1} B[(n-1)\Delta\tau] \cos \frac{1}{k}[(n-1)\Delta\tau] \Delta\tau$$

$$f_1(1 \text{ rad/sec}) = \frac{2}{\pi} \sum_{n=1}^{300-1} B[(n-1)\Delta\tau] \cos[(n-1)\Delta\tau] \Delta\tau$$

Figure 23 is a typical plot of the power spectral density multiplied by frequency (i.e., $\omega f(\omega)$ versus frequency).

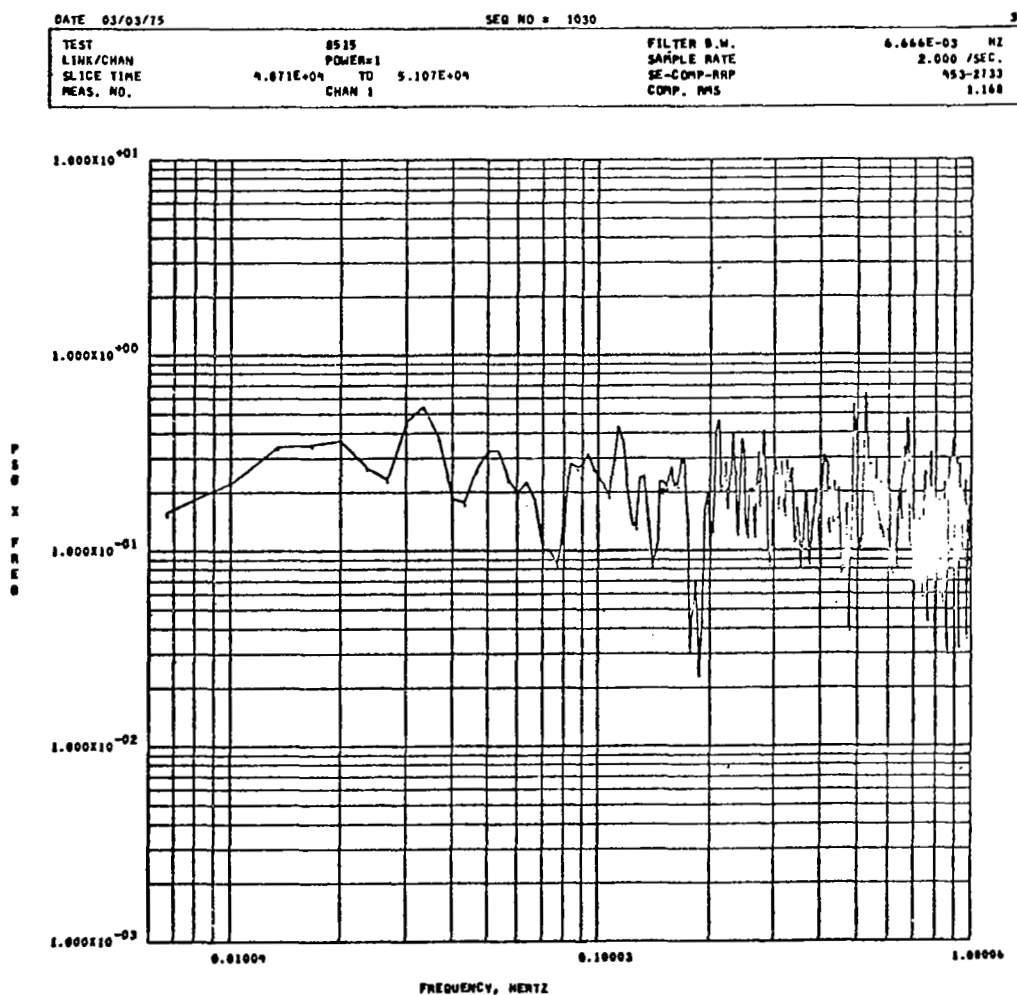


Figure 23. Typical power spectral density.

CHAPTER V

RUNS DOCUMENTATION

The data has been tabulated in a number of ways to facilitate location and cross referencing. Table V lists the run numbers according to the direction of the wind. The value of the wind angles given are the values averaged over the four levels of tower number 6. The data is tabulated in 30 degree increments. The majority of the runs were recorded for a 180-210 degree wind. For a number of runs all direction recorded where 360 degrees which are probably bad data, and hence are listed separately.

Table VI is a complete listing of all data collected to the date of this report. The symbol (C) denotes that a complete set of data is available for the runs, the symbol (P) denotes only partial data is available for the run and the symbol (-) denotes no data for the run. A complete set of data consists of mean values for all three components \bar{u} , \bar{v} , \bar{w} and turbulence data including the instantaneous values of u'' , v'' , w'' , the autocorrelations, the spectrum, the distribution, the rms values, etc. for all three components.

Table VII presents the computer printout of horizontal, direction, and vertical mean wind speeds and Table VIII gives the root mean square values of u' , v' , and w' of selected data. Table VII represents the three mean wind

TABLE VI
RUN NUMBERS FOR WHICH DATA IS AVAILABLE

Test No.	Mean Data	Turbulence Data	Test No.	Mean Data	Turbulence Data	Test No.	Mean Data	Turbulence Data
8001	C*	-**	8035	C	C	8404	C	C
8002	C	-	8036	C	C	8405	C	C
8003	C	C	8037	C	C	8406	C	C
8004	C	C	8038	C	-	8407	C	C
8005	C	C	8039	C	-	8408	C	C
8006	C	C	8040	-	C	8409	C	C
8007	C	C	8041	C	C	8504	-	C
8008	C	C	8042	C	C	8502	-	C
8009	C	-	8043	C	C	8503	-	C
8010	C	-	8044	C	C	8504	C	C
8011	C	-	8045	C	C	8505	C	C
8012	C	C	8046	C	-	8506	C	C
8013	C	C	8047	C	C	8507	C	C
8014	C	C	8048	C	-	8508	C	C
8015	C	C	8049	C	-	8509	C	C
8016	C	C	8050	C	-	8510	C	C
8017	C	C	8051	C	C	8511	C	C
8018	C	-	8052	C	C	8512	C	P
8019	C	-	8053	C	-	8513	C	C
8020	C	C	8054	-	C	8514	C	C
8021	C	C	8055	-	C	8515	C	C
8022	-	C				8516	C	C
8023	C	-	Small Building			8517	C	C
8024	C	C	8061	-	C	8518	C	C
8025	C	C	8065	-	P***	8519	C	C
8026	C	C	8076	C	C	8520	C	C
8027	C	C	8077	C	C	8521	C	C
8028	C	-	8078	C	C	8522	C	C
8029	C	-	8079	C	C	8523	C	C
8030	C	-				8524	C	-
8031	C	C	Large Building			8531	C	-
8032	C	C	8401	C	P	8541	C	-
8033	C	C	8402	C	C	8541	C	-
8034	C	C	8403	C	-	8542	C	-

*C = complete set of data

** - = no data

***P = partial data

TABLE VII
COMPUTER PRINTOUT OF HORIZONTAL, DIRECTION AND
VERTICAL MEAN SPEEDS

TOWER NO. 1												DATA SET
HORIZONTAL WIND SPEED				WIND DIRECTION				VERTICAL WIND SPEED				
1	2	3	4	1	2	3	4	1	2	3	4	
3.311	3.964	4.735	5.411	136.78	161.20	153.05	154.90	.157	.109	-.045	-.200	8001
4.305	5.575	9.516	6.359	65.58	91.26	92.56	90.10	.129	.097	-.070	-.159	8002
4.438	5.802	6.530	7.269	223.88	256.25	244.06	239.27	.256	.231	.436	.518	8003
4.502	5.044	5.608	6.072	232.90	264.38	253.64	249.51	.237	.231	.407	.592	8004
4.801	5.329	6.041	6.666	224.14	259.80	245.96	241.28	.257	.246	.448	.574	8005
5.720	6.327	7.375	8.300	211.47	242.33	232.69	229.16	-.443	-.544	-.544	-.544	8011
3.392	3.431	3.934	4.377	174.54	206.26	194.94	192.22	.332	.388	.142	.097	8013
4.856	5.423	6.251	6.572	58.32	85.29	84.66	85.16	.180	-.017	-.180	-.347	8014
5.857	6.526	7.445	7.792	51.94	77.06	78.45	76.61	.239	.068	-.108	-.197	8015
3.712	3.730	4.365	4.830	152.00	179.10	173.65	170.80	.665	.251	.208	-.136	8019
4.498	4.920	5.757	6.532	143.28	177.50	67.65	166.89	.351	.119	.054	-.080	8023
4.134	4.568	5.294	5.654	110.87	141.15	137.72	136.16	.344	.090	-.013	-.201	8024
5.151	5.050	6.722	7.944	208.45	246.61	234.24	231.84	.359	.272	.677	.361	8028
5.770	5.574	6.167	6.450	23.69	41.62	47.30	47.80	.338	.169	.070	.023	8034
5.279	5.073	5.631	5.938	40.25	57.36	63.25	62.68	.325	.119	-.060	-.094	8035
4.732	5.345	6.110	6.609	133.83	157.13	153.15	151.69	.429	.184	.146	-.090	8042
3.043	4.112	4.234	4.827	177.17	196.06	199.86	198.07	.388	.140	.135	.002	8044
2.963	8.065	4.028	4.243	234.07	251.83	253.71	251.94	.309	.188	.208	.303	8046
6.097	5.197	8.125	8.681	324.60	340.42	345.34	343.90	.381	.229	.390	.567	8047
4.890	5.214	6.331	6.678	321.13	341.19	342.62	341.66	.361	.236	.314	.602	8048
4.034	4.736	6.441	5.415	303.29	343.54	340.50	339.91	.348	.220	.272	.524	8049
4.941	5.091	7.124	7.254	330.50	357.73	353.50	353.70	.406	.357	.409	.765	8051
4.250	4.475	6.321	6.215	330.47	359.87	1.73	4.81	.375	.288	.256	.564	8052
4.746	5.475	6.408	7.497	231.26	257.00	251.32	246.57	.293	.262	.293	.449	8054
4.244	4.918	6.250	7.995	222.09	252.75	242.06	236.87	.307	.283	.344	.486	8055
3.136	3.950	4.539	4.965	197.01	268.46	223.40	244.64	.230	.124	.087	.205	8056
2.936	3.599	4.463	5.565	202.35	243.39	233.82	228.49	.271	.212	.186	.268	8057

TOWER NO. 2												DATA SET
HORIZONTAL WIND SPEED				WIND DIRECTION				VERTICAL WIND SPEED				
1	2	3	4	1	2	3	4	1	2	3	4	
3.813	4.614	5.571	5.955	161.41	149.11	140.91	155.59	.090	.086	.214	.211	8001
4.509	5.018	5.884	6.390	95.49	77.43	78.51	89.98	.308	.026	.169	.068	8002
5.288	5.790	6.582	7.215	248.75	230.77	232.06	227.59	.113	-.172	.441	.420	8003
4.575	5.005	5.593	6.102	259.33	242.63	241.32	237.07	.128	.192	.396	.428	8004
4.884	5.263	5.997	6.744	248.60	231.56	233.50	226.84	.148	-.115	.469	.425	8005
5.290	6.165	7.281	8.231	229.43	219.72	221.04	223.78	.000	.000	.000	.000	8011
2.994	3.354	4.014	4.529	196.33	186.85	181.51	186.04	.043	-.091	.267	.197	8013
4.750	5.487	6.242	6.498	78.17	73.01	71.32	92.86	.058	-.082	-.017	-.194	8014
5.904	6.640	7.449	7.713	72.09	64.60	60.04	74.20	.127	.039	.075	-.070	8015
3.344	3.708	4.292	4.767	173.44	162.63	162.56	170.85	.116	-.017	.576	.314	8019
4.413	4.967	5.784	6.523	170.42	156.96	156.22	169.61	.045	.060	.351	.265	8023
3.736	4.419	5.235	5.637	139.10	125.47	125.84	139.83	.066	.015	.250	.084	8024
4.834	5.515	6.585	6.577	222.96	219.52	222.19	191.09	.149	.207	.257	.025	8028
4.946	5.612	6.009	6.368	35.97	32.65	29.05	43.37	.115	-.170	.110	-.126	8034
4.509	5.058	5.537	5.887	51.24	49.25	44.92	54.41	.110	-.154	.032	-.186	8035
4.605	5.363	6.119	6.620	147.86	142.75	137.83	146.49	.124	.135	.405	.246	8042
3.022	3.226	4.068	4.701	185.76	166.72	183.99	197.57	.035	-.109	.217	.124	8044
2.836	3.279	3.951	4.210	242.44	242.19	238.34	252.75	-.006	-.239	.253	.227	8046
5.406	7.135	8.035	8.655	325.47	320.50	329.55	349.04	.210	-.295	.397	.212	8047
4.347	5.543	6.289	6.724	324.01	329.42	326.70	334.73	.144	-.309	.305	.194	8048
3.748	4.463	5.158	5.453	327.27	327.23	327.87	329.76	.142	-.285	.533	.186	8049
4.743	5.552	6.736	7.565	340.09	341.24	342.00	346.86	.214	-.176	.483	.429	8051
3.680	4.824	5.973	6.724	348.66	349.26	350.89	353.14	.188	-.180	.366	.270	8052
4.361	5.327	6.385	7.496	238.53	238.41	235.35	247.02	-.007	-.221	.334	.332	8054
4.148	4.998	6.201	7.577	231.58	229.58	226.18	229.36	.022	-.157	.420	.443	8055
3.113	3.607	4.377	4.930	240.92	214.85	216.02	251.02	-.039	-.235	.147	.140	8056
2.969	3.431	4.635	5.511	224.27	218.67	217.53	216.05	.017	-.166	.247	.210	8057

TABLE VII (continued)

TOWER NO. 3												DATA SET
HORIZONTAL WIND SPEED				WIND DIRECTION				VERTICAL WIND SPEED				
1	2	3	4	1	2	3	4	1	2	3	4	
3.605	5.128	5.899	6.456	137.22	148.69	143.95	145.73	-.159	.168	.088	-.101	8001
5.027	5.699	6.478	6.924	79.07	79.59	81.11	84.45	.167	-.003	.105	.084	8002
5.372	5.989	6.631	7.270	230.91	229.58	232.53	230.31	.182	.339	.322	.055	8003
4.640	5.176	5.648	6.048	241.92	242.73	242.48	243.30	.185	.391	.583	.178	8004
4.963	5.504	6.055	6.677	233.23	231.29	233.05	232.80	.185	.385	.472	.071	8005
5.920	6.539	7.401	8.314	219.88	219.13	222.30	226.39	.000	.000	.000	.000	8011
3.335	3.465	3.953	4.371	188.68	187.37	177.07	188.40	.157	.209	.052	.172	8013
6.287	5.765	6.411	6.844	76.17	76.00	76.72	94.86	.159	-.022	-.143	.184	8014
6.768	6.875	7.444	8.069	67.40	70.66	68.88	87.81	.233	.097	-.049	.329	8015
4.666	3.848	4.333	4.841	164.88	168.27	170.03	171.37	.349	.425	.549	-.280	8019
5.131	5.084	5.814	6.554	159.68	163.41	165.45	165.14	.183	.229	.360	.022	8023
4.474	4.495	5.241	5.621	128.87	132.25	136.31	131.60	.122	.110	.224	-.052	8024
5.149	5.820	6.692	7.993	223.91	226.31	225.85	236.71	.033	.305	.527	.274	8028
4.874	5.656	6.071	6.367	36.17	38.61	54.48	39.23	.210	.107	.351	-.077	8034
4.350	6.610	7.226	7.492	52.80	54.64	77.25	53.67	.237	.097	.299	-.091	8035
4.637	5.292	6.053	6.609	145.52	147.99	165.97	143.35	.221	.223	.329	-.025	8042
3.147	3.381	3.957	4.674	187.67	192.63	212.43	190.35	.156	.154	.256	-.205	8044
3.147	3.386	3.856	4.248	244.29	247.04	266.13	241.31	.175	.230	.432	-.049	8046
5.776	5.695	7.213	8.303	336.13	338.61	355.20	336.60	.132	.269	.748	.264	8047
4.928	5.228	6.164	6.605	332.50	335.58	356.93	332.42	.180	.209	.633	.137	8048
3.950	4.274	5.190	5.339	329.35	335.18	322.83	338.59	.223	.229	.639	.135	8049
5.421	5.886	6.655	7.529	346.54	349.08	340.70	356.83	.123	.253	.817	.398	8051
4.884	5.538	5.939	6.654	353.97	356.16	353.78	357.94	.192	.180	.672	.272	8052
4.782	5.440	6.411	7.533	241.07	243.85	261.89	238.19	.144	.289	.511	-.041	8054
4.496	5.256	6.277	7.634	232.74	234.89	252.85	224.20	.109	.228	.456	-.039	8055
3.516	3.647	4.684	4.995	217.24	241.45	217.11	241.01	.095	.123	.260	-.190	8056
3.192	3.622	8.801	5.590	224.80	226.19	223.36	225.28	.133	.147	.239	-.186	8057

HORIZONTAL WIND SPEED				WIND DIRECTION				VERTICAL WIND SPEED				DATA SET
1	2	3	4	1	2	3	4	1	2	3	4	
4.685	5.070	5.833	6.474	147.69	154.86	150.84	153.69	.315	.200	.326	.085	8001
4.887	5.445	6.203	6.698	75.65	82.69	85.86	87.30	.130	.166	.079	.212	8002
4.655	5.124	5.854	6.340	266.30	272.90	267.36	268.75	.438	.249	.676	.321	8003
4.766	5.150	5.694	6.132	246.14	246.08	253.57	253.92	.444	.308	.705	.455	8004
5.342	5.521	6.314	6.906	360.00	360.00	360.00	360.00	.428	.292	.754	.505	8005
6.127	6.739	7.582	8.358	223.92	236.18	230.74	227.98	.000	.000	.000	.000	8011
3.255	3.514	3.929	4.586	190.10	200.10	193.56	191.66	.346	.233	.563	.283	8013
5.075	5.593	6.229	6.534	68.54	81.52	81.50	82.46	.118	.199	.106	.114	8014
6.248	6.848	7.527	7.948	66.71	74.65	79.31	76.42	-.341	.114	.024	.095	8015
3.592	3.851	4.341	5.969	163.63	176.87	172.99	172.64	.298	.182	.426	.163	8019
4.660	5.062	5.827	6.598	153.96	168.72	164.14	165.31	.362	.298	.558	.213	8023
3.871	4.362	5.195	5.649	122.55	136.55	136.42	136.50	.214	.167	.318	.108	8024
5.267	5.926	6.870	8.124	221.85	238.94	232.41	358.07	.389	.185	.358	.528	8028
5.098	5.709	6.101	6.437	31.17	43.54	43.09	50.59	.071	.136	-.002	.137	8034
4.563	5.071	5.470	5.924	54.27	61.75	63.27	69.11	.094	.149	.068	.147	8035
1.626	2.323	3.018	4.123	217.16	215.17	212.67	208.68	.302	.195	.469	.161	8042
3.201	3.528	4.025	4.792	190.01	196.04	197.81	202.45	.353	.244	.500	.111	8044
3.160	3.650	3.860	5.449	243.55	248.92	249.67	244.26	.350	.258	.489	.224	8046
5.991	6.697	7.665	8.461	332.18	340.02	340.29	344.12	.328	.282	.305	.611	8047
5.117	5.570	6.259	6.622	331.61	330.65	339.57	344.92	.284	.196	.308	.499	8048
4.081	4.500	5.233	5.439	315.30	341.98	341.48	343.29	.286	.203	.310	.441	8049
5.333	5.657	6.816	7.374	330.50	353.52	352.28	356.62	.319	.387	.386	.727	8051
4.849	5.287	6.204	6.476	339.62	1.05	359.94	5.73	.257	.297	.283	.604	8052
4.849	5.535	6.532	7.462	240.13	246.13	247.22	248.93	.407	.277	.577	.303	8054
4.836	5.570	6.644	7.796	236.30	240.26	240.59	241.16	.595	.269	.581	.293	8055
3.333	3.742	4.457	5.092	218.57	239.44	236.96	238.27	.303	.195	.394	.125	8056
3.322	3.794	5.070	5.610	215.60	234.64	232.05	234.19	.328	.217	.486	.215	8057

TABLE VII (continued)

TOWER NO. 5					WIND DIRECTION				VERTICAL WIND SPEED				DATA SET
HORIZONTAL WIND SPEED					1	2	3	4	1	2	3	4	
1	2	3	4		1	2	3	4	1	2	3	4	
5.416	4.996	5.782	6.420		154.14	155.14	147.29	153.18	.460	.241	.414	-.163	8001
5.515	5.896	5.819	7.045		84.04	79.01	84.95	79.57	.387	.108	.493	.221	8002
4.530	5.495	6.117	6.500		250.22	259.18	260.60	258.33	.179	.194	.331	.007	8003
4.886	5.268	5.796	4.670		254.20	242.98	246.54	243.23	.168	.235	.244	.064	8004
5.331	5.345	6.476	6.300		360.00	360.00	360.00	360.00	.226	.292	.307	.118	8005
6.382	7.029	7.747	8.924		222.35	220.74	225.12	219.60	.000	.000	.000	.000	8011
3.433	3.658	4.188	4.807		191.79	187.54	187.23	180.14	.278	.195	.403	.077	8013
5.174	5.675	6.150	6.791		78.87	78.88	77.66	74.73	.274	.102	.443	.263	8014
6.471	7.089	7.661	8.199		69.24	71.10	69.21	71.36	.324	.151	.443	.469	8015
3.604	3.860	4.451	4.766		170.58	164.97	169.53	163.31	.292	.140	.416	.077	8019
4.786	5.312	6.041	6.799		159.05	155.49	159.73	154.25	.468	.258	.523	.103	8023
4.107	4.601	5.324	5.705		127.75	126.32	132.00	127.26	.363	.157	.458	.058	8024
5.550	6.447	7.291	8.240		206.97	222.84	228.27	360.00	.027	-.108	.437	.435	8028
5.081	5.642	6.147	6.520		37.71	36.85	41.07	36.33	.028	.032	.279	.201	8034
4.560	5.067	5.615	5.872		54.85	56.33	60.21	55.75	.146	.063	.390	.235	8035
2.770	3.227	4.319	3.893		206.73	199.66	197.15	198.85	.471	.208	.501	.060	8042
3.468	3.877	5.180	4.922		195.85	190.64	193.12	187.91	.231	.175	.304	-.092	8044
3.620	3.675	4.776	4.521		245.92	239.59	243.04	238.28	.053	.123	.169	-.076	8046
5.863	6.067	7.471	8.426		335.79	329.65	335.20	332.70	-.170	.139	.299	.430	8047
5.026	5.226	6.655	6.602		331.69	329.78	334.90	331.79	-.128	.115	.356	.463	8048
4.071	4.258	5.280	5.412		334.46	326.81	334.31	332.20	-.081	.107	.362	.264	8049
5.595	5.861	6.982	7.643		346.95	341.22	348.15	344.01	-.156	.150	.346	.506	8051
5.034	5.429	6.286	6.700		354.79	349.10	356.08	353.22	-.116	.147	.423	.555	8052
4.893	5.872	6.665	7.594		242.63	237.19	242.07	237.56	.101	.163	.164	.053	8054
5.303	6.228	7.077	7.917		235.50	232.46	235.77	231.09	.132	.165	.112	-.047	8055
3.342	4.162	4.587	5.017		231.19	226.60	231.25	224.94	.166	.192	.257	-.033	8056
3.605	4.356	5.249	5.701		224.07	220.43	226.19	220.68	.155	.142	.207	-.098	8057

TOWER NO. 6					WIND DIRECTION				VERTICAL WIND SPEED				DATA SET
HORIZONTAL WIND SPEED					1	2	3	4	1	2	3	4	
1	2	3	4		1	2	3	4	1	2	3	4	
2.847	5.323	6.034	8.927		87.17	151.95	153.87	150.56	.172	.187	.414	.163	8001
5.541	6.031	6.166	6.715		85.45	78.10	83.07	81.76	.316	.169	.264	.282	8002
4.966	5.944	6.493	9.230		267.10	208.65	213.42	207.43	.137	.426	.295	.149	8003
4.684	5.323	5.129	6.090		250.51	240.37	247.11	243.14	.149	.240	.317	.177	8004
5.206	5.699	5.773	6.632		360.00	360.00	360.00	360.00	.189	.331	.412	.384	8005
6.677	7.313	7.826	8.351		227.65	219.01	224.28	223.85	.000	.000	.000	.000	8011
3.664	3.948	4.229	4.650		189.71	181.92	193.69	188.36	.126	.149	.004	.344	8013
5.192	5.569	5.953	6.288		79.76	74.51	76.59	94.17	.284	.107	.130	.435	8014
6.290	6.857	7.356	7.600		74.84	69.89	71.39	85.48	.353	.158	.260	.043	8015
3.718	3.578	4.388	4.788		169.41	166.66	171.93	166.47	.138	.179	.489	.069	8019
5.351	5.860	6.556	6.939		165.24	162.44	169.14	165.30	.162	.167	.330	.043	8023
4.364	4.786	5.242	5.572		136.99	132.40	141.73	131.35	.155	.073	.332	.136	8024
5.893	6.572	7.240	7.950		227.07	232.14	225.75	231.91	.112	.181	.296	-.088	8028
4.879	5.468	5.960	6.394		45.94	47.68	59.86	37.66	.285	.141	.554	.186	8034
4.639	5.077	5.470	5.812		64.70	67.25	81.67	53.27	.266	.094	.436	.125	8035
2.570	3.820	3.155	2.199		211.73	205.27	228.88	208.17	.190	.226	.388	.095	8042
3.841	4.285	4.623	5.107		195.93	196.81	214.72	186.39	.092	.165	.386	.102	8044
3.521	3.917	3.986	5.363		245.20	239.49	264.07	233.82	.102	.205	.310	.053	8046
5.381	5.928	7.141	7.953		338.06	341.12	355.42	332.26	.392	.359	.613	.047	8047
4.803	5.068	5.865	6.626		340.06	342.94	352.78	330.96	.352	.295	.622	.275	8048
4.145	4.290	4.923	5.510		336.97	341.40	328.13	336.23	.300	.226	.560	.352	8049
5.434	5.577	6.340	7.798		351.36	354.33	339.82	349.69	.381	.290	.487	.194	8051
5.097	5.185	5.378	7.062		360.00	1.71	352.91	356.10	.344	.269	.474	.474	8052
5.116	5.712	6.582	7.343		245.39	241.26	263.29	236.54	.108	.292	.393	.174	8054
5.214	5.838	6.783	7.627		238.66	239.09	255.62	225.23	.105	.259	.345	.120	8055
3.682	3.919	4.475	5.079		234.96	238.47	232.45	228.77	.105	.191	.305	.136	8056
3.957	4.503	5.199	5.900		227.16	232.78	223.11	221.77	.113	.251	.337	.192	8057

TABLE VII (continued)

TOWER NO. 1				WIND DIRECTION				VERTICAL WIND SPEED				DATA SET
HORIZONTAL WIND SPEED												
1	2	3	4	1	2	3	4	1	2	3	4	
5.335	5.923	7.016	7.573	67.36	77.88	80.08	71.25	-.408	-.692	-.797	.045	8401
.226	2.668	2.902	3.099	244.27	256.00	249.56	247.94	.122	.403	.136	.569	8404
4.341	5.013	5.915	.231	189.30	199.40	203.64	197.32	.303	.033	-.222	-.586	8405
3.079	4.499	5.345	.231	186.37	195.34	196.72	189.96	-.009	-.297	.024	-.104	8406
3.084	3.995	4.512	5.210	169.55	182.14	185.25	178.41	-.259	-.185	.338	.699	8407
3.063	3.621	4.353	4.921	176.95	188.34	184.62	175.28	-.617	-.065	.490	.789	8408
1.789	2.560	4.192	4.531	.70	2.49	8.66	3.64	.241	-.096	.098	-.128	8409
TOWER NO. 2				WIND DIRECTION				VERTICAL WIND SPEED				DATA SET
HORIZONTAL WIND SPEED												
1	2	3	4	1	2	3	4	1	2	3	4	
5.643	6.421	7.033	7.445	66.86	63.56	162.31	85.10	-.884	.282	-.645	2.760	8401
2.418	2.646	2.922	3.209	257.69	249.55	236.54	257.44	1.099	.470	.094	.320	8404
3.518	4.894	6.023	7.173	208.59	199.84	284.33	201.60	-.476	-.016	.729	-.506	8405
3.074	4.411	5.456	6.488	201.57	196.59	282.49	196.76	.599	.093	.474	-.029	8406
2.637	3.695	4.608	5.341	182.85	179.21	174.76	182.35	.716	-.049	-.556	-.010	8407
2.622	3.696	4.539	5.357	175.20	180.07	181.47	193.59	.439	-.443	-.842	-.185	8408
.476	3.872	4.623	4.905	206.66	1.84	1.26	3.92	.316	.478	.559	2.092	8409
TOWER NO. 3				WIND DIRECTION				VERTICAL WIND SPEED				DATA SET
HORIZONTAL WIND SPEED												
1	2	3	4	1	2	3	4	1	2	3	4	
4.646	6.224	7.165	6.862	75.78	60.09	64.25	43.29	1.418	.458	.586	.450	8401
1.935	2.788	2.961	3.204	240.43	235.45	242.02	229.42	1.007	.309	5.442	.296	8404
.298	5.617	6.036	7.400	37.41	188.09	195.68	188.49	-.013	-.186	5.442	-.723	8405
.211	5.106	5.518	6.413	340.45	185.03	189.72	182.91	-.149	.074	5.442	.508	8406
.180	4.408	4.726	5.323	115.57	174.68	178.87	167.87	-.023	.247	.442	.528	8407
.056	4.371	4.695	5.350	145.73	172.55	174.53	163.12	.135	.210	-.442	.119	8408
1.804	3.471	4.437	5.100	353.97	353.37	359.33	354.93	1.364	1.028	.377	.089	8409
TOWER NO. 4				WIND DIRECTION				VERTICAL WIND SPEED				DATA SET
HORIZONTAL WIND SPEED												
1	2	3	4	1	2	3	4	1	2	3	4	
5.589	6.366	7.003	7.419	78.88	83.63	77.66	75.87	.284	.745	.647	.078	8401
.226	2.837	3.070	3.213	253.32	261.67	245.49	243.90	.141	.323	.512	.221	8404
2.156	4.390	6.070	7.101	212.00	206.33	197.43	192.25	.138	-.019	.139	-.647	8405
2.066	4.085	5.520	6.424	191.43	198.09	191.65	192.60	.155	-.061	-.264	-.382	8406
2.559	3.772	4.774	5.356	172.49	189.61	184.49	186.08	.349	-.068	-.187	-.629	8407
2.651	3.776	4.733	5.381	170.76	184.58	176.91	176.21	-.003	.906	.860	.647	8408
3.373	3.989	4.286	4.817	358.71	8.79	2.43	.47	-.336	-.044	.431	.390	8409
TOWER NO. 5				WIND DIRECTION				VERTICAL WIND SPEED				DATA SET
HORIZONTAL WIND SPEED												
1	2	3	4	1	2	3	4	1	2	3	4	
5.924	6.385	7.060	7.560	67.57	83.76	81.08	251.02	.609	.173	.551	1.187	8401
2.639	2.817	3.071	3.218	240.11	258.77	252.05	253.00	-.193	-.370	.077	.127	8404
4.755	5.287	6.146	6.657	190.22	208.57	202.76	197.00	-.497	-.010	-.752	-.442	8405
4.296	4.822	5.596	5.735	188.01	208.63	195.71	201.14	-.023	.434	.005	.048	8406
3.971	4.390	4.925	5.101	174.05	189.48	179.92	176.18	.076	.461	.184	.158	8407
3.065	4.280	4.878	5.058	168.43	189.61	183.57	173.89	.100	-.084	-.353	.117	8408
3.921	4.394	4.807	4.833	353.24	19.80	2.48	6.38	.552	-.079	-.133	-.160	8409
TOWER NO. 6				WIND DIRECTION				VERTICAL WIND SPEED				DATA SET
HORIZONTAL WIND SPEED												
1	2	3	4	1	2	3	4	1	2	3	4	
6.256	6.695	7.080	7.734	77.43	73.53	75.82	91.32	1.077	.473	.303	.356	8401
2.737	2.957	2.640	3.315	248.64	244.53	245.30	258.18	.109	.164	.014	-.156	8404
9.413	6.006	6.543	.232	199.04	196.41	198.39	212.62	-.129	-.074	-.442	-.178	8405
4.903	5.410	5.880	.231	192.42	191.82	195.96	213.55	-.031	-.302	-.282	.171	8406
3.770	4.527	4.070	4.850	4.40	3.39	2.77	14.14	.199	.343	.851	.341	8409

TABLE VII (continued)

TOWER NO. 1												
HORIZONTAL WIND SPEED				WIND DIRECTION				VERTICAL WIND SPEED				DATA SET
1	2	3	4	1	2	3	4	1	2	3	4	
4.108	4.923	6.027	6.726	176.38	184.34	187.17	175.01	-.010	.117	-.062	1.098	8504
3.890	4.851	5.884	6.148	142.76	153.90	162.53	158.36	.216	.054	-.154	-.124	8505
3.549	4.513	5.408	4.978	143.36	160.13	167.15	156.66	1.920	.004	-.035	4.809	8506
3.623	4.049	4.713	5.069	194.55	207.02	211.46	200.17	.324	-.104	-.309	-.128	8507
3.851	4.290	5.026	5.360	207.29	214.19	215.09	207.73	-.029	.269	-.190	.337	8508
3.244	3.690	4.339	4.521	192.94	207.66	211.18	203.50	.732	.091	-.379	-.352	8509
3.547	4.461	5.265	6.022	138.24	150.82	155.61	148.08	-.135	.063	.066	.300	8510
4.344	5.508	6.467	7.262	131.19	141.41	146.86	142.38	-.972	-.377	-.109	-.184	8511
3.434	4.129	5.143	6.228	162.95	168.40	167.87	162.38	1.830	.543	.429	-.354	8512
2.976	3.157	3.593	3.944	221.61	234.68	238.14	225.90	.876	.221	.392	.502	8513
3.165	3.722	4.673	5.603	329.72	344.58	356.31	342.71	-.050	.159	.835	.387	8514
2.680	2.924	3.357	3.099	360.00	120.68	127.86	122.37	5.411	.123	.317	.001	8515
3.435	4.182	5.432	5.880	338.84	356.20	2.34	357.84	.466	-.033	.394	.022	8516
3.273	4.344	6.627	7.666	344.12	354.00	359.92	351.37	-.155	-.311	.330	.371	8517

TOWER NO. 2												
HORIZONTAL WIND SPEED				WIND DIRECTION				VERTICAL WIND SPEED				DATA SET
1	2	3	4	1	2	3	4	1	2	3	4	
3.611	5.117	6.277	7.598	177.33	182.77	189.03	201.42	.770	.733	.280	2.552	8504
3.785	5.113	6.224	7.233	157.61	166.68	166.83	174.57	.743	.605	.177	.398	8505
3.626	4.827	5.742	6.636	153.00	162.84	164.87	179.40	.854	.749	.364	.248	8506
2.997	3.973	4.828	5.682	204.04	199.51	202.66	219.85	.852	.807	1.752	.331	8507
3.273	4.245	5.090	5.860	221.98	219.78	220.49	229.40	.567	.805	.634	.430	8508
2.781	3.659	4.479	5.197	216.66	210.95	209.70	219.32	.761	1.084	1.574	.507	8509
3.651	4.739	5.616	6.323	137.34	148.82	153.33	171.98	.439	.435	-.645	1.754	8510
4.520	5.749	6.808	7.576	140.73	152.13	150.25	161.19	.267	.899	1.582	-.092	8511
3.099	4.299	5.307	5.491	162.64	170.36	179.19	188.03	.016	.082	.488	.528	8512
2.602	3.150	3.667	4.170	229.44	224.56	229.58	1.39	.293	-.043	-.753	.117	8513
.225	3.566	4.847	5.206	282.49	353.42	353.90	5.90	.763	.985	.473	.447	8514
2.388	2.861	3.316	3.673	121.56	130.57	129.71	140.24	-.122	-.545	-.256	2.522	8515
.175	4.165	5.747	6.223	320.66	354.35	357.88	7.56	-.126	-.104	-.697	3.788	8516
.517	5.181	7.088	7.878	211.94	.48	4.17	11.20	.576	.597	-.238	.377	8517

TOWER NO. 3												
HORIZONTAL WIND SPEED				WIND DIRECTION				VERTICAL WIND SPEED				DATA SET
1	2	3	4	1	2	3	4	1	2	3	4	
.185	6.014	6.560	6.466	97.31	187.35	185.66	186.65	.600	.707	.267	.186	8504
1.543	5.946	6.515	6.276	116.65	168.43	167.75	166.70	1.453	.559	.087	.107	8505
1.903	5.469	6.047	4.983	126.45	171.49	168.27	167.98	1.397	.486	3.868	-.039	8506
.264	4.581	4.903	4.646	304.82	200.67	201.69	206.67	-.016	.478	1.444	.617	8507
1.135	4.875	5.176	4.886	575.46	205.07	211.11	211.64	1.006	.604	-.131	.335	8508
.999	4.299	4.557	3.477	272.31	203.58	207.70	231.96	.652	.542	.152	.456	8509
2.243	5.352	5.821	5.721	124.37	159.42	151.18	1.07	1.385	.390	2.951	-.177	8510
3.216	6.441	7.031	6.858	123.26	155.56	149.07	8.59	1.591	.085	.034	-.621	8511
.698	5.058	5.437	2.468	131.50	171.14	162.28	196.65	1.188	.717	-.109	-.386	8512
1.919	3.538	3.795	3.301	263.37	221.34	225.21	39.35	1.518	.668	.314	.013	8513
2.209	3.423	4.574	2.939	338.20	351.27	347.65	284.61	2.169	1.270	.689	1.187	8514
2.985	2.937	3.381	3.422	116.70	134.18	129.45	5.46	.366	.277	.088	-.711	8515
2.498	3.850	5.332	5.134	349.55	358.34	358.09	332.33	1.893	1.175	.467	.246	8516
2.830	4.589	6.222	6.430	348.91	356.28	354.41	339.68	1.848	1.493	1.023	1.106	8517

TABLE VII (continued)

TOWER NO. 4												DATA SET
HORIZONTAL WIND SPEED				WIND DIRECTION				VERTICAL WIND SPEED				
1	2	3	4	1	2	3	4	1	2	3	4	
3.810	4.933	6.581	7.640	164.21	168.75	176.13	176.58	-.128	-.237	.127	-.070	8504
4.460	5.320	6.497	7.351	150.34	162.88	156.89	161.36	.732	.320	.503	-.046	8505
4.466	5.497		6.929	152.94			156.30	.015	-.263	-.082	.122	8506
2.463	3.693	4.872	5.621	229.05	210.73	216.67	207.53	-.102	-.302	-.053	.037	8507
3.065	4.013	5.126	5.850	226.01	213.98	216.82	211.79	-.192	-.320	.224	.081	8508
2.784	3.572	4.604	5.223	222.64	215.19	212.47	206.09	-.640	-.091	.544	.479	8509
4.307	5.057	5.736	6.342	154.55	333.07	158.06	152.04	-.176	.396	.346	-.373	8510
5.105	6.083	6.924	7.624	151.76	327.08	148.33	145.64	-.343	.047	.586	.406	8511
3.572	4.425	5.491	6.499	155.41	162.23	172.46	173.09	-.771	-.747	-.238	.247	8512
3.091	3.342	3.819	4.114	233.19	56.97	220.22	234.83	.318	-.113	-.321	-.521	8513
3.377	3.655	4.650	5.503	352.05	185.27	355.28	347.29	.852	1.008	1.144	1.393	8514
2.331	2.967	3.336	3.585	127.45	305.46	130.90	129.12	.296	-.112	-.543	-.451	8515
3.609	4.403	5.294	6.431	348.61	181.03	354.15	354.81	.262	.089	-.331	.165	8516
4.629	6.047	6.638	7.944	357.38	191.76	2.09	.66	-.331	.123	.278	1.162	8517

TOWER NO. 5												DATA SET
HORIZONTAL WIND SPEED				WIND DIRECTION				VERTICAL WIND SPEED				
1	2	3	4	1	2	3	4	1	2	3	4	
5.441	6.048	6.605	7.776	175.73	184.06	182.54	166.68	.846	4.233	.558	-.115	8504
5.234	5.826	6.614	7.364	163.34	173.20	171.07	159.13	.238	4.961	.767	.461	8505
4.909	5.515	6.287	7.077	152.23	163.99	166.69	155.83	1.733	-.367	.627	-.238	8506
4.050	4.490	4.999	5.661	204.90	219.65	218.62	210.11	.207	-.424	.420	.060	8507
4.328	4.780	5.275	5.889	212.90	224.18	218.85	206.90	.356	4.902	.395	-.090	8508
3.776	4.186	4.698	5.220	211.72	223.36	218.16	202.97	.248	-.317	.003	-.339	8509
4.476	5.037	5.734	6.448	145.56	153.68	156.33	156.25	1.037	5.338	.316	-.056	8510
5.375	5.948	6.845	7.657	145.42	158.57	158.26	151.81	.510	-.680	.100	-.425	8511
4.526	5.087	5.745	6.640	169.65	173.81	173.68	165.88	.941	-.344	.208	-.598	8512
3.335	3.641	3.791	4.111	233.60	246.91	228.81	225.56	-.020	5.000	.547	.283	8513
4.106	4.099	4.901	5.512	340.81	351.97	354.97	356.04	.844	4.066	.955	1.292	8514
2.809	3.145	3.445	3.711	120.65	132.52	131.27	128.67	.362	5.114	.602	.206	8515
4.836	4.798	5.777	6.383	351.82	358.82	352.68	344.43	.197	5.377	.483	.709	8516
6.178	6.041	7.133	7.874	356.98	4.11	.15	358.84	.407	3.253	.024	.276	8517

TOWER NO. 6												DATA SET
HORIZONTAL WIND SPEED				WIND DIRECTION				VERTICAL WIND SPEED				
1	2	3	4	1	2	3	4	1	2	3	4	
6.003	6.663	7.386	8.023	178.69	177.55	187.74	175.62	-.034	.279	-.009	.093	8504
5.889	6.414	7.330	7.829	163.01	159.71	174.16	165.18	.344	.388	-.143	-.158	8505
5.208	5.831	6.534	7.144	161.35	155.74	165.10	154.34	-.057	.214	.355	.722	8506
4.512	4.921	5.425	5.789	213.48	210.80	217.50	206.77	-.123	-.041	-.48	.270	8507
4.592	5.063	5.574	5.991	217.24	216.24	222.99	213.72	-.146	.247	.143	.497	8508
4.262	4.678	5.119	5.328	212.13	209.05	220.75	211.75	.100	.382	.374	.019	8509
4.954	5.551	6.233	6.674	156.86	154.90	159.13	148.79	.234	.025	-.182	.498	8510
5.610	6.277	7.117	7.651	152.48	150.27	159.08	152.92	.343	.463	.560	-.158	8511
5.129	5.674	6.297	6.888	172.88	171.73	184.25	171.68	-.392	-.050	.283	.512	8512
3.243	3.510	3.806	4.035	227.99	230.78	239.57	232.04	-.275	-.324	-.394	.173	8513
4.139	4.157	5.048	5.493	352.93	352.08	350.55	346.70	1.023	.933	1.396	1.057	8514
2.860	3.103	3.360	3.528	130.65	129.34	139.18	126.06	-.129	-.351	-.249	.211	8515
4.759	4.866	5.909	6.399	351.69	354.16	358.54	355.98	.131	-.128	.220	.525	8516
6.112	6.525	7.433	7.476	1.22	.92	6.26	.67	.258	.403	1.185	.620	8517

TABLE VIII

COMPUTER PRINTOUT OF ROOT MEAN SQUARE OF u' , v' AND w'

TOWER NO. 1												
URMS				VRMS				WRMS				DATA SET
1	2	3	4	1	2	3	4	1	2	3	4	
0.926	0.987	1.063	1.099	1.227	1.250	1.303	1.330	1.360	1.649	1.659	1.689	8013
1.113	0.967	0.951	0.962	0.0	0.0	0.0	0.0	0.785	1.032	1.095	1.238	8019
1.048	1.117	1.159	1.178	1.219	1.276	1.268	1.295	0.0	0.0	0.0	0.0	8023
0.934	0.962	0.994	1.043	0.0	0.0	0.0	0.0	0.0	0.0	0.0	0.0	8044
TOWER NO. 2												
URMS				VRMS				WRMS				DATA SET
1	2	3	4	1	2	3	4	1	2	3	4	
0.973	1.001	0.992	1.072	1.192	1.220	1.303	1.336	1.631	1.656	1.650	1.713	8013
0.940	0.994	0.982	0.994	0.0	0.0	0.0	0.0	0.889	1.007	1.198	1.268	8019
1.096	1.134	1.154	1.177	1.226	1.227	1.273	1.285	0.0	0.0	0.0	0.0	8023
0.926	0.976	1.000	1.053	1.115	1.055	1.100	1.045	0.704	0.814	0.946	0.936	8044
TOWER NO. 3												
URMS				VRMS				WRMS				DATA SET
1	2	3	4	1	2	3	4	1	2	3	4	
1.002	1.010	0.995	1.072	1.219	1.241	1.309	1.349	1.581	1.639	1.722	1.700	8013
0.953	1.001	1.000	0.958	0.0	0.0	0.0	0.0	0.916	0.998	1.261	1.277	8019
0.956	1.126	1.140	1.156	1.270	1.232	1.205	1.315	0.0	0.0	0.0	0.0	8023
0.863	0.978	0.956	1.055	1.080	1.067	1.100	1.043	0.658	0.795	0.991	0.918	8044
TOWER NO. 4												
URMS				VRMS				WRMS				DATA SET
1	2	3	4	1	2	3	4	1	2	3	4	
1.011	1.068	1.054	0.988	1.210	1.246	1.309	1.364	1.498	1.628	1.574	1.718	8013
0.947	0.993	1.026	0.875	1.099	1.144	1.149	1.261	0.675	0.740	0.769	0.913	8019
1.043	1.094	1.128	1.128	1.197	1.245	1.257	1.308	0.0	0.0	0.0	0.0	8023
0.954	0.971	0.991	1.023	1.078	1.050	1.045	1.049	0.692	0.800	0.877	0.944	8044
TOWER NO. 5												
URMS				VRMS				WRMS				DATA SET
1	2	3	4	1	2	3	4	1	2	3	4	
0.994	1.005	1.014	1.133	1.214	1.235	1.314	1.385	1.485	1.649	1.642	1.710	8013
0.944	0.995	1.011	1.060	1.101	1.093	1.140	1.143	0.616	0.729	0.789	0.873	8019
1.038	1.078	1.140	1.121	1.214	1.237	1.300	1.313	0.0	0.0	0.0	0.0	8023
0.914	0.965	0.851	1.006	1.111	1.067	1.189	1.040	0.621	0.735	0.849	0.888	8044
TOWER NO. 6												
URMS				VRMS				WRMS				DATA SET
1	2	3	4	1	2	3	4	1	2	3	4	
1.010	1.047	1.104	1.091	1.270	1.311	1.356	1.273	1.558	1.633	1.657	1.660	8013
0.921	0.966	1.019	0.977	1.146	1.123	1.101	1.188	0.599	0.716	0.633	0.473	8019
1.053	1.109	1.144	1.116	1.243	1.272	1.250	1.346	0.0	0.0	0.0	0.0	8023
0.921	0.937	0.986	0.981	1.064	1.086	1.063	1.040	0.569	0.767	0.720	0.473	8044
TOWER NO. 7												
URMS				VRMS				WRMS				DATA SET
1	2	3	4	1	2	3	4	1	2	3	4	
1.081	1.115	1.109	0.164	1.210	1.233	1.220	0.265	1.492	1.156	1.359	1.695	8013
0.949	0.975	0.995	0.894	1.072	1.120	1.116	1.163	0.527	0.628	0.729	0.032	8019
1.069	1.111	1.141	1.148	1.184	1.237	1.202	1.205	0.0	0.0	0.0	0.0	8023
0.959	0.968	0.750	1.000	0.926	0.940	1.063	0.952	0.544	0.625	0.748	0.739	8044
TOWER NO. 8												
URMS				VRMS				WRMS				DATA SET
1	2	3	4	1	2	3	4	1	2	3	4	
1.129	1.154	1.515	1.111	1.202	1.202	1.591	1.181	1.524	1.576	1.656	1.557	8013
0.984	1.002	0.925	0.992	0.997	1.044	1.159	1.043	0.545	0.639	0.717	0.637	8019
1.101	1.140	1.048	1.139	1.140	1.151	1.181	1.138	0.0	0.0	0.0	0.0	8023
0.954	1.043	1.251	1.046	1.055	0.969	1.663	0.936	0.522	0.604	0.620	0.812	8044

TABLE VIII (continued)

TOWER NO. 1					TOWER NO. 2					TOWER NO. 3					TOWER NO. 4														
URMS					VRMS					WRMS					URMS					VRMS					WRMS				
1	2	3	4		1	2	3	4		1	2	3	4		1	2	3	4		1	2	3	4		1	2	3	4	
1.123	1.189	1.224	1.395		1.207	1.266	1.280	1.211		0.883	0.847	0.927	1.001		1.431	1.269	1.209	1.316		1.259	1.218	1.344	1.136		0.871	0.785	0.990	0.996	
1.103	1.155	1.243	1.360		1.181	1.194	1.214	1.158		0.967	0.919	0.978	1.080		1.313	1.251	1.223	1.271		1.163	1.179	1.154	1.138		1.070	0.787	0.910	0.920	
1.086	1.193	1.215	1.326		1.129	1.160	1.167	1.113		0.979	0.852	0.909	0.937		1.224	1.191	1.158	1.212		1.076	1.261	1.178	1.181		0.961	0.762	0.967	0.959	
1.032	1.102	1.127	1.338		1.073	1.112	1.161	1.110		1.145	0.708	0.826	1.389		1.097	1.104	1.186	1.129		1.045	0.032	1.249	1.083		0.909	0.692	0.828	0.868	
0.944	1.006	1.076	1.170		0.989	1.025	1.055	1.081		0.851	0.554	0.812	0.902		1.219	1.118	1.053	1.103		1.050	1.136	1.065	1.113		0.905	0.741	0.815	0.933	
0.990	1.025	1.087	1.180		1.064	1.091	1.155	1.104		0.946	0.666	0.767	0.960		1.281	1.174	1.091	1.158		0.979	1.192	1.115	1.105		0.916	0.703	0.741	0.795	
0.883	0.932	0.988	1.164		1.009	1.035	1.050	1.050		0.930	0.663	0.779	0.847		1.171	1.095	0.993	1.031		1.011	1.190	1.101	1.100		0.920	0.695	0.756	0.813	
1.059	1.149	1.200	1.261		0.964	0.992	1.013	1.060		0.872	0.744	0.789	0.860		1.118	1.160	1.204	1.249		0.962	0.931	0.978	0.987		0.908	0.750	0.800	0.936	
1.058	1.128	1.140	1.149		0.950	0.962	0.992	1.024		0.907	0.733	0.894	1.087		1.068	1.116	1.109	1.092		1.007	0.973	1.034	1.012		0.840	0.701	0.844	0.868	
1.032	1.099	1.167	1.270		1.062	1.056	1.047	1.245		0.0	0.0	0.0	0.0		1.200	1.163	1.162	1.219		0.986	1.061	1.074	1.079		0.0	0.0	0.0	0.0	

TABLE VIII (continued)

TOWER NO. 5												
URMS				VRMS				WRMS				DATA SET
1	2	3	4	1	2	3	4	1	2	3	4	
1.204	1.237	1.293	1.298	1.219	1.298	1.322	1.182	0.819	0.695	0.825	0.906	8501
1.139	1.165	1.192	1.228	1.124	1.154	1.192	1.179	0.739	1.565	0.883	1.023	8504
1.160	1.208	1.241	1.246	1.107	1.137	1.146	1.167	0.884	1.081	0.790	0.955	8505
1.052	1.109	1.126	1.120	1.039	1.089	1.097	1.083	0.819	0.742	0.809	0.898	8506
0.974	1.001	1.044	1.064	1.091	1.140	1.116	1.110	0.875	1.297	0.751	0.822	8507
1.093	1.118	1.146	1.164	1.010	1.034	1.123	1.158	0.776	1.188	0.766	0.844	8508
0.939	0.965	0.980	0.997	1.041	1.091	1.099	1.154	0.762	2.257	0.727	0.830	8509
1.083	1.122	1.188	1.213	0.946	1.012	1.016	1.013	0.843	0.746	0.784	0.878	8510
1.035	1.075	1.101	1.063	1.016	1.040	1.028	1.075	0.767	2.149	0.772	0.860	8511
1.042	1.075	1.141	1.184	1.045	1.027	1.031	1.064	0.0	0.0	0.0	0.0	8512
TOWER NO. 6												
URMS				VRMS				WRMS				DATA SET
1	2	3	4	1	2	3	4	1	2	3	4	
1.183	1.219	1.257	1.561	1.217	1.283	1.272	1.000	0.567	0.774	0.942	0.940	8501
1.092	1.139	1.198	1.257	1.104	1.125	1.155	1.222	0.600	0.771	0.854	0.918	8504
1.134	1.247	1.192	1.197	1.060	1.252	1.121	1.152	0.585	0.738	0.863	0.936	8505
1.024	1.068	1.120	1.105	0.952	0.995	1.088	1.102	0.574	0.692	0.797	0.871	8506
0.934	0.952	0.994	1.027	1.069	1.084	1.085	1.141	0.539	0.679	0.863	0.891	8507
1.045	1.087	1.106	1.138	1.011	1.048	1.029	1.060	0.550	0.669	0.807	0.881	8508
0.935	0.952	0.973	0.976	1.048	1.077	1.071	1.101	0.533	0.640	0.807	0.864	8509
1.039	1.061	1.114	1.107	0.930	0.947	0.975	0.993	0.578	0.683	0.831	0.867	8510
1.057	1.084	1.106	1.090	0.958	0.996	1.045	1.036	0.616	0.745	0.801	0.826	8511
1.027	1.075	1.116	1.146	0.978	1.026	1.086	1.116	0.0	0.0	0.0	0.0	8512
TOWER NO. 7												
URMS				VRMS				WRMS				DATA SET
1	2	3	4	1	2	3	4	1	2	3	4	
1.259	1.293	1.190	1.249	1.201	1.228	1.179	1.198	0.915	0.860	0.802	0.857	8501
1.192	1.224	1.156	1.188	1.148	1.168	1.092	1.112	0.988	0.879	0.777	0.894	8504
1.141	1.200	1.138	1.206	1.137	1.134	1.110	1.099	0.924	0.800	0.705	0.776	8505
1.059	1.117	1.058	1.105	0.0	0.0	0.0	0.0	0.879	0.716	0.715	0.752	8506
1.031	1.061	0.960	1.001	0.940	1.110	1.078	1.112	0.938	0.790	0.718	0.803	8507
1.198	1.126	1.071	1.102	1.020	1.056	1.002	1.038	0.906	0.747	0.778	0.852	8508
1.122	1.012	0.948	0.987	1.069	1.110	1.072	1.125	0.918	0.720	0.714	0.763	8509
1.067	1.114	1.037	1.104	0.997	0.970	1.013	0.998	1.005	0.725	0.723	0.807	8510
1.039	1.098	1.008	1.063	0.971	0.980	0.991	1.016	0.944	0.771	0.696	0.731	8511
1.105	1.137	1.067	1.116	1.043	1.064	1.055	1.019	0.0	0.0	0.0	0.0	8512
TOWER NO. 8												
URMS				VRMS				WRMS				DATA SET
1	2	3	4	1	2	3	4	1	2	3	4	
1.158	1.234	1.248	1.270	0.804	1.283	1.007	1.325	0.930	0.908	0.949	0.884	8501
1.059	1.167	1.024	1.190	0.991	1.150	1.075	1.231	0.918	0.993	0.871	0.893	8504
1.182	1.189	1.236	1.160	0.856	1.137	0.953	1.209	0.967	0.887	0.983	0.852	8505
0.934	1.154	1.009	1.121	0.0	0.0	0.0	0.0	0.942	0.895	0.967	0.784	8506
1.079	1.003	0.897	1.033	0.876	0.980	0.834	0.981	0.882	0.829	0.757	0.835	8507
1.303	1.140	1.190	1.064	0.887	1.072	0.834	1.013	1.031	0.851	0.815	0.804	8508
1.193	0.977	1.083	0.995	0.861	1.038	0.795	0.993	0.865	0.754	0.804	0.790	8509
1.016	1.266	1.086	1.230	0.736	1.034	0.832	1.033	0.907	0.826	0.992	0.814	8510
0.896	1.164	1.004	1.131	0.771	1.037	0.854	1.049	0.834	0.826	1.014	0.842	8511
1.049	1.102	1.000	1.108	0.899	1.090	0.965	1.164	0.0	0.0	0.0	0.0	8512

velocity components for the no building, small building, and large building cases, respectively. Similarly, Table VIII represents the rms values for selected data of the no building and the large building case.

CHAPTER VI

SMOKE STUDY

On April 3, 1975, two tests were conducted at the field site when the wind was approximately 12 mph (5.36 m/s) blowing almost directly down the array (down the array is from tower number 1 to tower number 6). These two tests are as follows:

1. Smoke bombs were used to define the extent of the wake on the center line behind the building and to visualize and qualitatively define other flow patterns about the building.
2. Hand held anemometer and simple directional vanes were used to estimate the nature of the wake along the center line and at the corners of the building.

Simultaneously all towers were operating and standard measurements were taken. Detailed measurements of the locations of the trees, road, and fence from the building and tower array were made. Figure 24 shows these measurements.

Photographs of the smoke patterns are shown in Figures 25 through 28 which illustrate essentially the same basic flows observed in wind tunnels. Figure 25 shows the upstream region of flow separation. Although reversed flow would, on occasion, occur as far upstream as the smoke bomb

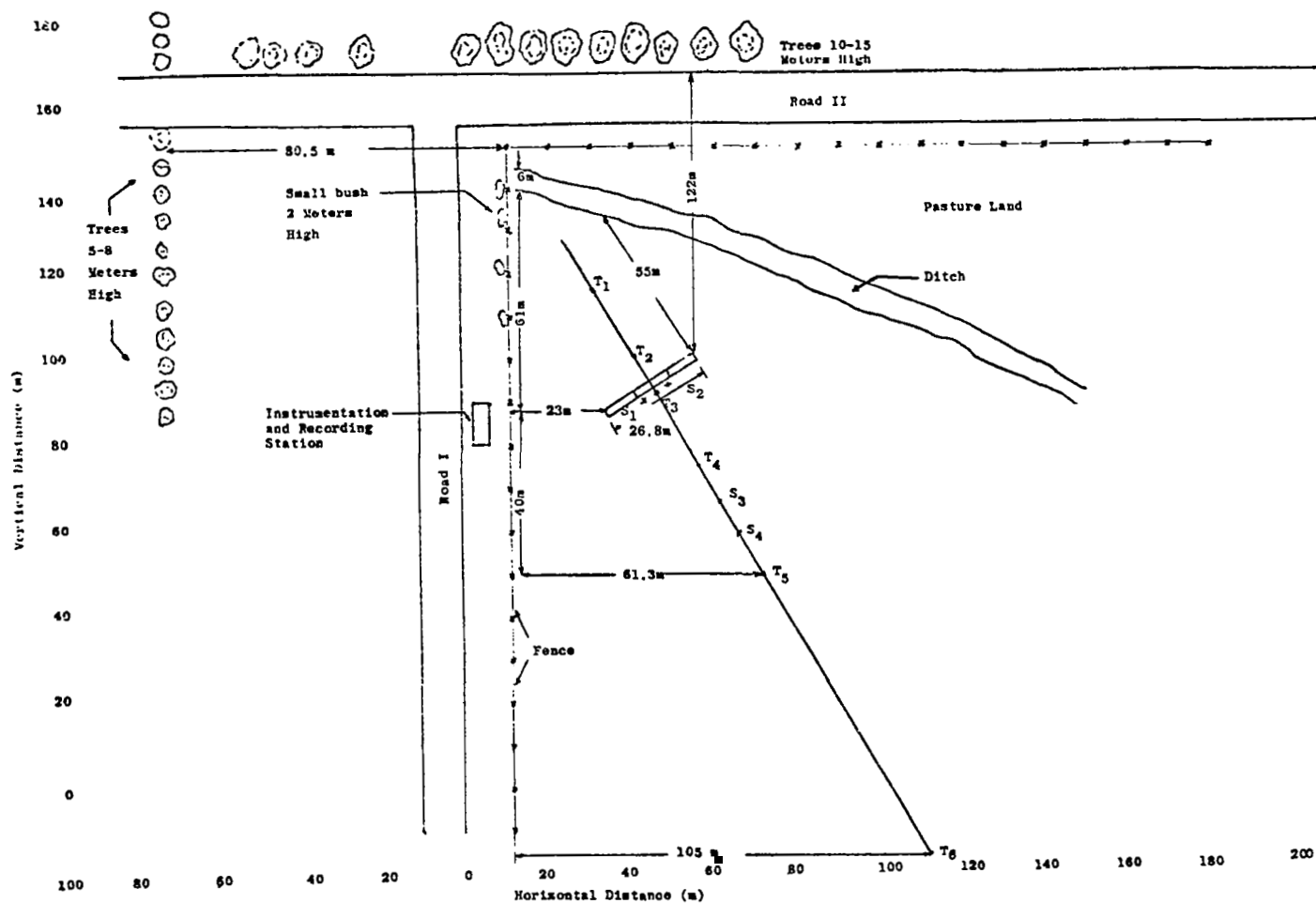


Figure 24. Top view of the eight tower facility site (all dimensions in meters).

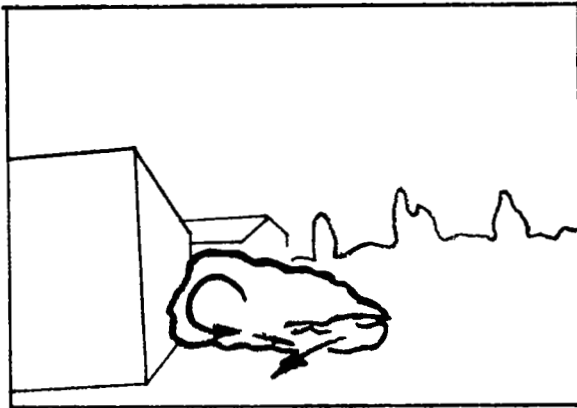
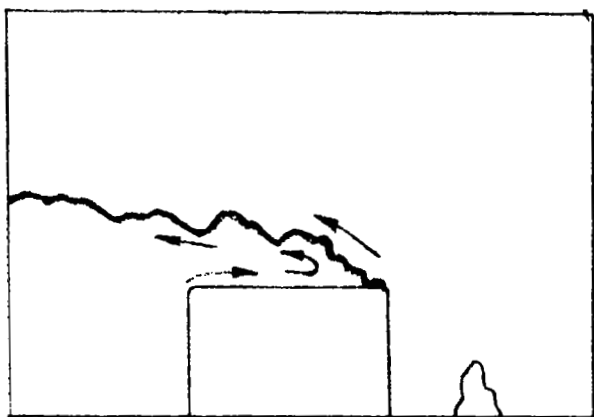
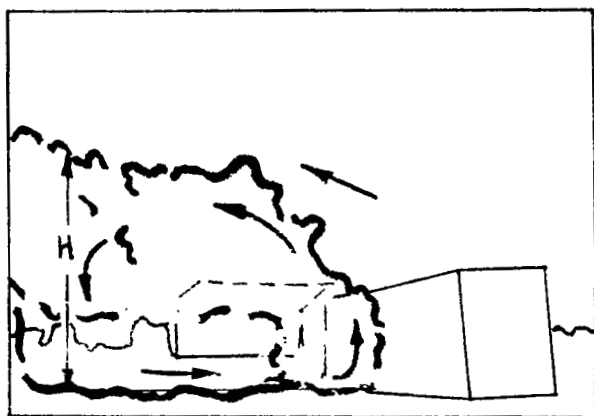


Figure 25. Upstream flow separation.



(a)



(b)

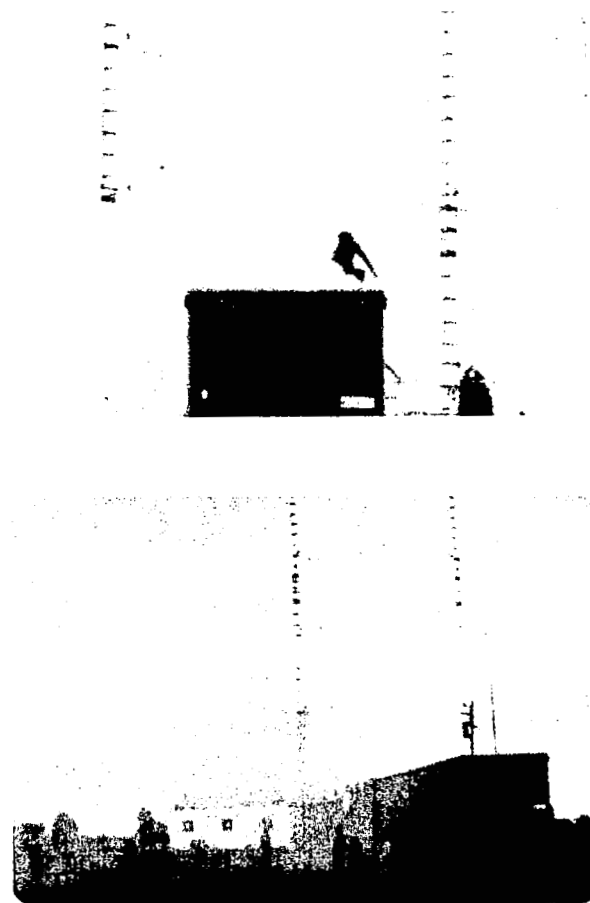


Figure 26. Wake formation.



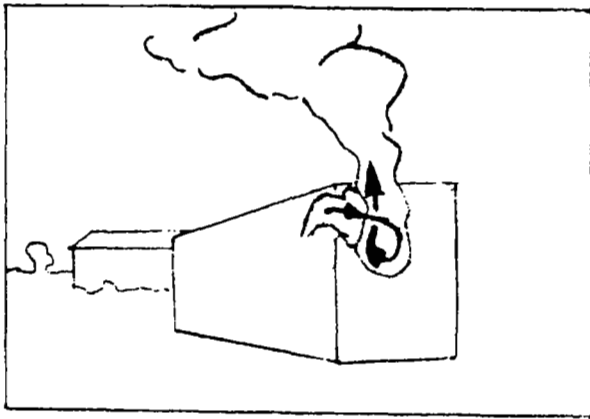
(a)



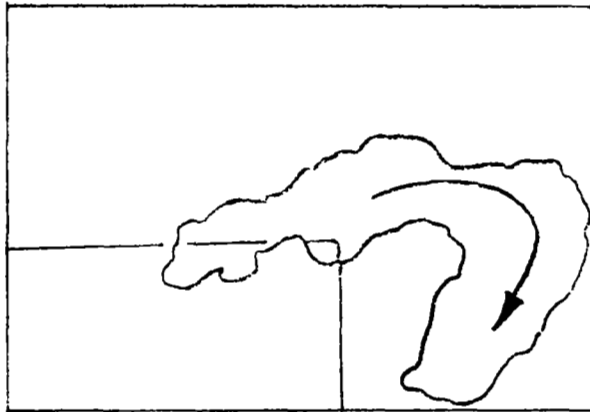
(b)



Figure 27. Recirculation and reattachment flow.



(a)



(b)



Figure 28. Vortex shedding.

illustrated in the picture (approximately 2.9 m), most of the time the reversed flow regions were less than this in extent. The smoke released at ground level approximately 3 m upstream normally separated and followed along the front of the building passing around the ends of the building, and then flowing downstream indicating substantial three-dimensional effects on the front face of the building.

The size of the upstream recirculation and the side to which the smoke passed around the building was highly fluctuating as was also the position of the rearward wakes and other flow patterns observed. This fluctuation came primarily from directional variations in the upstream wind. The field data, through necessity, must therefore depart from wind tunnel data since these pronounced directional variation in the wind cannot readily be simulated in the laboratory.

The rms value of the wind direction, $\bar{\theta}_{\text{rms}}$ measured in the undisturbed flow at tower 6 for this particular day was on the order of 7.5 degrees and the maximum deviations of $\bar{\theta}$ is on the order of ± 56 degrees. Reference [6] shows that there is appreciable difference between wind tunnel flow normal to a model block building and that at a 47 degree angle to the building. Hence the wake pattern can be expected to show considerable fluctuation with this kind of angular variation in wind.

Figures 26a and 26b illustrate that the height of the wake, approximately 1.5 building heights downstream,

extends on an average to almost twice the building height. This agrees with reported values [5].

Figure 27, page 71, clearly illustrates the extent of the wake near the ground. In Figure 27a the smoke from the bombs closest to the building is seen to move directly upstream and that from the bomb farthest from the building is seen to move directly downstream. In Figure 27b three smoke bombs are positioned along the downstream center line behind the building. Smoke from the upstream location flows upstream, smoke from the downstream location flows downstream, and smoke from the center location flows partly upstream and partly downstream indicating that the center location coincides with the reattachment zone. The location of this reattachment zone like the upstream separation region is highly fluctuating.

Several rough measurements of the extent of the wake along the center line were made by holding a smoke candle at a given level and walking either away from or toward the building. The distance from the building where the smoke began to depart from a definite upstream or downstream flow was recorded on a tape measure laid along the ground. Continuing to walk downstream the distance at which the smoke flow was distinctly flowing in the opposite direction (see Figure 27b) was recorded. The two distances represent the extent of the reattachment zone. The length of the wake was taken as the midpoint of this zone. Table IX gives the measured distances determined from the smoke candle held at

TABLE IX

SMOKE PATTERN MEASUREMENT OF THE WAKE EXTENT

Run No.	Height of Measurement	1 ft		3 ft		5 ft		7 ft	
		L_b^*	L_e^{**}	L_b	L_e	L_b	L_e	L_b	L_e
1		29.0	44.0↓***	22.0	40.0↑****	38.0	45.0↓	28.0	47.0↑
2		23.0	41.0↑	27.0	49.0↓	29.0	47.0↓	29.0	48.0↓
3		31.0	44.0↓	20.0	49.0↑	27.0	46.0↑	18.0	41.0↑
4		40.0	57.0↓					21.0	45.0↑
5		43.0	55.0↓						
Average		32.0	48.0	23.0	46.0	31.0	46.0	24.0	45.0
Midpoint		40.0		34.5		38.5		34.5	
Variance		8.0	7.0	4.0	5.0	6.0	1.0	5.0	3.0

* L_b represents length of traverse at which reattachment begins.

** L_e represents length of traverse at which reattachment ends.

***↓ represents traverse toward the building.

****↑ represents traverse away from the building.

the 1, 3, 5, and 7 ft level above the ground. Table IX gives an indication of the extent of the wake with respect to height.

The average midpoint of reattachment at the 1 ft level above the ground from Table IX is 12.5 ± 2.34 building height. Typical values measured for two-dimensional bluff bodies in wind tunnels range from 13 building height to 17 building height. For three-dimensional geometries, Leutheusser, et al. [8] present wind tunnel data indicating reattachment will occur at 4 building height downstream which is not consistent with the field results. One might conclude from the above observations that the length of the separation region along the center line behind the building behaves almost two-dimensionally.

Also, quantitative measurements of the wind speed were made with a hand held anemometer at the 1, 3, 5, and 7 ft levels along the center line and these are recorded in Table X. The experimental results show that the mean velocity 7.9 ft away from the building is approximately 2.5 mph and increases to 5 mph at 27.6 ft. The speed then decreases to 3.5 mph at 38.6 ft which indicates the presence of the reattachment zone. This value of 38.6 ft corresponds very well with the location of reattachment determined from the smoke bomb tests. After reattachment the wind speed again increases downstream.

Figure 28, page 72, illustrates vortex shedding from the building corners as depicted in Figures 1 and 2,

TABLE X
MEASUREMENT OF WIND SPEED AT DIFFERENT HEIGHTS

Wind Speed and Location	Height of Measurement Above the Ground (ft)			
	1	3	5	7
Distance (ft)	7.9	7.9	7.9	7.9
Wind Speed (mph)	2-3	3-4	3-4	3-4
Distance (ft)	27.6	27.6	27.6	27.6
Wind Speed (mph)	4-6	5-8	2-4	5-6
Distance (ft)	38.6	38.6	38.6	38.6
Wind Speed (mph)	3-4	4-5	3-4	3-4
Distance (ft)	49.3	49.3	49.3	49.3
Wind Speed (mph)	6-7	8-10	10-12	10-12
Distance (ft)	81.7	81.7	81.7	81.7
Wind Speed (mph)	6	10-11	10-12	15-18
Distance (ft)	100.0	100.0	100.0	100.0
Wind Speed (mph)	8-9	10-11	11	13-16

pages 2 and 4. In Figure 28a, page 72, the smoke released near the corner of the building is drawn down and circles toward the building due to the corner vortex. Looking essentially down the center line of the vortex in Figure 28b the smoke is observed to form a large swirl as it departs from the corner of the building.

A Super 8mm motion picture film of the smoke pattern formation about the building is available on loan from The University of Tennessee Space Institute, Tullahoma, Tennessee, 37388, attn: Dr. Walter Frost.

CHAPTER VII

INTERPRETATION OF DATA

I. DESCRIPTIONS

Three complete data sets were taken on April 3, 1975. These runs were performed the same day as the smoke bomb test was conducted (the direction of the wind was within $192^\circ < \bar{\theta} < 202^\circ$ where the bar over θ means averaging over the four instrumentation levels). These three runs are numbered 8540, 8541 and 8542. Note that the instruments at level 4 (20.01 m) of tower number 3 were again located at the 9 m level.

The data are analyzed in the same manner as runs 8504, 8505 and 8512 described in Frost, et al. [9] and lead to essentially the same conclusions. The only apparent difference between the test conditions of the data for 8504, 8505, and 8512 and that for 8540, 8541 and 8542 is the range of wind direction which was $165^\circ < \bar{\theta} < 180^\circ$ for the former and $192^\circ < \bar{\theta} < 202^\circ$ for the latter.

II. RAW VELOCITY DATA

In Reference [9] it was shown for 13 runs both with and without the building present that the wind speed data at tower number 6, non-dimensionalized with respect to the wind speed at level 4, $V(1,6)/V(4,6)$, clustered within an 8

percent accuracy band. This demonstrated that tower number 6 recorded the undisturbed wind and served as a reference velocity to which the other tower velocities could be compared. In the present data the horizontal wind sensor at level 4 read extremely low and therefore it was necessary to adjust the data to provide a reliable reference velocity as will be described later.

Figure 29 shows a computer plot of the velocities at each of the six towers non-dimensionalized with respect to the level 4 value. For tower number 3 it was, of course, necessary to interpolate between $V(4,2)$ and $V(4,4)$ to determine the upper level non-dimensionalizing velocity. Inspection of the tower number 6 data show some of the data to be badly in error. This is due to dividing by the previously mentioned low value of $V(4,6)$.

Near the building the velocity profiles show a pronounced deficit and slightly more scatter than profiles farther from the building. The significant influence of wind direction on the wake as described from the smoke bomb tests is believed responsible for the scatter.

To isolate the effects of the building on the flow, it is preferable to reference all velocities to the undisturbed velocity profile at tower number 6. This was achieved by curve fitting the tower number 6 data to the logarithmic velocity profile

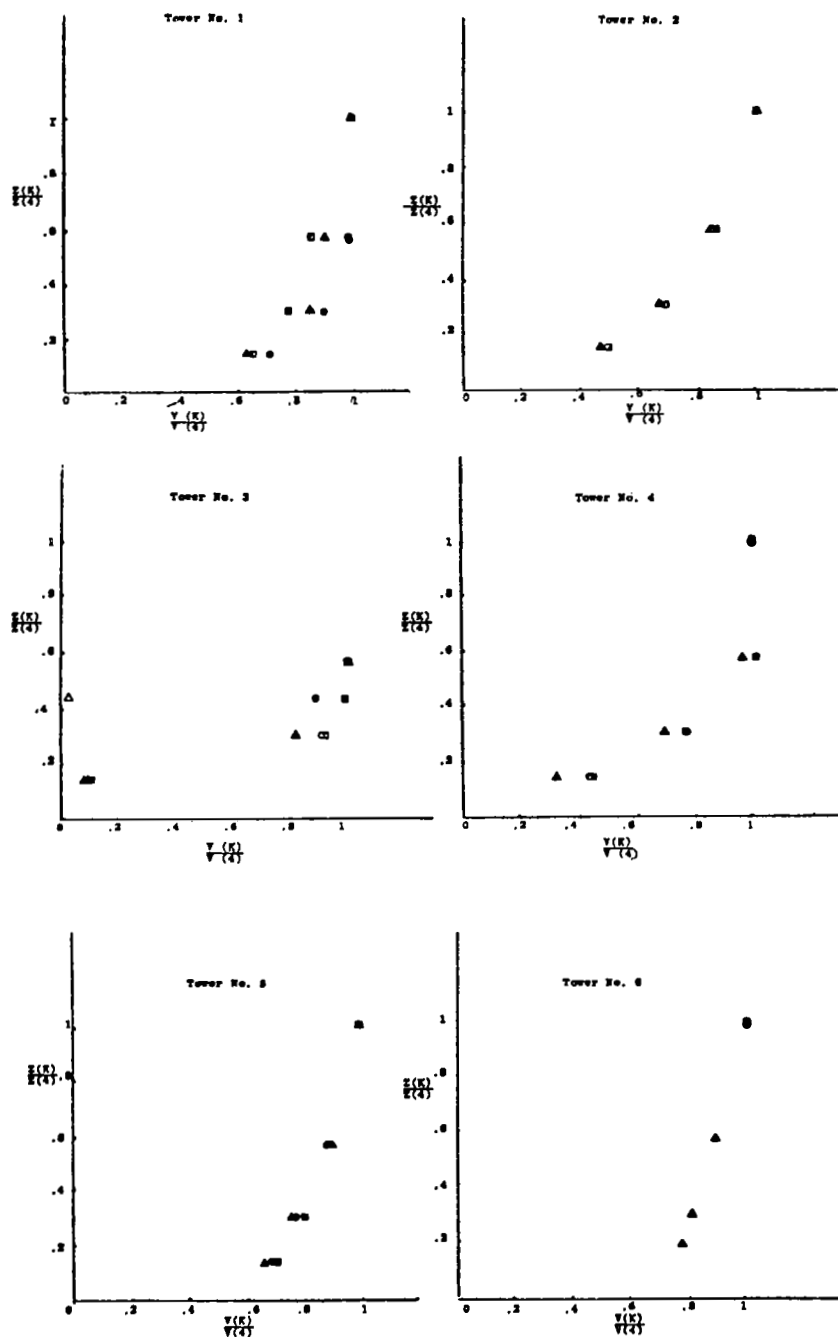


Figure 29. Basic data for test number 8540-42.

$$u(z) = \frac{u_*}{K} \ln \frac{z + z_o}{z_o} \quad (1)$$

The value of $z_o = 0.007$ m found applicable to this field site in Reference [9] was used in the curve fit. The friction velocity u_* for the three runs was

Run No.	u_* (m/sec)	$\bar{\theta}$ (deg)
8540	0.343	192
8541	0.367	201
8542	0.318	202

Figure 30 shows the correlation of the data with the curve fit and compares the results with that of Reference [9]. With the exception of the two bad points at level 4, the agreement is excellent. The solid symbols are the most recent data.

Referencing the velocity profiles at the remaining towers to the velocity curve, Equation 1, results in Figure 31 which compares the data of runs 8540-8542 with 8504, 8505, and 8512. The solid symbols are the most recent data. In general, the data for the recent runs display a higher recover toward the reference curve than the earlier data. This is hard to explain except that perhaps the upstream trees in April when runs 8540-8542 were taken may have had more or less foliage than in November when runs 8504, 8505, and 8512 were taken. Also the difference in mean wind angle may have influenced the result as is mentioned later.

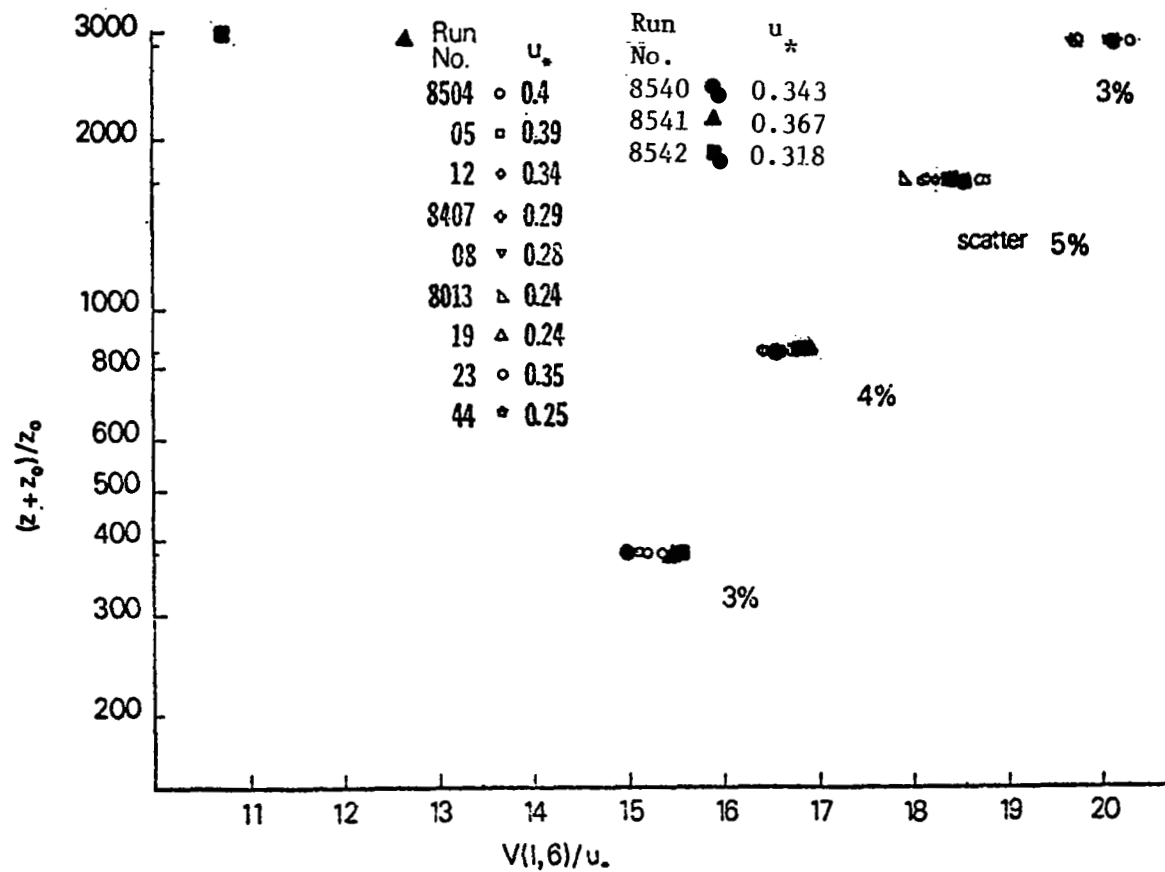


Figure 30. Correlation of reference velocity, tower number 6.

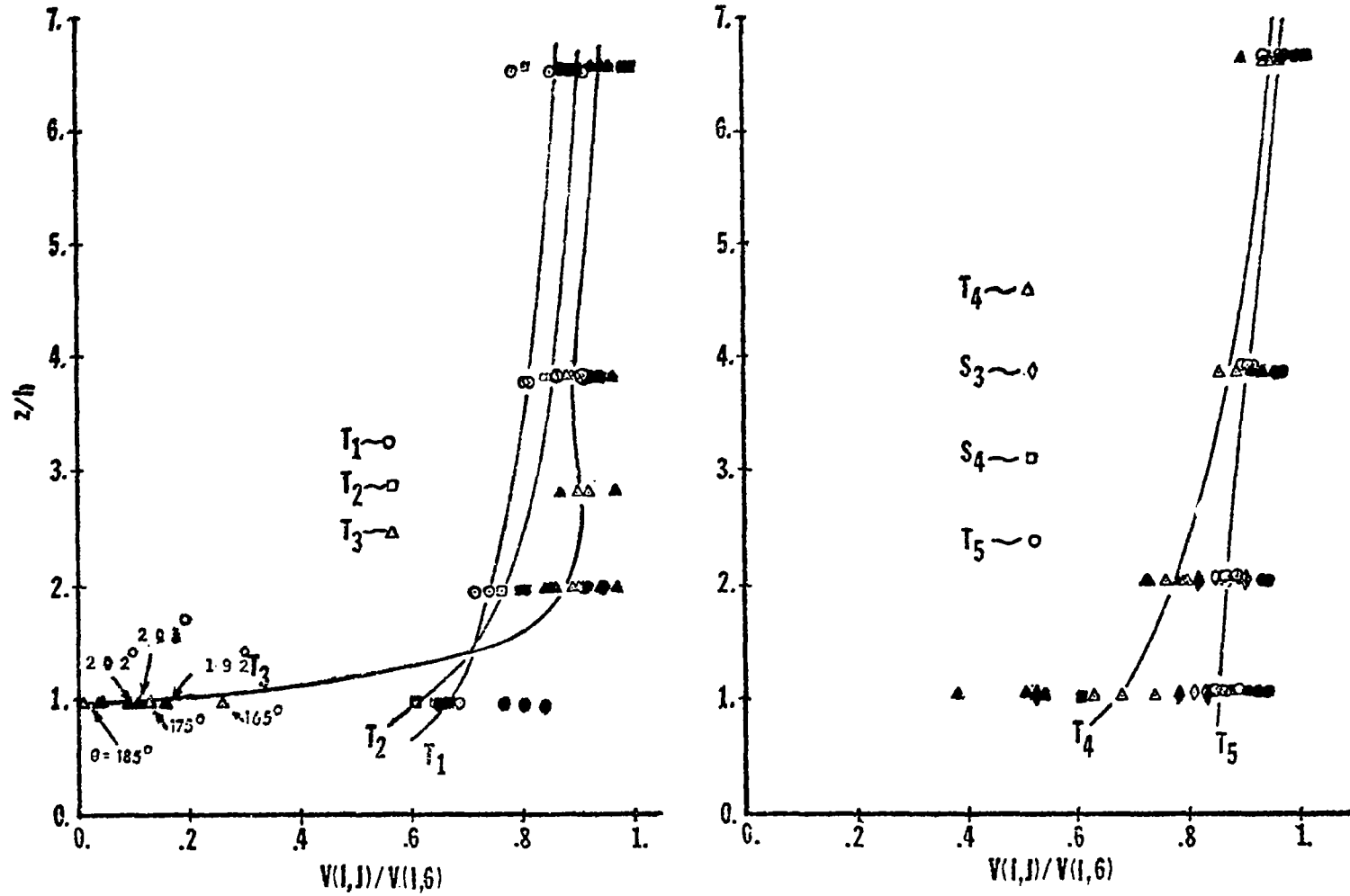


Figure 31. Wind speed nondimensionalized with reference wind speed.

Tower number 4 data show the overshoot in velocity to be carried further downstream than it was in the earlier data and to have a larger velocity deficit at the lower levels. The very low datum point registered for tower number 3 at the 9 m level is due to a malfunctioning instrument which was corrected after run 8540. In turn, the upper level data for tower number 1 are not recorded since the horizontal wind speed anemometer was frozen throughout the runs.

The same explanation of the physics of the flow as given in Reference [9] pertains here in describing the results of Figure 3, page 5. That is, at tower number 3 one observes a definite overshoot at the 6 m and 9 m levels in the local velocities with the velocity directly behind the building going almost to zero. The wind at no time exceeds tower number 6 values. The reason for this is that the building is in the wake of the upstream trees and consequently does not experience local winds as strong as those at tower number 6. If in both cases the velocity profile at tower number 3 is referenced to the velocity profile at tower number 6 for the no building case velocity ratio greater than one would occur.

The presence of a wake due to the trees which interacts with building disturbances which was reported in Reference [9] is again apparent from the data for tower number 1 and tower number 2. The velocity of tower number 1 is greater than that of tower number 2 at level one but

becomes lower at higher levels. This occurs due to tower number 2 being farther from the trees than tower number 1 and hence having recovered greater velocity as the wake decays at the 20 m level. However, at low levels the wind is now being retarded due to the building and this retardation is more strongly felt by tower number 2 which is closer to the source of disturbance. The data for tower number 1, tower number 2 and tower number 4 show considerable scatter which is attributed to the shifting of the tree wake with wind direction.

Figure 32 shows a plot of the velocity deficit $[V(1,6) - V(1,J)]/V(1,6)$ averaged over the 8540, 8541 and 8542 data set. The data correlate with

$$\frac{\Delta V}{V(1,6)} = 3.73 \left(\frac{x}{h} \right)^{-1.25}$$

which as noted in Reference [9] predicts a slower decay than normally reported [6]. However, if the effects of the tree wake is subtracted, the corrected data plot as shown by the square symbols in Figure 32 and correlate with

$$\frac{\Delta V}{V(1,6)} = 5.59 \left(\frac{x}{h} \right)^{-1.50} \quad (2)$$

The exponent on this correlation (-1.50) is in near perfect agreement with the wind tunnel results of [6] and that for the same field site reported in [9].

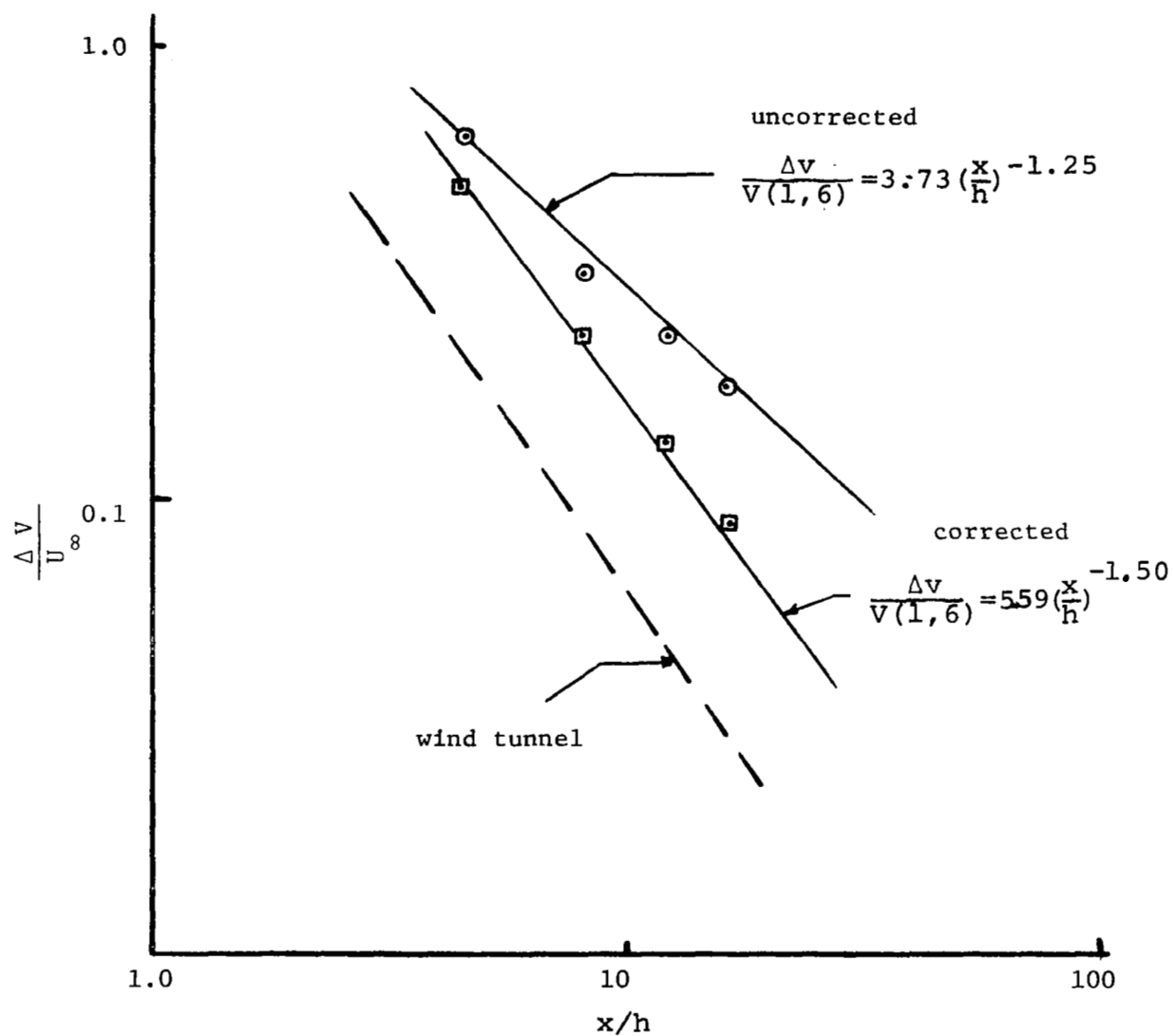


Figure 32. Decay of velocity deficit along center line of wake.

The coefficient in Equation 2 is higher than reported in Reference [6], however. This is in agreement with the higher velocity deficits shown in Figure 32 to occur in the wake region at the lower levels for the 8540-8542 runs as compared to the earlier data [9]. One possible explanation of the higher deficit is that for runs 8504, 8505 and 8512 the average wind direction was $165^\circ < \bar{\theta} < 185^\circ$, whereas for runs 8540-8542 it was $192^\circ < \bar{\theta} < 202^\circ$. Inspection of Figure 33 shows that for the latter runs the wind was coming more directly over the trees than in the former case.

III. TURBULENCE CHARACTERISTICS OF THE FLOW

A preliminary look at the turbulence characteristics of the flow is given in the following paragraphs. Further analysis of the turbulence structure will be given in later reports.

Figures 34 and 35 show the variation with horizontal position of the longitudinal rms value divided by u_* for the 3 m and 12 m levels. The value of u_* is that for the undisturbed flow at tower number 6. In Figure 34 the average value of σ_u/u_* for the four runs with no building 8013, 8019, 8023, and 8044 is plotted and in Figure 35 the average value of σ_u/u_* for the two runs 8407 and 8408 and for the three runs 8504, 8505 and 8512 is plotted, respectively.

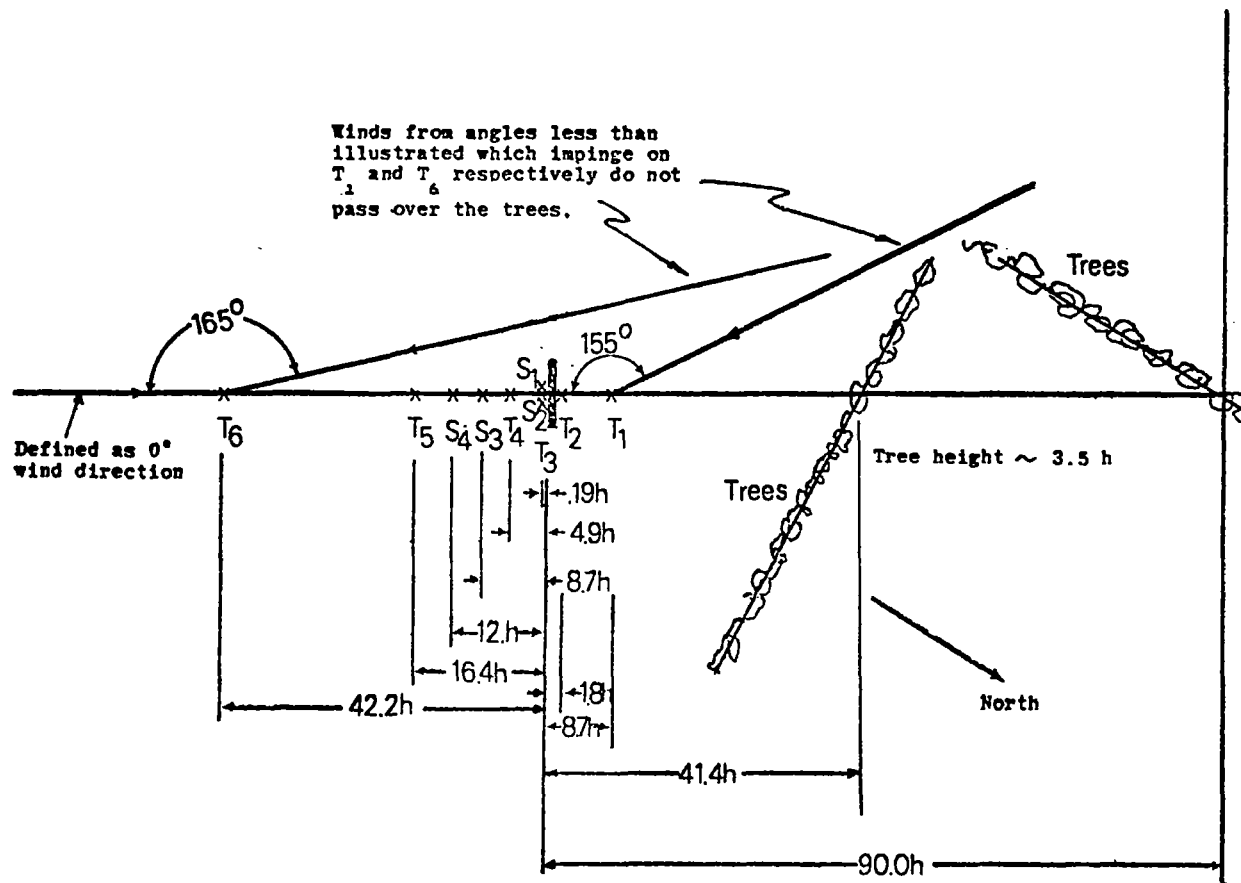


Figure 33. Plan view of tower array.

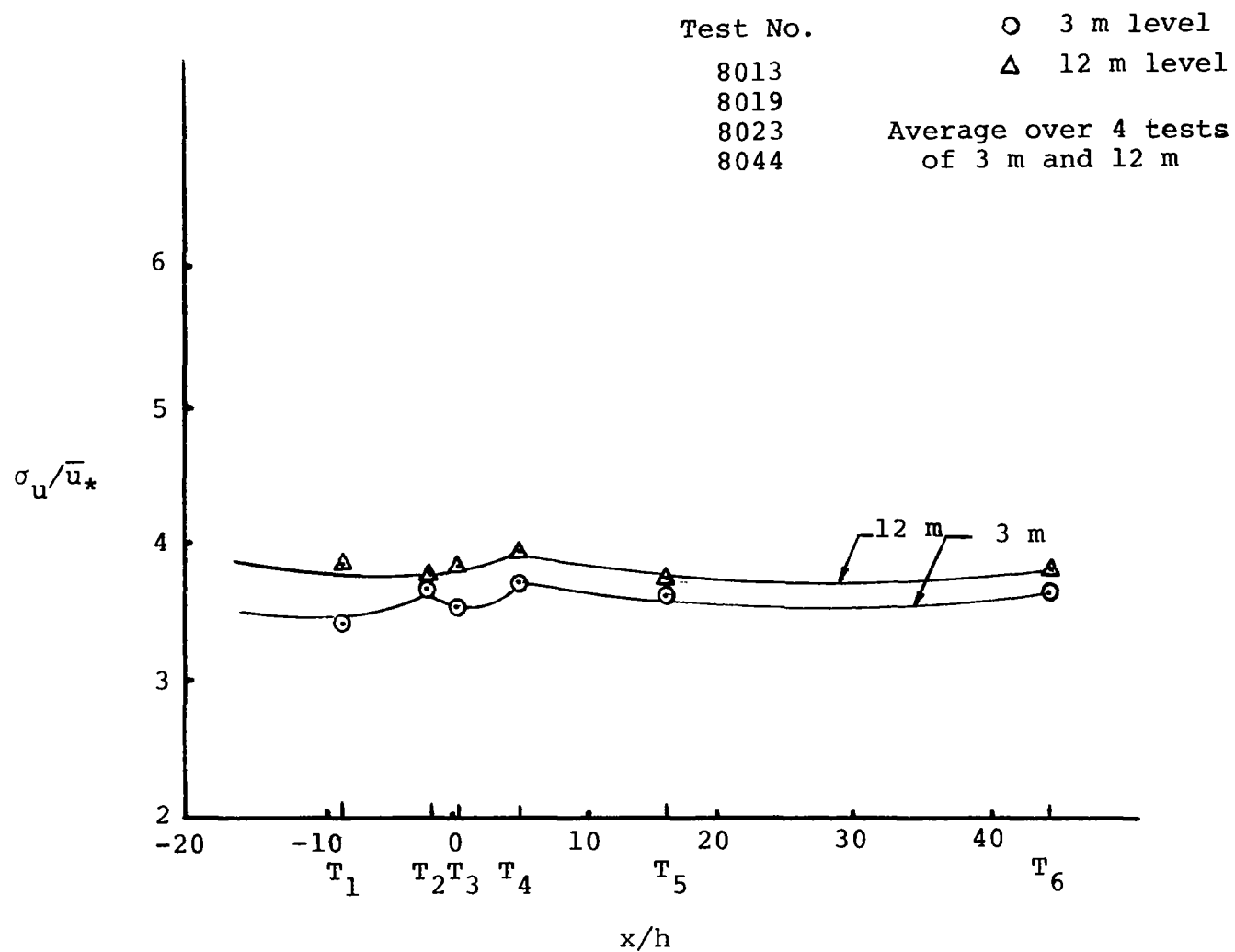


Figure 34. Variations of longitudinal velocity fluctuation σ_u (no building case).

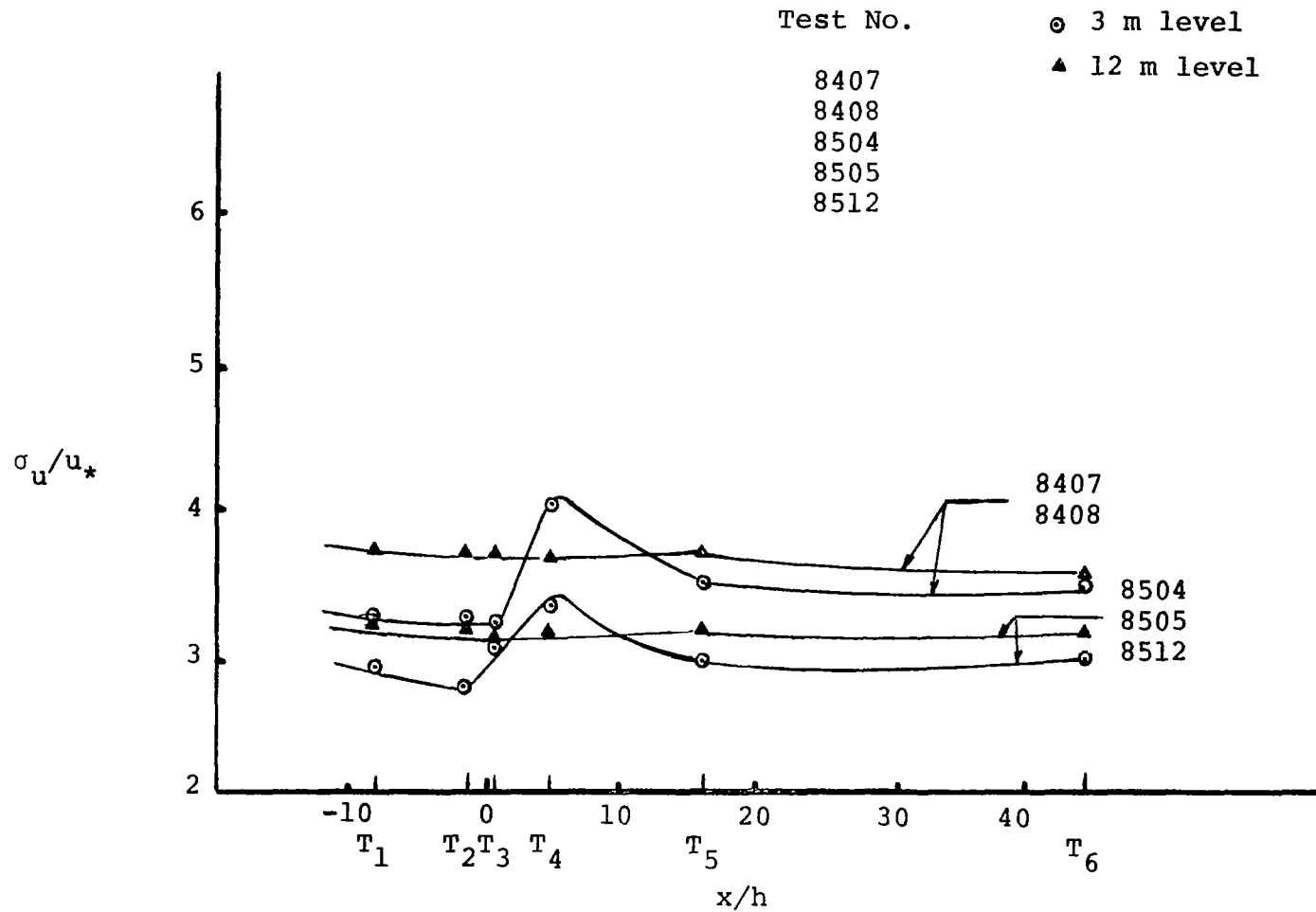


Figure 35. Variations of longitudinal velocity fluctuation σ_u (building case).

For the undisturbed atmospheric boundary layer (no building case) the mean velocity fluctuation remains relatively constant having a small unaccountable disturbance near towers 3 and 4. It is normally reported [10] that σ_u/u_* is constant with height for the neutral atmosphere. The magnitude of the fluctuation for the 3 m level is, however, approximately 6 percent lower than the 12 m level showing a slight increase with height. The overall average of σ_u/u_* for the two levels is 3.75. Reference [10] reports values of this ratio ranging from 2.9 to 2.10 which are 33 percent lower than found here.

Reference [10] does point out that the value of the constant of proportionality varies with terrain, however, one is lead to suspect the upstream tree line as behaving somewhat as a turbulence grid.

Figure 35 illustrates that the longitudinal component of turbulence has a pronounced peak in the building wake at the 3 m level of tower 4 and a large deficit at towers 1, 2, and 3. At the 12 m level the building appears to have little influence. For reasons that are not clear, the 8500 series runs are about 8 percent lower in magnitude than the 8400 series and 13 percent lower than the 8000 series. Assuming the 12 m level represents the undisturbed condition, the effect of the building at the 3 m level is to decrease the turbulence upstream approximately 12 percent and increase the turbulence in the wake at tower 4 about 7 percent. Beyond tower 5 the value of σ_u/u_* at level 3 has

returned to approximately 6 percent less than level 12, as it does for the undisturbed flow, Figure 34, page 90.

Figure 36 shows the horizontal variation of σ_v/u_* and σ_w/u_* at 3 m level for run 8044 and for the average of runs 8407 and 8408. The lateral and vertical turbulence fluctuations for the latter case show an increase at tower 2, a depression at tower 3 and another increase at towers 4 and 5. There is justification for this behavior as illustrated by the sketch in Figure 37. As the flow approaches the building there will be a suppression of longitudinal fluctuations due to the retardation of the flow by the solid structure. The vertical and lateral fluctuations should increase as the flow circumvents the building, hence the increase in σ_v and σ_w at tower 2, and tower 3. In the wake the flow is very still, hence, the depression in σ_v and σ_w . Finally, there should be a resurgence of turbulence at towers 4 and 5 which will be in the highly turbulent shear layer separated from the leading edge. If the rms values were referenced to the local velocity then the turbulence intensity directly behind the building would be very high since the local velocity is very small in that region.

Comparing the undisturbed case with the building case, both components of the turbulence fluctuations are greater for the undisturbed case. The constants of proportionality for σ_w/u_* and σ_v/u_* in the undisturbed flow are on the order of 2.3 and 4.3 respectively. Again these are larger by almost a factor of 2 than the reported values of

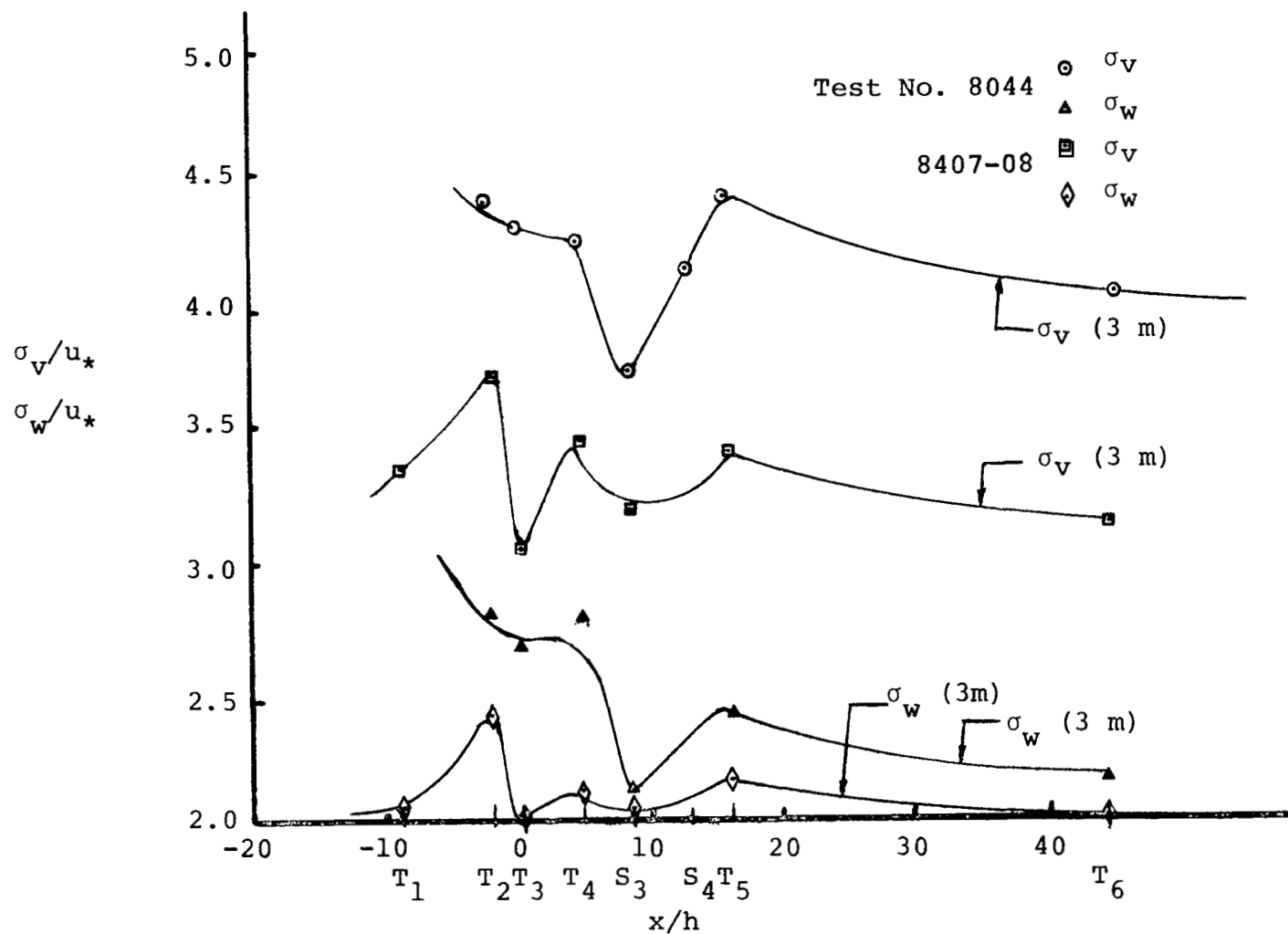


Figure 36. Variations of the lateral σ_v and vertical σ_w velocity fluctuations.

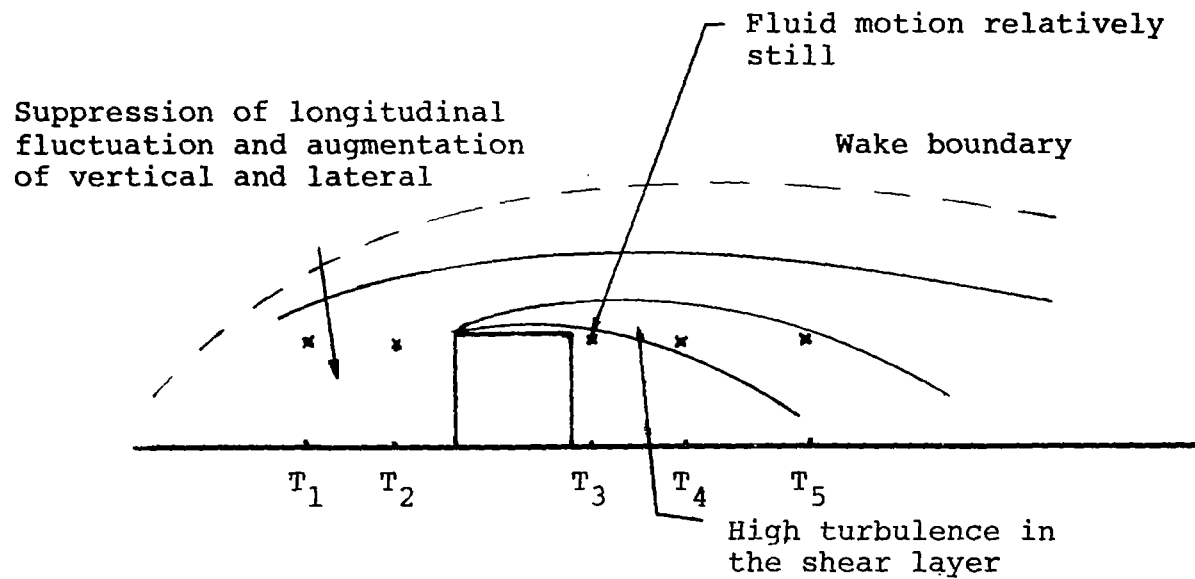


Figure 37. Turbulent regions in shear layer.

1.3 and 2.2 respectively. The ratio of $\sigma_u/\sigma_v/\sigma_w$ is 1.6/1.9/1.0 as compared to the most frequently quoted ratio of 2.4/1.9/1.0. It should be noted, however, that the reported values of this ratio vary greatly throughout the literature (see Reference [10]).

Some of the anomalous characteristics of the rms turbulence fluctuation for the undisturbed flow have been alluded to as occurring from the upstream trees creating a wake which sheds large eddies. Further evidence of this wake is given by Figure 38 which is a plot of σ_u divided by the local velocity. One observed a high local turbulence intensity which decays downstream analogous to turbulence decay behind a wind tunnel grid [11].

The influence of the wake is further illustrated in the nondimensionalized power spectral density functions for the undisturbed flow shown in Figures 39 and 40. Figures 39 and 40 are an "eyeball" curve fit of the computed power spectral density function (see Figure 39). Also plotted on the figures is the best fit curve for the near-neutral spectra over sufficiently homogeneous terrain reported by Kaimal, et al. [12]. Again u_* is the value for the tower 6 undisturbed velocity profile whereas \bar{u} is the local horizontal wind speed.

The figures illustrate higher energy in the larger eddies for the present data with an apparent loss of energy in the low eddy or high frequency region. The data is not

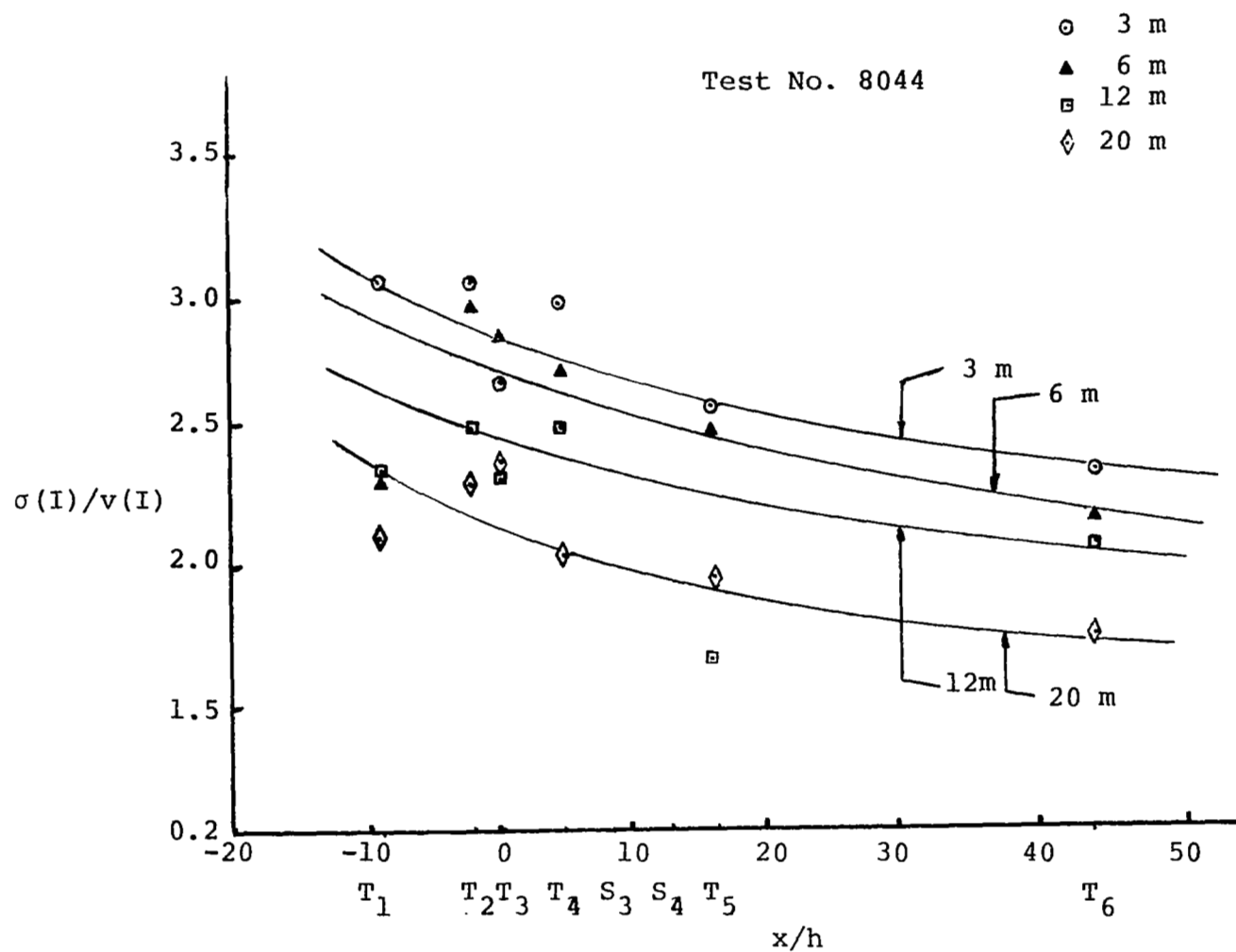


Figure 38. Turbulence intensity (no building case).

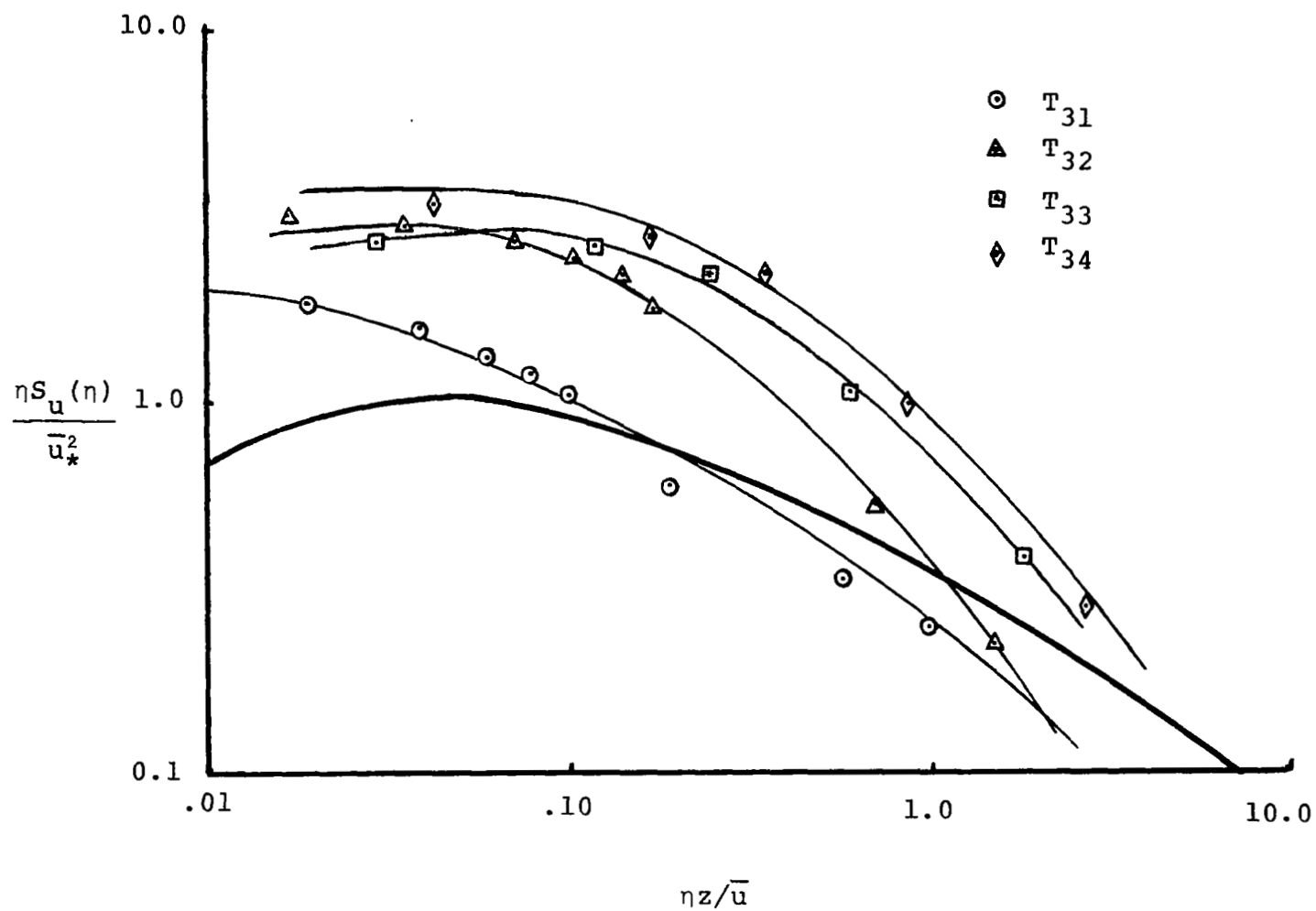


Figure 39. Test 8044, tower number 3, nondimensionalized spectral density (no building).

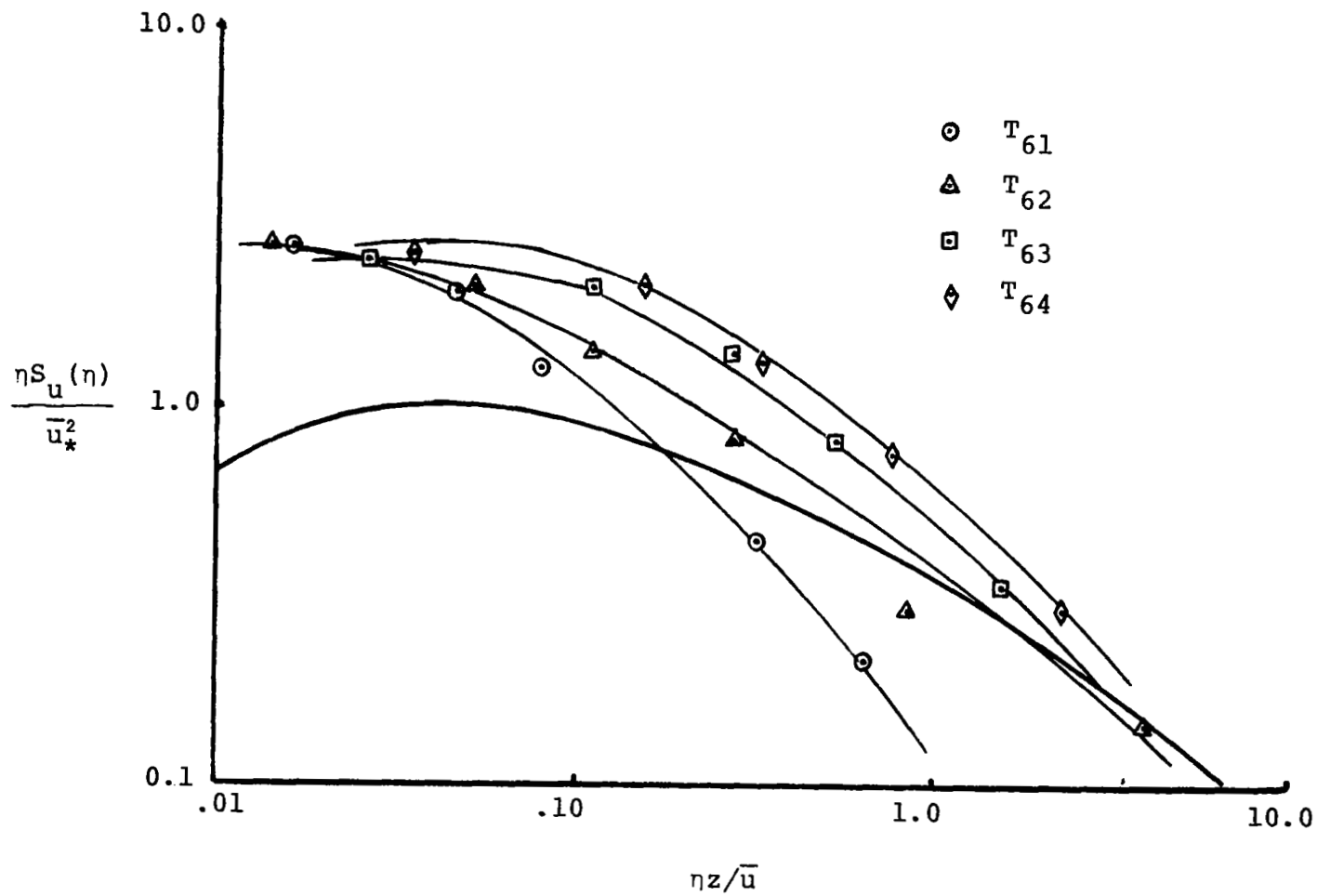


Figure 40. Test 8044, tower number 6, nondimensionalized power spectral density (no building).

sufficiently resolved to determine the true behavior of the flow at the higher frequency to see if the $-5/3$ law applies.

These curves do, however, point to some form of organized vortex shedding from the trees.

Interestingly, the spectral peaks with the exception of the 3 m and 6 m levels remain about the same as Kaimal's, et al. [12] data.

The building disturbed data in the same non-dimensionalized form is given in Figures 41 and 42. The curves have approximately the same form as the near-neutral homogeneous data curve but are considerably higher. The spectral peaks are shifted to higher frequencies, particularly behind the building at tower number 3. This shift is contrary to what one would expect.

Normally, the building would be expected to shift the energy to smaller frequencies. The observed reverse effect is probably due to nondimensionalizing with Taylor's hypothesis, i.e., $\eta_{\text{ref}} = \bar{U}/z$, which is of questionable validity in the building wake where u'/U_{ref} may be very large.

Further analysis of the spectra is required and is being conducted on the present project. The capability of reducing the data stored on magnetic tape using The University of Tennessee Space Institute facilities has now been developed and cross-correlations and other statistics can be computed.

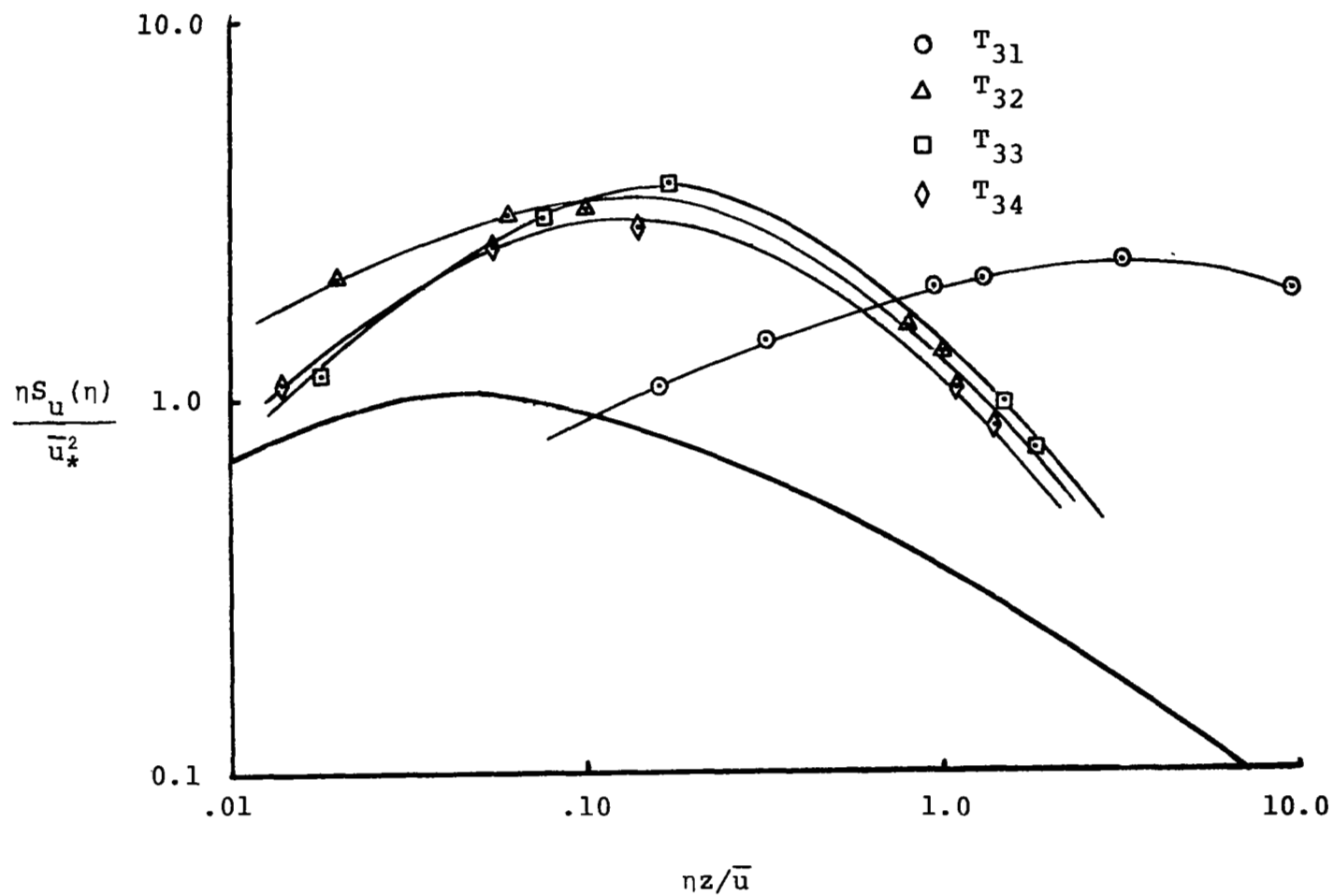


Figure 41. Test 8504, tower number 3, nondimensionalized spectral density (building case).

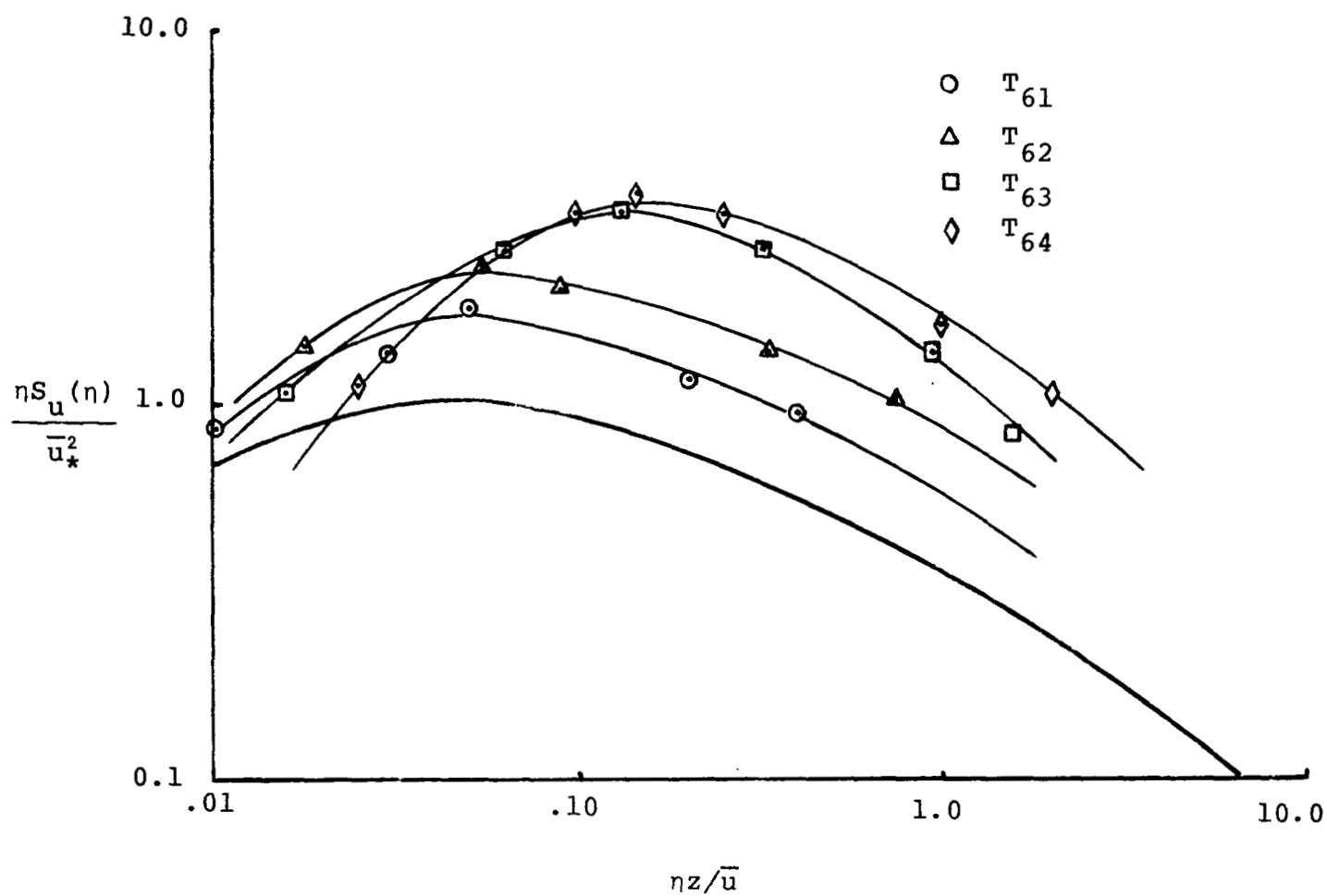


Figure 42. Test 8504, tower number 6, nondimensionalized spectral density (building case).

CHAPTER VIII

CONCLUSIONS

An experiment has been conducted which provides data from which a fundamental understanding of the mean wind field and its turbulence structure about a simulated block building in a large open field can be determined. The data demonstrate the typical features of laboratory flows over bluff bodies; however, the existence of a wake from a line of trees approximately 122 m upstream is clearly evident and the data must be interpreted accordingly.

Analysis of the mean longitudinal velocity at building level shows an overshoot at tower number 3 and a velocity deficit decay in the wake which are in both qualitative and quantitative agreement with wind tunnel results. The mean extent of the wake measured with smoke patterns under conditions of approximately a 16 mph wind speed at the 20 m level was 12.5 ± 2.3 building heights at a height of approximately 1 ft above the ground. This can be compared with values of 13 h to 16 h reported for similar two-dimensional laboratory tests. The smoke patterns also indicate that the wake extends upward to a height of approximately 1.5 h to 2 h and the separation at the upstream face of the building extend forward about 0.9 h.

The rms values of the velocity components at the 3 m level were strongly influenced by the building but at the

12 m level this influence was not apparent, indicating that the disturbance from the building did not extend to that height. The maximum departure of the rms values from the no building case was ± 12 percent.

The ratio of $\sigma_u/\sigma_v/\sigma_w$ for the runs with no building is 1.6/1.9/1.0 as contrasted to 2.4/1.9/1.0 which is the ratio normally reported for level homogeneous terrain. The tree wake is believed to be a factor in this regard.

The turbulence energy spectra shows higher values than the neutrally stable atmosphere over homogeneous uniform terrain reported in the literature. Again, this is believed to be due to the tree wake. The shift in spectral peaks, however, is not in complete accord with intuitions and different nondimensionalizing parameters are likely required to resolve this difference.

Additional analysis of the lateral and vertical mean velocity components and of the statistics of the turbulence is required.

BIBLIOGRAPHY

BIBLIOGRAPHY

1. Frost, W. "Review of Data and Prediction Techniques for Wind Profiles Around Manmade Surface Obstructions, Flight in Turbulence," Agard-CP-140, Section 4, May, 1973.
2. Lighthill, M. J., and A. Silverleaf. "A Discussion on Architectural Aerodynamics," Phil. Trans. Roy. Soc. Lond. A. 269, pp. 321-554, October, 1971.
3. Chang, P. K. Separation of Flow. New York: Pergamon Press, 1970.
4. Nash, J. F. Lecture notes at Short Course on Flow Separation. The University of Tennessee Space Institute, Tullahoma, Tennessee, January, 1972.
5. Halitsky, J. "Meteorology and Atomic Energy," D. H. Slade, editor. U.S. Atomic Energy Commission, TID 24190, 221-255, March, 1968.
6. Hanson, A. C., J. A. Peterka, and J. E. Cermak. "Wind Tunnel Measurements in the Wake of a Simple Structure in a Simulated Atmospheric Flow," NASA Marshall Space Flight Center Report No. NASA-CR-2540; M-140, April, 1975.
7. Colmer, M. J. "Some Full-Scale Measurements of the Flow in the Wake of a Hangar," ARC-CP-1166, December, 1971.
8. Leutheusser, H. J. "Simulated Problems in Building Aerodynamics," Journal of the Hydraulics Division, Proceedings ASCE, 93:35-49, May, 1967.
9. Frost, W. "Mean Horizontal Profiles Measured in the Atmospheric Boundary Layer About a Simulated Block Building," Proceedings of Second U.S. National Conference on Wind Engineering Research, June, 1975.
10. Neal, M. B., G. Dagfinn, and R. S. Dwight. "Wind Models for Flight Simulator Certification of Landing and Approach Guidance and Control System," Report No. FAA-RD-74-206, December, 1974.

11. Hinze, J. O. Turbulence; An Introduction to Its Mechanisms and Theory. New York: McGraw-Hill Book Company, Inc., 1959.
12. Kaimal, J. C., J. C. Wyngaard, Y. Izumi, and O. R. Cote. "Spectral Characteristics of Surface Layer Turbulence," Quarterly Journal of Royal Meteorological Society, 98:563-589, November, 1972.

APPENDIX

FIGURES AND TABLE ARRANGEMENTS

The materials contained in the Appendix are the illustrations of tower arrangements, and the type, and the locations of the data acquired (Figures A-1 through A-5, and Table A-I).

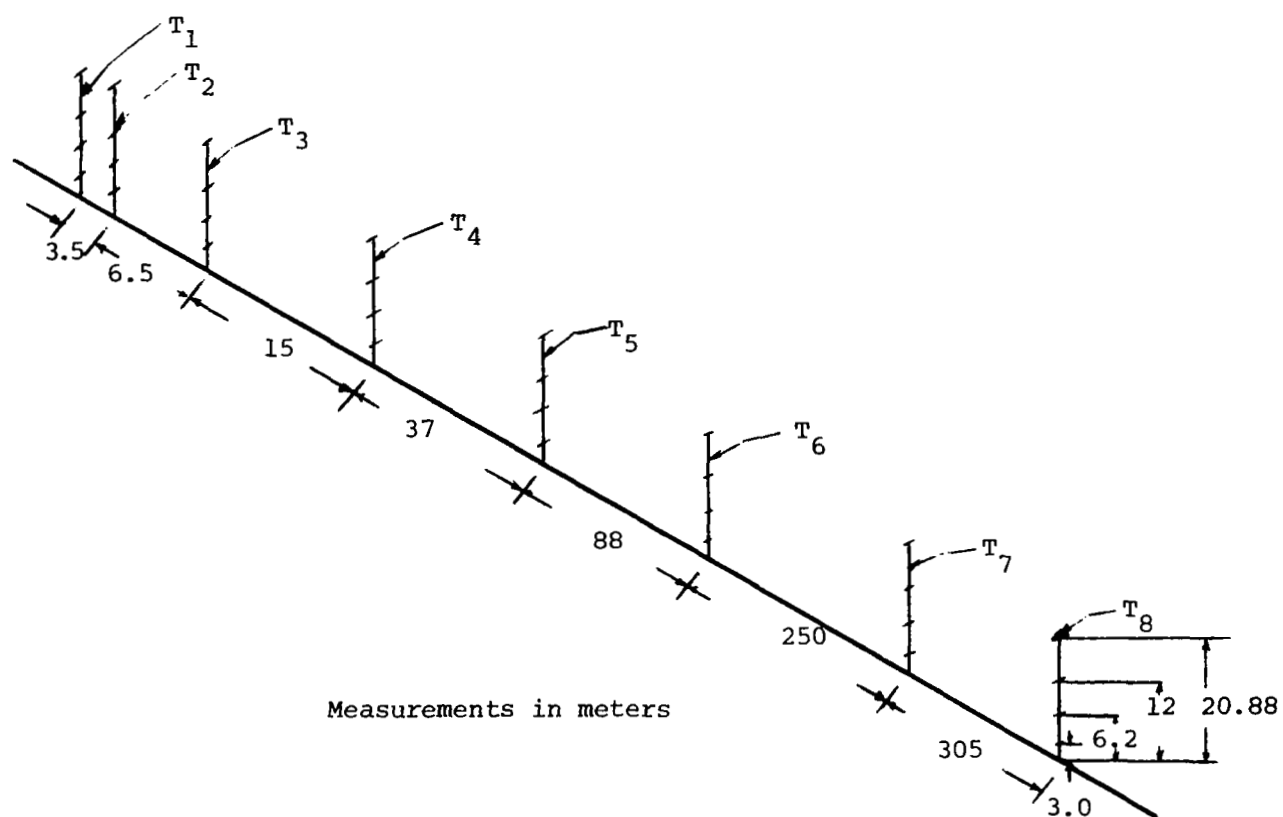


Figure A-1. Tower arrangements; runs 8001 through 8057, recorded between December 30, 1971 and May 22, 1972.

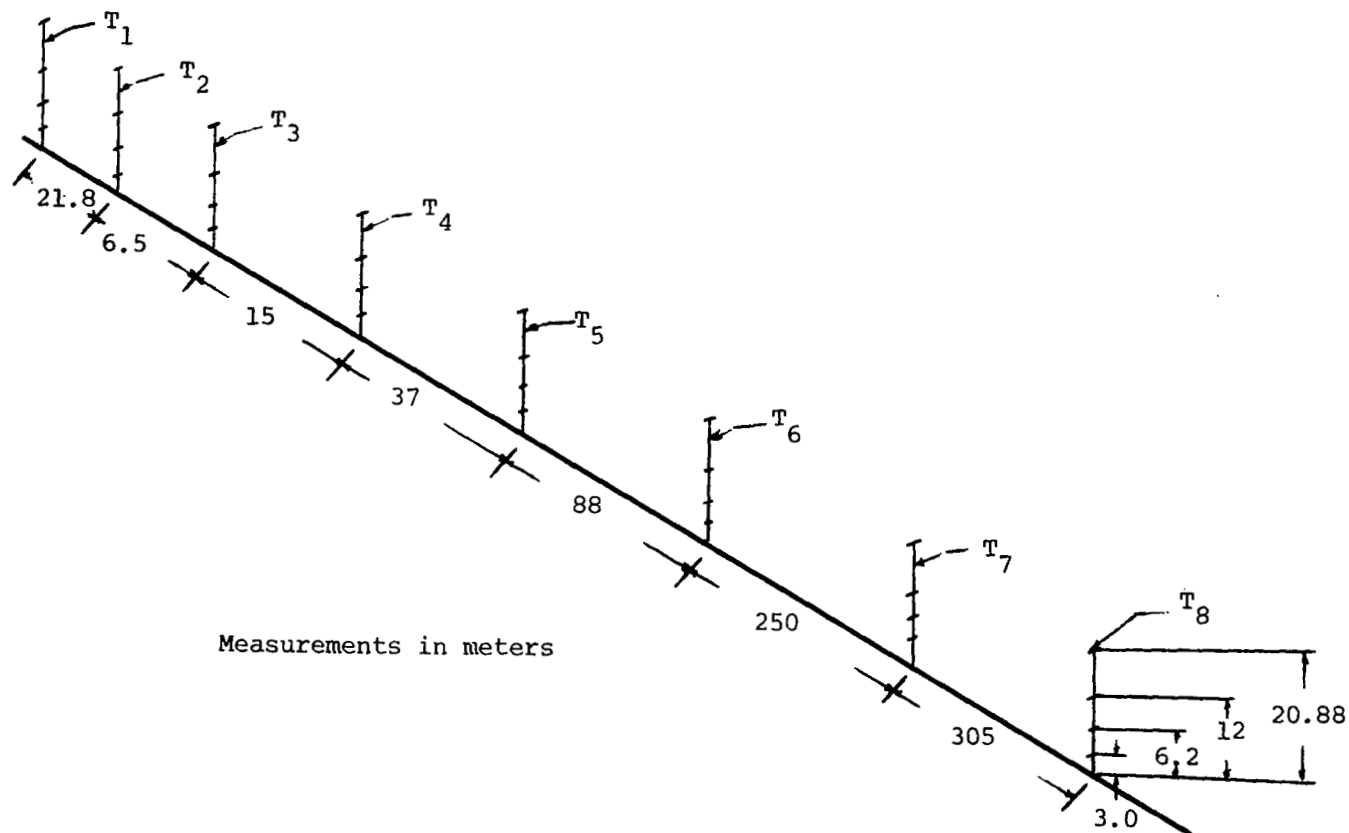


Figure A-2. Tower arrangements; runs 8058 through 8062, recorded between January 3, 1973 and January 22, 1973.

Figure A-3. Tower arrangements; runs 8063 through 8079, recorded between March 1, 1973 and April 27, 1973.

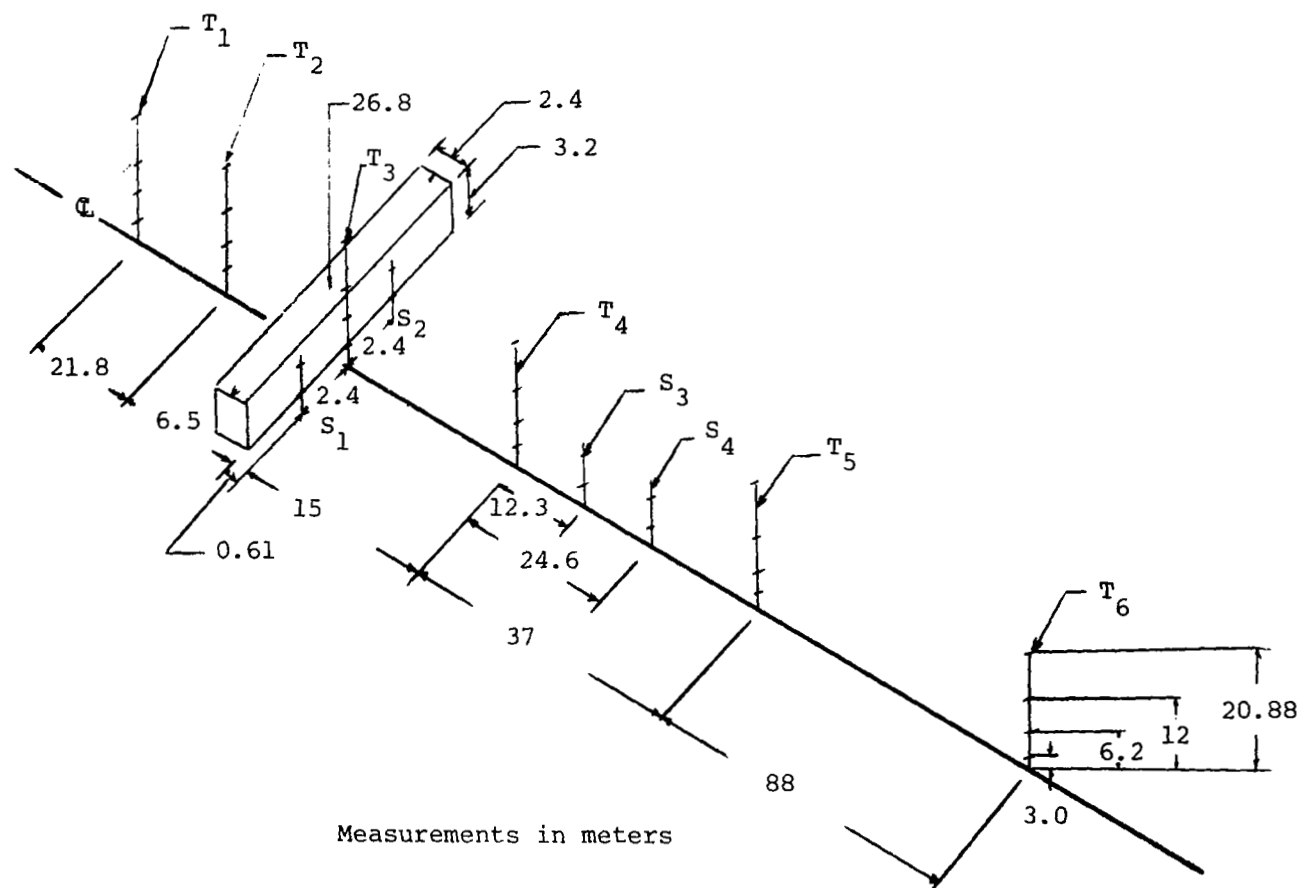
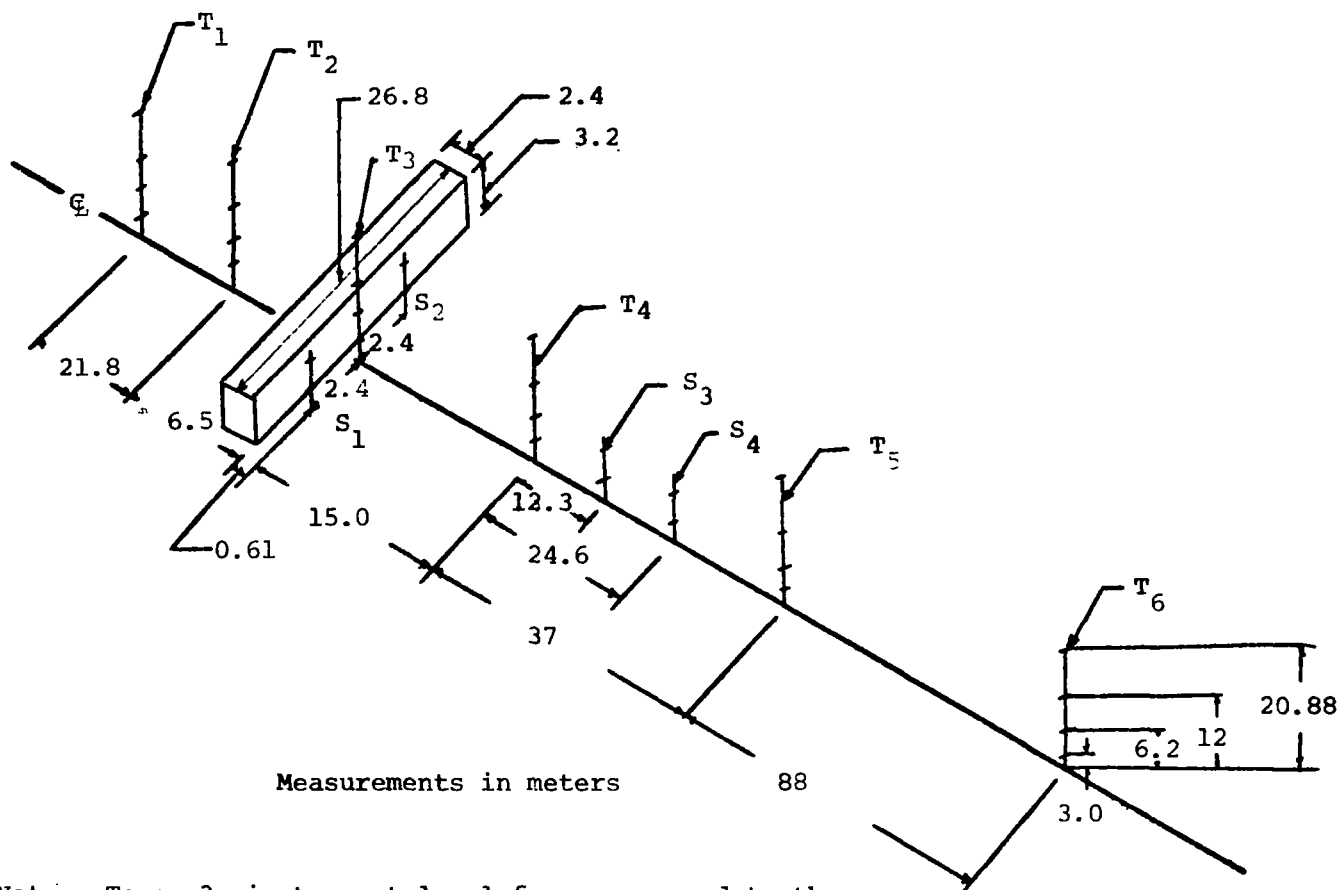


Figure A-4. Tower arrangements; runs 8401 through 8409, recorded between March 19, 1974 and May, 1974.



Note: Tower 3, instrument level four was moved to the 9 meter level, but still recorded as T₃L₄.

Figure A-5. Tower arrangements; runs 8501 to present, recorded between November, 1974 to present.

TABLE A-I

TOWER AND LEVELS ASSOCIATED WITH THE GIVEN CHANNEL NUMBER

Data	Recorder #-Channel	Data Systems Lab. Output		Tower and Level
		Data Channel	Type Data	
Wind Speed	1-1	1	Longitudinal Component Spectra	T ₁ L ₁
	-2	2		T ₁ L ₂
	-3	3		T ₁ L ₃
	-4	4		T ₁ L ₄
	-5	5		T ₂ L ₁
	-6	6		T ₂ L ₂
	-7	7		T ₂ L ₃
	-8	8		T ₂ L ₄
	-9	9		T ₃ L ₁
	-10	10		T ₃ L ₂
	-11	11		T ₃ L ₃
	-12	12		T ₃ L ₄
	2-1	13		T ₄ L ₁
	-2	14		T ₄ L ₂
	-3	15		T ₄ L ₃
	-4	16		T ₄ L ₄
	-5	17		T ₅ L ₁
	-6	18		T ₅ L ₂
	-7	19		T ₅ L ₃
	-8	20		T ₅ L ₄
	-9	21		T ₆ L ₁

TABLE A-I (continued)

Data	Recorder #-Channel	Data Systems Lab. Output		Tower and Level
		Data Channel	Type Data	
Wind Speed	-10	22	Longitudinal Component Spectra	T ₆ L ₂
	-11	23		T ₆ L ₃
	-12	24		T ₆ L ₄
	3-1	25		T ₇ L ₁
	-2	26		T ₇ L ₂
	-3	27		T ₇ L ₃
	-4	28		T ₇ L ₄
	-5	29		T ₈ L ₁
	-6	30		T ₈ L ₂
	-7	31		T ₈ L ₃
	-8	32		T ₈ L ₄
	4-1	33	Lateral Component Spectra	T ₁ L ₁
	-2	34		T ₁ L ₂
	-3	35		T ₁ L ₃
	-4	36		T ₁ L ₄
	-5	37		T ₂ L ₁
	-6	38		T ₂ L ₂
	-7	39		T ₂ L ₃
	-8	40		T ₂ L ₄
Wind Direction	-9	41		T ₃ L ₁
	-10	42		T ₃ L ₂
	-11	43		T ₃ L ₃

TABLE A-I (continued)

Data	Recorder #-Channel	Data Systems Lab. Output		Tower and Level
		Data Channel	Type Data	
Wind Direction	-12	44	Lateral Component Spectra	T ₃ L ₄
	5-1	45		T ₄ L ₁
	-2	46		T ₄ L ₂
	-3	47		T ₄ L ₃
	-4	48		T ₄ L ₄
	-5	49		T ₅ L ₁
	-6	50		T ₅ L ₂
	-7	51		T ₅ L ₃
	-8	52		T ₅ L ₄
	-9	53		T ₆ L ₁
	-10	54		T ₆ L ₂
	-11	55		T ₆ L ₃
	-12	56		T ₆ L ₄
	6-1	57		T ₇ L ₁
	-2	58		T ₇ L ₂
	-3	59		T ₇ L ₃
	-4	60		T ₇ L ₄
	-5	61		T ₈ L ₁
	-6	62		T ₈ L ₂
	-7	63		T ₈ L ₃
	-8	64		T ₈ L ₄

TABLE A-I (continued)

Data	Recorder #-Channel	Data Systems Lab. Output		Tower and Level
		Data Channel	Type Data	
Vertical Wind Speed	7-1	65	Vertical Component Spectra	T ₁ L ₁
	-2	66		T ₁ L ₂
	-3	67		T ₁ L ₃
	-4	68		T ₁ L ₄
	-5	69		T ₂ L ₁
	-6	70		T ₂ L ₂
	-7	71		T ₂ L ₃
	-8	72		T ₂ L ₄
	-9	73		T ₃ L ₁
	-10	74		T ₃ L ₂
	-11	75		T ₃ L ₃
	-12	76		T ₃ L ₄
	8-1	77		T ₄ L ₁
	-2	78		T ₄ L ₂
	-3	79		T ₄ L ₃
	-4	80		T ₄ L ₄
	-5	81		T ₅ L ₁
	-6	82		T ₅ L ₂
	-7	83		T ₅ L ₃
	-8	84		T ₅ L ₄
	-9	85		T ₆ L ₁

TABLE A-I (continued)

Data	Recorder #-Channel	Data Systems Lab. Output		Tower and Level
		Data Channel	Type Data	
Vertical Wind Speed	-10	86	Vertical Component Spectra	T ₆ L ₂
	-11	87		T ₆ L ₃
	-12	88		T ₆ L ₄
	9-1	89		T ₇ L ₁
	-2	90		T ₇ L ₂
	-3	91		T ₇ L ₃
	-4	92		T ₇ L ₄
	-5	93		T ₈ L ₁
	-6	94		T ₈ L ₂
	-7	95		T ₈ L ₃
	-8	96		T ₈ L ₄